LIÈGE université
Gembloux
Agro-Bio Tech

CHEMICAL DEFENSES OF SEA CUCUMBERS: INTERACTIONS BETWEEN SAPONINS AND MODEL PLASMA MEMBRANES

CLAEREBOUDT Emily

Travail de fin d'études présenté en vue de l'obtention du diplôme de Master bioingénieur en Chimie et Bio-industries

Année académique 2016-2017

(Co)-promoteur(s): Magali Deleu (ULg) et Igor Eeckhaut (UMons)

LIÈGE université
Gembloux
Agro-Bio Tech

CHEMICAL DEFENSES OF SEA CUCUMBERS: INTERACTIONS BETWEEN SAPONINS AND MODEL PLASMA MEMBRANES

CLAEREBOUDT Emily

Travail de fin d'études présenté en vue de l'obtention du diplôme de Master bioingénieur en Chimie et Bio-industries

Année académique 2016-2017

(Co)-promoteur(s): Magali Deleu (ULg) et Igor Eeckhaut (UMons)

ACKNOWLEDGMENTS

I would first like to thank my thesis advisors Pr. Magali Deleu of the Laboratoire de Biophysique Moléculaire aux Interfaces (LBMI) of the Gembloux Agro Bio-tech faculty of the University of Liege and Pr. Igor Eeckhaut of the “Biologie des organismes Marins et Biomimétisme” (BOMB) lab of the faculty of Science of the University of Mons for their undivided aid and mentorship through my thesis. In addition I would like to thank Pr. M-L Faucconier’s and Dr. L.Lins who's office doors were always open whenever I ran into an obstacle or had a question about my research or writing. Everyone consistently allowed this paper to be my own work, but steered me in the right the direction whenever they thought I needed it.

I would also like to thank the experts who were involved in helping me in learning new techniques through out this research project: Guillaume Caulier, Lola Brasseur, Corentin Decroo, Thomas Bertrand and Estelle Deboever. Thank you for putting up with my endless curiosity and always being there for even the tiniest of questions.

Finally, I must express my very profound gratitude to my parents and to my partner in life, Nico, for providing me with unfailing support and continuous encouragement throughout my years of study and through the process of researching and writing this thesis. This accomplishment would not have been possible without them. Thank you.

-Emily

“The more that you read,

the more things you will know.

The more that you learn,

the more places you’ll go.”

-Dr.Seuss

Abstract

Saponins are a very diverse class of secondary metabolites found in plants and some marine invertebrates. They are amphiphilic molecules composed of a hydrophilic sugar moiety, and a hydrophobic steroid/triterpenic-like part known as the aglycone. Saponins are studied for their pharmacological properties such as their anti-fungal, anti-microbial and anti-tumoral activity. Holothuroids, or sea cucumbers, produce saponins as a chemical defense against predators and parasites, but interestingly, are immune to the cytotoxic nature of these chemicals. This immunity is extremely poorly understood. The standing hypothesis, based purely on observation, is that the rare Δ^{7} and $\Delta^{9(11)}$ sterols that replace cholesterol in the cellular plasma membranes of sea cucumbers are responsible for this immunity, however, the molecular mechanism remains obscure.

The aim of this study was to elucidate the mechanisms behind the immunity of holothuroid to the cytotoxic saponins (e.g. Frondoside A) they produce but also to describe, at a molecular level, the interactions that occur between model plasma membranes and saponins. This investigation was conducted using complementary biophysical tools, using both *in silico* approaches such as the Hypermatrix, IMPALA and Big Monolayer simulation models and with an *in vitro* technique called Isothermal Titration Calorimetry (ITC). The Hypermatrix method calculates energies of interaction between a central molecule and a surrounding lipid monolayer, allowing to determine if certain interactions are more favorable than others. The Big Monolayer uses these energies to simulate a monolayer composed of different proportions of lipids and saponin. ITC is a technique used to describe interactions in a thermodynamic framework, and allows for the enthalpy, entropy, free Gibbs energy and the binding constant of a particular interaction to be determined from a recorded thermogram.

The structural differences of the holothuroid sterols were first described and compared to the mammalian membrane sterol: cholesterol. Structural differences of saponins and sterols were associated with different interaction affinities and mechanisms. Saponin-lipid (both phospholipids and sterols) interactions were mainly apolar in nature. Interactions with phospholipids were more favorable than with sterols, and among the sterols, saponins interacted more favorably with cholesterol than the holothuroid Δ^{7} and $\Delta^{9(11)}$ sterols. Liposomes containing cholesterol resulted in exothermic interactions with Frondoside A whereas liposomes containing the Δ^{7} sterol were endothermic with the same saponin. Big Monolayer simulations using experimental settings previously developed for plant saponins revealed that the holothuroid saponin Frondoside A has an agglomerating effect on cholesterol domains, similarly to the plant saponin. However when interacting with the Δ^{7} sterols, the sterol domains were fragmented into small clusters.

The coevolution of a saponin-Δ^{7} sterol pair may be an adaptation required for holothuroid membranes to inhibit the formation of large membrane disruptive sterol domains in the presence of saponin.

Key-words: Saponin, holothuroid, *Holothuria scabra*, model plasma membrane, membrane interactions, sterol, biophysics, ITC

Résumé

Les saponines constituent une classe composée de divers métabolites secondaires trouvés dans de nombreuses plantes mais aussi dans certains invertébrés marins. Ce sont des molécules amphiphiles composées d'une moitié saccharidique polaire et d'une moitié stéroïdique/ triterpénique hydrophobe appelée l'aglycone. Les saponines particulièrement étudiées pour leurs propriétés pharmacologiques telles que leur activité antifongique, antimicrobienne et antitumorale. Les holothuries, ou concombres de mer, produisent des saponines ayant un rôle de défense chimique envers les prédateurs/parasites mais ne semblent pas affectés par leurs effets cytotoxiquesL'hypothèse , uniquement baséesur des observations, est que les stérols rares Δ^7 et $\Delta^{9(11)}$ qui remplacent le cholestérol dans les membranes plasmiques des holothuries, sont responsables de cette résistance. Toutefois, les mécanismes moléculaires impliqués dans cette résistance restent obscurs.

Cette étude avait pour but d'élucider le mécanisme qui explique la résistance des holothuries contre les saponines (e.g. Frondoside A) qu'elles produisent, mais aussi de décrire les interactions «membrane plasmique–saponines» au niveau moléculaire au travers d'une série d'outils biophysique complémentaires : des approches *in silico* tels que les modèles Hypermatrix, IMPALA et Big Monolayer, et une approche *in vitro*, la Titration Calorimétrique Isothermique (TIC). Les modèles Hypermatrix calculent les énergies d'interaction entre une molécule cible et une monocouche de lipides qui identifie les interactions plus favorables que d'autres. Le logiciel Bigmonolayer utilise ensuite ces énergies pour simuler une monocouche composée de proportions variables de lipides différents avec ou sans saponine. Le TCI décrit les interactions d'un point de vue thermodynamique et permet de déterminer l'enthalpie, l'entropie, l'énergie libre de Gibbs et la constante de liaison d'une interaction en particulier, à partir d'un thermogramme.

Les stérols d'holothuries et le stérol membranaire des mammifères (le cholestérol) sont structurellement différents et les différences structurelles entre les saponines et les stérols résultent en affinités et mécanismes d'interaction différents. Les interactions saponines-lipides sont de nature plutôt apolaire. Les interactions entre saponines et phospholipides étaient plus favorables que celles avec les stérols et les saponines interagissent de manière plus favorables avec le cholestérol qu'avec les stérols d'holothuries. Les liposomes contenant du cholestérol ont interagi avec la saponine Frondoside A de manière exothermique, alors que les liposomes contenant le stérol Δ^7 ont réagit de manière endothermique avec cette même saponine. Les simulations Big Monolayer, basées sur des conditions expérimentales décrites préalablement avec des saponines de plante, ont montré que la saponine Frondoside A avait un effet agglomératif sur les domaines de cholestérol, alors qu'elle a au contraire induit une fragmentation des domaines du stérols Δ^7.

La co-évolution de la paire saponine-stérol Δ^7 pourrait être une adaptation nécessaire aux holothuries pour conserver l'intégrité des membranes cellulaires.

Table of Contents

Abbreviations

PL	Phospholipids
PC	Phosphatidylcholine
DPPC	1,2-dipalmitoyl-*sn*-glycero-3-phosphocholine
DMPC	1,2-Dimyristoyl-sn-glycero-3-phosphorylcholine
DOPC	1,2-Dioleoyl-sn-glycero-3-phosphocholine
Chol	Cholesterol
Δ^7-sterol	5α-Cholest-7-en-3β-ol
$\Delta^{9(11)}$-sterol	4α,14α-dimethyl-5α-cholest-9(11)-en-3β-ol
Frondo	Frondoside A
HPLC	High Performance Liquid Chromatography
UV	Ultra violet
MeOH	Methanol
ACN	Acetonitrile
HM	Hypermatrix
BM	Big Monolayer
AFM	Atomic Force Microscopy
ITC	Isothermal Titration Calorimetry
LUV	Large Unilamellar Vesicles
DLS	Dynamic Light Scattering
ΔG	Free Gibbs energy (J/mol)
ΔH	Enthalpy (J/mol)
TΔS	Entropy (J/mol)
K	Binding constant (mM^{-1})
mAU	Milli absorbance units
Å	Ångström (=0.1nm)

1. Introduction

Chemical Defense Mechanisms in Nature

Some organisms can escape dangerous or unfavorable circumstances. Others can defend themselves with claws, teeth, or cunning and some can protect themselves by retreating into a shell or can avoid attack by blending into their surroundings. Many organisms that do not possess mobility, weapons, intelligence, structural defenses or crypsis utilize chemical means of defense against predators, pathogens and spatial competitors (Kubanek, 2009).

Generally speaking there are two mechanisms by which an organism can acquire chemical defensive compounds; either through endogenous means (products of the metabolism of the defended organism) or exogenous means (products of another organism)(Kubanek, 2009; Good heart *et al.*, 2016). In endogenous accumulation of chemical compounds, organisms synthesize toxins using their own metabolic pathways; alternatively in exogenous accumulation it is the diet that provides the toxin. This process is also known as sequestration (Fürstenberg-Hägg *et al.*, 2014). *De novo* bio-synthesis of toxin is common among plants to ward off herbivores and pathogens, for example the milky latex produced by plants of the Euphorbia genus (Wittstock and Gershenzon, 2002). Examples of sequestration can be found at all levels of the tree of life. The monarch butterfly represents a classic case of acquired defense, where caterpillars not only tolerate, but also sequester cardenolides from their milkweed host plants (*Asclepias spp.,* Apocynaceae) and transfer these toxins to the butterfly stage for their own defense against predators and parasites (Petschenka and Agrawal, 2015). Among other organisms, nudibranchs of the family Chromodorididae are known to sequester defensive terpenes extracted from their diet of sponges (Dewi *et al.*, 2016).

Living organisms produce thousands of different organic compounds of which many have no apparent function in the basic processes of growth and development, and have therefore been referred to as secondary metabolites (Berenbaum, 1995). They defend many species of plants, animals and microorganisms against predators, pathogens and competitors, and can also be involved in conveying messages to conspecifics and mutualists regarding the presence of food, mates and enemies (Gershenzon and Dudareva, 2007; Caulier *et al.*, 2013). It is believed that many of these defensive secondary metabolites are the consequence of the coevolution and adaptation of predator-prey interactions (Ferrari *et al.*, 2010).

These secondary metabolites whether sequestered or synthesized represent a wide range of chemical families from acids, small organic molecules or even proteins, and their ecological and biological activities are divers. These metabolites can be unpalatable or can injure, sicken or kill predators or pathogens (Kubanek, 2009). Overall, chemical defenses seem to be an ubiquitous strategy that enhances the fitness of organisms be it plants, microorganisms, or animals.

Marine chemical defense mechanisms

Typically, a single cm^3 of seawater contains 10^3 fungal cells, 10^6 bacteria, and 10^7 viruses, including pathogens that can cause widespread mortalities and microbes that initiate fouling of host surfaces (Kubanek *et al.*, 2003). The large biodiversity found in marine habitats is mirrored by an even larger molecular diversity of secondary metabolites synthesized in marine animals, plants and microbes (König *et al.*, 2005). Over 20,000 new compounds have been isolated from sponges, ascidians, soft corals, sea-weeds, marine microbes, and many other benthic and pelagic organisms, with more being discovered daily (Blunt *et al.*, 2015). This array of secondary metabolites, include terpenes (Ebel, 2010), steroids (Ivanchina *et al.*, 2013), polyketides (Lorente *et al.*, 2014), peptides (Kim and Wijesekara, 2009), alkaloids (Kuramoto *et al.*, 2004), porphyrins (He *et al.*, 2012), and many more (Table 1.1). Marine invertebrates, in particular have yielded a larger number of bioactive natural products than algae have, which is in sharp contrast to the terrestrial environment where plants (primary producers) are by far the richest source of secondary metabolites (Proksch, 1994).

However the natural function of many of these marine secondary metabolites remains unclear, although they have often been assumed to be part of defense mechanisms against consumers, competitors, fouling organisms, and pathogens (Hay, 1996). This suspected function is supported by a correlation observed between the absence of obvious physical defense mechanisms of an organism and the presence of unusual chemistry in its tissue (Pawlik, 1993).

In the marine world the most accomplished chemists, rich in secondary metabolites are soft bodied sessile invertebrates such as sponges, anthozoan corals, echinoderms, polchaetes, bryozoans, brachiopods, and tunicates, whereas mobile and armored species generally lack secondary metabolite diversity (Pawlik 1993; Berenbaum, 1995).

For instance, despite their simple morphology, cnidarians (the phylum that includes jellyfish and corals) are one of the oldest extant lineage of venomous animals and are capable of subduing or repelling prey and predator species with far more complex body structures (Goodheart *et al.*, 2016). Utilizing specialized penetrating nematocysts, cnidarians inject the “venom” that initiates toxic and immunological reactions in the targeted organism (Cuypers *et al.*, 2006). These venoms contain enzymes, potent pore forming toxins, and neurotoxins (Jouiaei *et al.*, 2015) and can induce local but also systemic responses in both vertebrates and invertebrates (Suput, 2009).

Table 1.1. A few examples of marine organisms that use natural chemical products (secondary metabolites) to defend themselves.

Organism	Taxon	Active substance	Action	Reference
Dendryphiella salina (Marine fungus)	Fungi	Terpenes	Cytotoxic	Ebel, 2010
Anthopleura elegantissim (Sea anemone)	Cnidaria	Polypeptides	neurotoxic and cardiotoxic	Bruhn *et al.*, 2000
Sarcophyton sp (Soft Coral)	Cnidaria	Hexadecyl palmitate	Antimicrobial	Dobrestrov *et al.*, 2015
Miamira magnifica (Nudibranch)	Mollusca	Oxy-polybrominated diphenyl ethers (O-PBDEs)		Dewi, 2016
Aplysina cauliformis (Sponge)	Porifera	Alkaloid	Inhibition of acetylcholinesterase	Loh and Pawlik 2014
Toxopneustes pileolus (Sea urchin)	Echinodermata	Lectin	Agglutinating activitiy	Nakagawa *et al.*, 2003
Holothuria forskali (Sea cucumber)	Echinodermata	Triterpene glycosides (Saponins)	Cytotoxic	Vandenspiegel *et al.*, 2000; Van Dyke *et al.*, 2011

Like nematocysts in cnidarians, many marine organisms have evolved a variety of specialized organs to deliver chemical signals, others localize them to the tissues most vulnerable or most accessible to enemies, or release them gradually as a cloud of repulsive chemistry (Kubanek, 2009).

Nudibranchs of the family Chromodorididae for example are known to sequester defensive terpenes from the sponges they feed on (Dewi *et al.*, 2016), in addition to chemical sequestration aeoloid nudibranchs have been documented to sequester the entire nematocyst structure from their prey. In both instances the materiel sequestered is stored in high concentrations in the fleshy dorsal organs called cerata (Obermann *et al.*, 2012). Chemical sequestration is widespread among animals, but the ability to sequester entire structures, such as organelles, appears to be rare. Nematocyst sequestration has evolved multiple times, and has been documented in Ctenophora, Acoelomorpha, Platyhelminthes, and Mollusca (Goodheart *et al.*, 2016).

A repulsive cloud of secondary metabolites is the type of delivery system involved in the antifouling nature of some marine natural products. In fact several marine natural products exhibit antifungal

and antibacterial properties in laboratory conditions (Pawlik 1993), unfortunately adequate methods for testing the antifouling role of these metabolites *in vivo* are lacking (Krug, 2006).

Another group of species rich in secondary metabolites, in the phylum Cnidaria are the Alcyonacea also known as soft corals, that contrary to scleractinian corals, do not produce an extensive calcium carbonate skeleton. The large, fleshy colonies rely on a vast array of defensive secondary metabolites. For example methanol: chloroform (1:1) extracts of some soft coral species have demonstrated antimicrobial activity due to the presence of a mixture of hexadecyl palmitate and hexadecyl stearate, which when pure inhibited the growth and attachment of marine biofouling bacteria. This suggest that soft corals have developed a chemical mechanism to combat microbial infections and inhibit bacterial fouling (Dobrestrov *et al.*, 2014). This could also be true for other slow moving or sessile marine invertebrates.

Defenses mechanisms in echinoderms

Echinoderms form a phylum of mostly benthic marine invertebrates, found in a continuous distribution from the intertidal zone to the deepest depths of the ocean. They are a sister group to the chordates and are basal deuterostomes (Bourlat *et al.*, 2006). Approximately 7,000 extant echinoderm species have been described, falling into five classes: Echinoidea (regular and irregular sea urchins), Holothuroidea (sea cucumbers), Asteroidea (sea stars or starfish), Crinoidea (sea lilies and feather stars) and Ophiuroidea (brittle stars and basket stars), as well as a number of extinct classes known only from the fossil records (Fig. 1.1.). Echinoderms feed in a variety of ways, some are suspension feeders (Crinoidea Ophiuroidea), some are scavengers of even predators (Asteroidea) and the majority of holothuroids are deposit feeders that actively contribute to the bioturbation of sedimentary organic matter and play an important role in the detritus food web by recycling the organic matter and oxygenating the sediment (Coulon and Jangoux, 1993; MacTavish *et al.*, 2012; Purcell *et al.*, 2016).

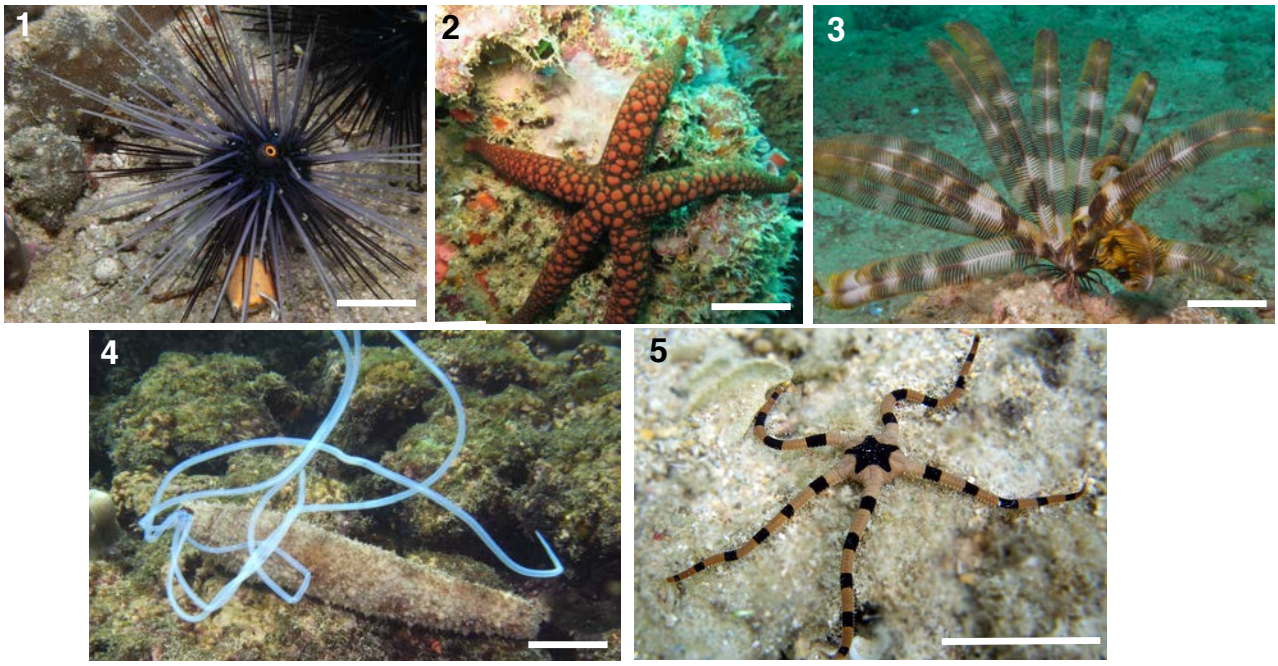

Figure 1.1. Photographs of the 5 classes of the phylum of echinoderms. 1. Echinoidea (sea urchins); 2. Asteroidea (starfish); 3. Crinoidea (sea lilies and feather stars); 4. Holothuroidea (sea cucumbers) expelling its Cuvier tubules; 5.Ophiuroidea (brittle stars). Scale bars represent 5 cm. Sources: Photographs 1, 3 and 4 from Michel Claereboudt, Photograph 2 from Emily Claereboudt and photograph 5 from www.amongthereef.com

Echinoidea have characteristic spines which play key functional roles. They protect the body from predators and water born particles, are involved in locomotion (acting as stilts in some taxa) and burrowing (in the so-called "irregular sea urchins") and are part of a photoreceptor system (Al-Wahaibi and Claereboudt, 2017). If for some species, for example *Paracentrotus lividus* (also known as the purple sea urchin) each fully grown spine is a single crystal of magnesium calcite (Moureaux *et al.*, 2010), for others, the spines of the *Diadema* genera are made of a spiral stack of triangular pieces (Coppard *et al.*, 2004). For some species this physical barrier is accompanied by venomous proteins with agglutinating properties. The venom is delivered either by a venomous membrane covering the tips of the spines, or via small structures known as pedicellariae that contain venom glands and fangs (Nakagawa *et al.*, 2003). Sea urchins also produce secondary metabolites called spinochromes, primarily known to be involved in pigmentation, but also have anti-microbial properties suggesting a role in defense against the external environment (Brasseur *et al.*, 2017).

In some starfish such as *Acanthaster planci*, the numerous spines of the aboral surface contains venomous cells that liberate a complex mixture of venom into possible predators (Lee *et al.*, 2014).

On the other hand, a common defensive practice in some starfish, crinoids and ophiuroids is autotomy which refers to the adaptive, and voluntary detachment of an arm or part of an arm. The detachment, and regeneration of a limb when under attack, allows the organism to make its escape, while the predator is distracted by the limb (Wilkie, 2001).

The typically large, often fleshy body of sea cucumbers lack external spines and have developed a unique system of defense mechanism. Within the class Holothuroidea many species of the Aspidochirotida order (deposit feeding sea cucumbers with spade like oral tentacles), but not all, possess a very specialized defensive system: the Cuvierian tubules (Fig. 1.1.3). When irritated, the animal curves its aboral end toward the irritating object and undergoes a general contraction that increases the hydrostatic pressure inside the general cavity of the animal. The Cuvierian tubules, together with some coelomic fluid, are then vigorously expelled. The tubules lengthen, instantly become sticky and rapidly immobilize the threatening organism (Vandenspiegel *et al.*, 2000; Flammang 2002). This effective physical defense is also coupled with a group of cytotoxic secondary metabolites called saponins concentrated in the tubules (Van Dyke *et al.*, 2011). Among echinoderms, only holothuroids and asteroids produce these saponins (Mackie *et al.*, 1976; Friess *et al.*, 2002).

There are numerous phylogenetic parallels in the biosynthesis of low molecular weight natural products between starfishes, sea cucumbers, and the other echinoderms that suggest a monophyletic origin of many biosynthesis pathways in echinoderms (Bondoc *et al.*, 2013). However, at the same time metabolites such as triterpene glycosides (saponins), some gangliosides, $\Delta^{9(11)}$ sterols, steroid oligo-glycosides are associated to distinct classes. Of particular interest among them as chemotaxonomic characters are triterpene glycosides from sea cucumbers, which have been used in a classification of Holothurioidea that mirrors the classic phylogeny of the class (Stonik, 1988; Kalinin *et al.*, 2005).

Saponins: a chemical defense system for many

Saponins form a large and diverse group of secondary metabolites produced by several terrestrial and marine organisms. These natural products are well documented in plants (Vincken *et al.*, 2007), but also occur in marine sponges (Kubanek *et al.*, 2002; Genta-Jouve *et al.*, 2015), starfish (Demeyer *et al.*, 2014; 2015), and sea cucumbers (Kalinin *et al.*, 2008; Bondoc *et al.*, 2013; Caulier *et al.*, 2011; 2016).

The term ‘saponin’ is derived from the Latin *sapo* (Engl.: soap) reflecting their ability to form stable soap-like foams in aqueous solutions. This characteristic is caused by the amphiphilic nature of saponins due to the covalent linkage of a lipophilic isoprenoidal-derived aglycone to a hydrophilic saccharide moiety (Augustin *et al.*, 2011).

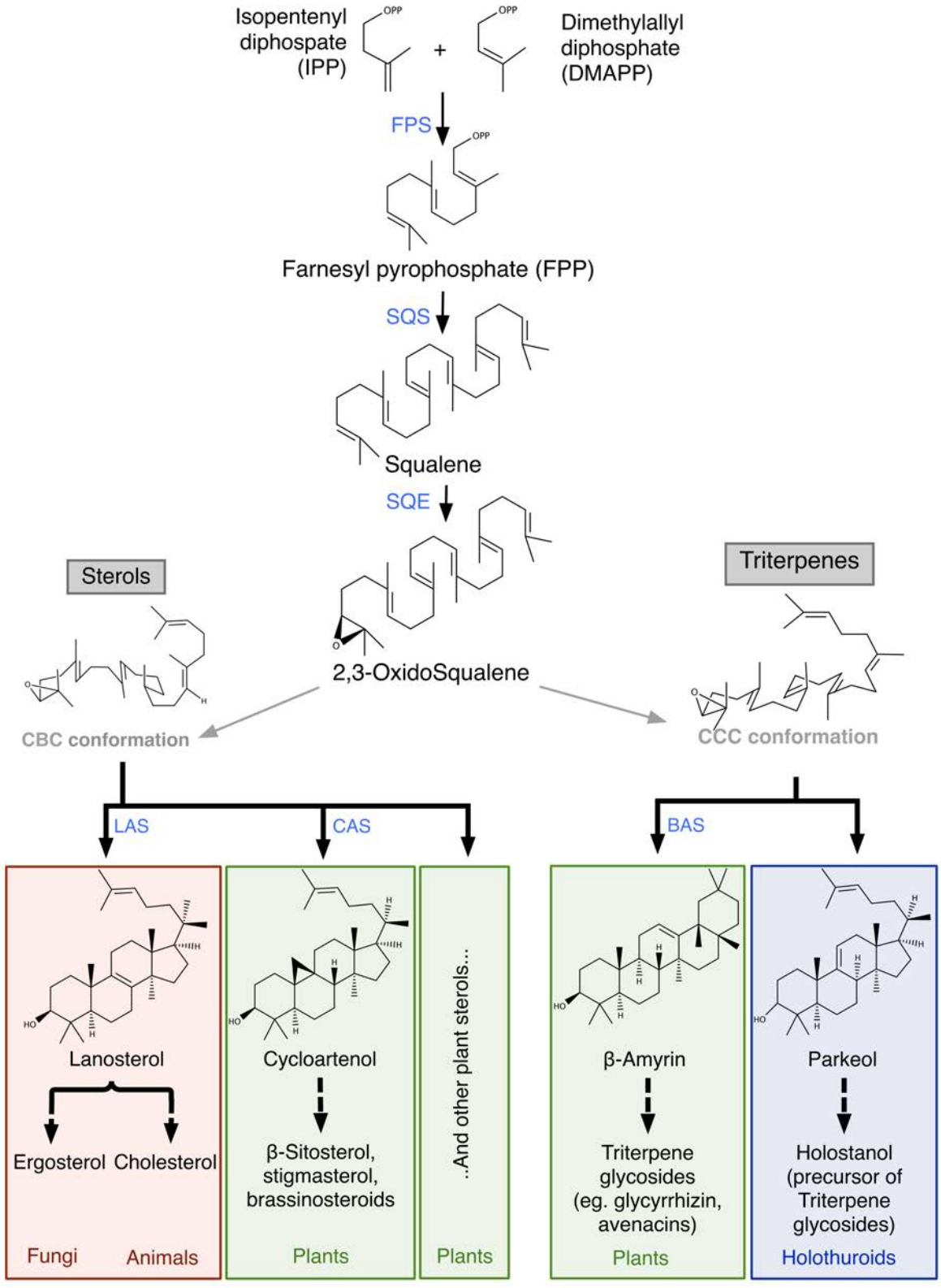

Figure 1.2. The proposed biosynthetic route of sterols and triterpenes in plants (adapted from Thimmappa *et al.*, 2014). Sterols and triterpenes are synthesized via the mevalonic acid (MVA) pathway. The enzymes that catalyze the various steps are indicated in Blue. Enzyme abbreviations: FPS, farnesyl pyrophosphate synthase; SQS, squalene synthase; SQE, squalene monooxygenase or epoxidase; SHC, squalene-hopene cyclase; LAS, lanosterol synthase; CAS, cycloartenol synthase; BAS, β-amyrin synthase. Other abbreviations: CBC, chair-boat-chair; CCC, chair-chair-chair.

Saponin structure and classification

Saponins are often subdivided into two main classes, the triterpenoid and the steroid saponins (Vincken *et al*., 2007), which are both derived from the linear 30 carbon atom containing precursor oxidosqualene (Moses *et al*., 2014). Both the triterpenoid and steroidal aglycone backbones are isoprenoids that are synthesized from isopentenyl pyrophosphate (IPP) units generated by the mevalonate (MVA) pathway (Moses *et al*., 2014) (Fig. 1.2). The 2,3-oxidosqualene is then cyclized by a variety of oxidosqualene cyclases (OSCs) to form a vast variety of polycyclic structures (Fig. 1.2). As such, nine main classes of triterpene backbones have been documented to be synthesized by plants (Vincken *et al*., 2007; Moses *et al*., 2014). In plants the aglycones can then be tailored with oxidoreductases, and a series of cytochrome P450-dependent monooxygenases (P450s) before being glycosylated with multiple sugar moieties (Friedman, 2006).

Holothuroid saponins

Historically it has been known that some holothurian species contain toxins. In the southern Pacific and Tokara Islands (islands of southern Japan), a peculiar fishing method using sea cucumbers is employed. The autochthones catch paralyzed fish after they throw extracts or fragments of sea cucumbers into tidal pools. This toxic effect has been attributed to the presence of saponins in the sea cucumber (Matranga and Muller, 2005).

Over 700 saponins have been described so far in holothuroidae (Bahrami *et al*., 2015). Holothuroid saponins are of the triterpenoid class. Similarly to plants, these marine saponins are synthesized from the precursor, squalene. In sponges and starfish, the squalene is cyclized into lanosterol which gives way to steroidal saponins (Fig. 1.2). However in holothroidae squalene is cyclized into parkeol, which is then rearranged to form the most abundant holothuroid aglycone, holostanol (Fig. 1.3). These two aglycone backbones differ due to the position of the double bond that is positioned between C8 and C9 in lanosterol (Fig. 1.2) and between C9 and C11 in parkeol (Fig. 1.3) (Ker *et al*., 1995). In sea cucumbers, the sugar residue has only one branch (Kalinin *et al*., 2005), whereas plant saponins may contain one, two or three saccharide chains, with a few having an acyl group bound to the sugar moiety (Bahrami *et al*., 2015). The oligosaccharide moiety of holothuroid saponins can contain up to six sugar units including mainly glucose, 3-O-methylglucose, quinovose and xylose which can be sulfated or non-sulfated (Caulier *et al*., 2016; Decroo, 2014).

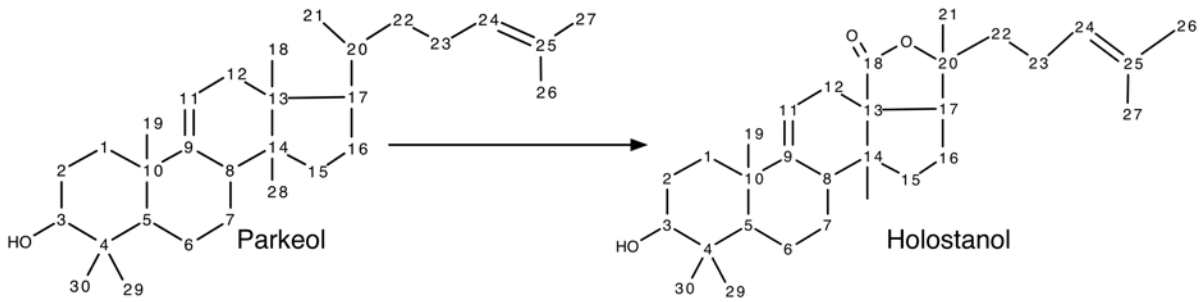

Figure 1.3. Parkeol rearranges to give Holostanol the most abundant aglycone precursor of Holothuroid triterpene saponins.

Saponin profiles differ in function of the species (Caulier *et al.*, 2011), of the body component (Kobayashi *et al.*, 1991; Van Dyck *et al.*, 2009, 2010), the sex (Decroo, 2014), and the maturity of the individual (Iyengar and Harvell, 2001), both qualitatively (different saponin mixtures) and quantitatively (different concentrations).

If saponins have been recovered from most tissues of sea cucumbers, their concentration seems to increase in Cuverian tubules (Van Dyck *et al.*, 2010). This localization of saponins in the Cuverian tubules is consistent with their cytotoxic effect on most organisms. They probably act as a chemical defense repelling predators (Kalinin *et al.*, 1996). In addition, Van Dyck *et al.* (2011) highlighted that some saponins could be specifically emitted by holothuroids in the surrounding seawater, potentially acting as chemical “aposematic” signals, deterring predators and settling larvae. All combined reports therefore suggests saponins have an important and complex ecological function, the most important being probably defense (Van Dyck *et al.*, 2011; Eeckhaut *et al.*, 2015; Bahrami *et al.*, 2016; Park *et al.*, 2014).

In addition to the toxic nature of saponins, some organisms including the Harlequin crab, *Lissocarcinus orbicularis*, are involved in a symbiotic relationship with sea cucumbers and uses these secondary metabolites: it has been shown that saponins act as kairomones recognized by these crabs, allowing them to locate their hosts (Caulier *et al.*, 2013). Additional functions of saponins are currently being explored including the possible role that saponins may play in intraspecific communication during gonad maturation and spawning (Watson *et al.*, 2003).

Triterpene glycosides also have some taxonomic specificity for different species and genera of sea cucumbers and even for taxa of supra-genus level (Bondoc *et al.*, 2013). The glycosides have quite complicated structures and may be distinguished by many independent characters: the type and number of monosaccharide units in the carbohydrate chain, the number and positions of sulfate groups attached to monosaccharide units, the position of double bond in the cyclic system of the aglycone, the number and position of double bonds in the side chain of the aglycone and the number and different position of hydroxy-, epoxy-, acetyl- and oxo- groups in the aglycone etc. (Kalinin *et al.*, 2005).

Biosynthesis of saponins

In general very little is known about the site, enzymes or biochemical pathways involved in saponin biosynthesis both in plants and marine invertebrates. The genes involved in the biosynthesis of both types of saponins (triterpenoid and steroid) in plants can however be grouped into four main categories based on their characteristic reactions. This includes the OSCs (oxidosqualene cyclases) that cyclizes squalene, P450s (P450-dependent monooxygenases) that modify the aglycone, UGTs (UDP-dependent glycosyltransferases) and other tailoring enzymes (mostly encoding transferases) (Moses *et al.*, 2014; Thimmappa *et al.*, 2014). Recently, numerous examples of gene clusters for the biosynthesis of different classes of specialized metabolites have been discovered in a variety of plant species, including clusters for saponin biosynthesis (Moses *et al.*, 2014). Although there is still a wide gap in our understanding of saponin biosynthesis in plants, recent molecular insights continue to be published. Saponin biosynthesis in echinoderms and more particularly in sea cucumbers remains more obscure, and research is outdated. Older research has identified that a “Cuvier gland” is the site of saponin biosynthesis (Kerr and Chen, 1995). However this gland has never previously been described in the anatomy of sea cucumbers. Perhaps the author intended to identify Cuverian tubules (defensive sticky filaments) as the site of the biosynthesis. If so, this would not be coherent with saponin production in holothuroid species lacking Cuverian tubules. A tentative relationship between the biosynthesis of rare holothuroid sterols, triterpene saponin, and the metabolism of dietary cholesterol has been briefly explored, but the research is outdated and merits re-investigation (Mackie *et al.*, 1976; Stonik *et al.*, 1998; 1999). Further research therefore needs to be carried out on the biosynthesis of saponins in these marine invertebrates.

Holothuria scabra: a sustainable source of saponins

For centuries, sea cucumbers have been consumed by Chinese people as a food delicacy and also have been used in traditional Chinese and Malaysian medicine. Therefore, processed sea cucumbers, also called trepangs or Bêche-de-mer, have a high commercial value on Chinese markets (Conand, 2004). Although around 60 holothurian species are fished commercially around the world, only a few yield first grade trepang. The sandfish *H. scabra* is one of these species and can fetch between around 40 and 85 € per kg of dry weight (Hamel *et al.*, 2001).

Figure 1.4. Sea cucumber farm for *H. scabra* in southwest Madagascar. *Source:* BlueVenture NGO

Indian Ocean Trepang (IOT) is a sea cucumber aquaculture farm industry based in the southwest of Madagascar, Toliara, which produces and prepares trepang from the most valuable local exploited sea cucumber species, the sandfish *Holothuria scabra* (Jaeger, 1833) (Caulier *et al.*, 2013). Trepang processing involves sea cucumber evisceration, salting, cooking for several hours in boiling water, and finally drying into trepang (Conand, 1979). The viscera of the animals are by-products that are currently discarded during the processing of the sea cucumber into trepang, and are therefore an ideal sustainable source of saponins (Fig. 1.4). The valorization of this by-product of the sustainable aquaculture of sea cucumbers could potentially be very profitable for the industry. Although a few patents exist for the extraction and purification of holothuroid saponins (US Patent 7,163,720 B1; Avilov *et al.*, 2007), the industrialization and profitability of this way of valorizing this by-product has not been investigated.

The saponin profile of the discarded digestive tubes of *H. scabra* has not yet been described in the literature, however six saponins have been described in the body wall of the species (Fig. 1.5) (Caulier *et al.*, 2013). Scabraside B and Scabraside A are the most abundant saponins found in the body wall of *H. scabra* (Han *et al.*, 2009), and are therefore the most interesting to isolate and purify for commercialization.

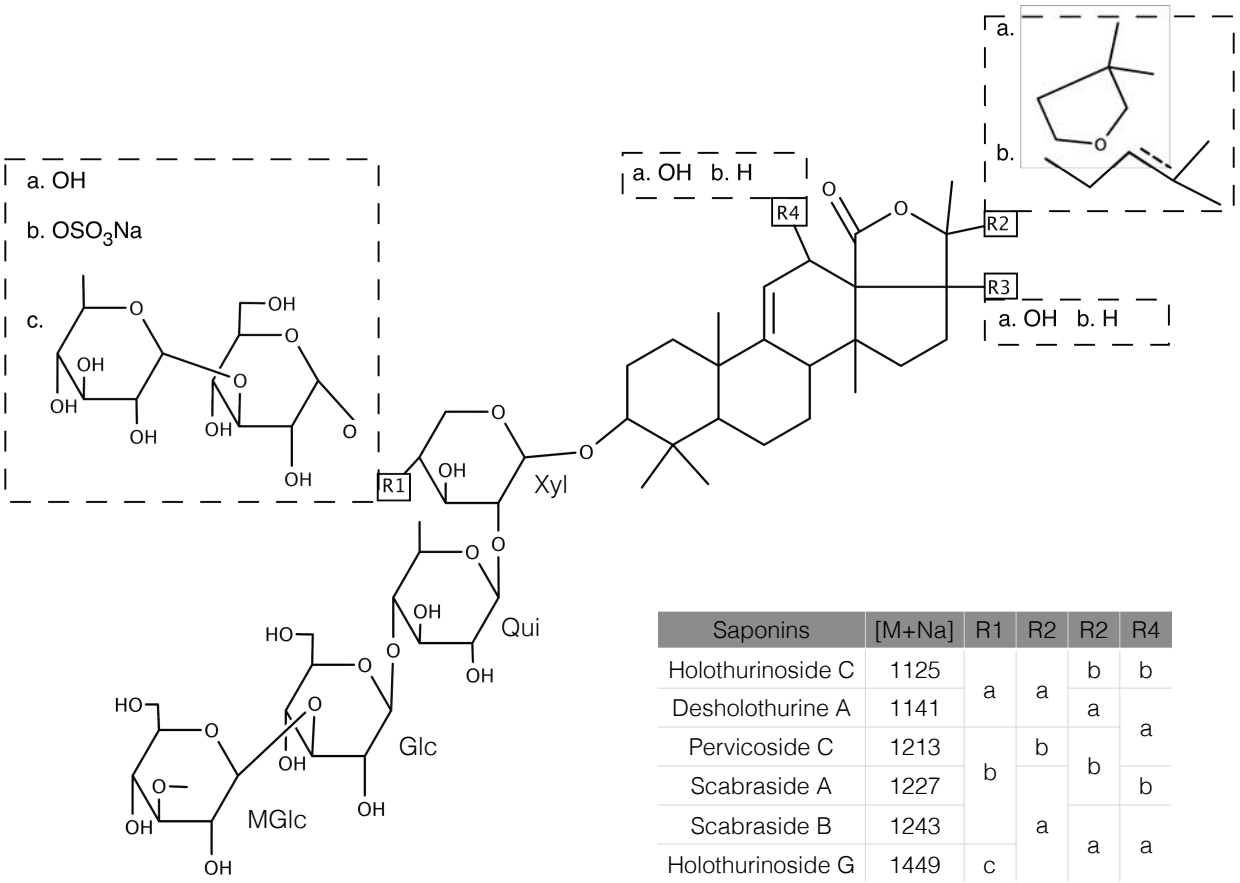

Saponins	[M+Na]	R1	R2	R2	R4
Holothurinoside C	1125	a	a	b	b
Desholothurine A	1141			a	a
Pervicoside C	1213	b	b	b	
Scabraside A	1227		a		b
Scabraside B	1243			a	a
Holothurinoside G	1449	c			

Figure 1.5. Structural diversity of saponins in the body wall off *Holothuria scabra.* Scheme adapted from Caulier *et al.* (2013).The sugar chain on the C3 of the aglycone is composed of β-D-xylose, β-D-quinovose, β-D-glucose, and 3-O-methylglucose.

Biological activities of saponins

Saponins are characterized by a large chemical diversity and a wide variety of pharmacological activities. Several patents have been filed throughout the world in relation to triterpene glycosides and includes various industrial or semi-industrial extraction methods, isolation of individual compounds, quantification and modification using isotopes for pharmacokinetic studies (Yu *et al.*, 2012), inclusion of saponins in functional foods (Bordbar *et al.*, 2011) and other products (US Patent Nº5,166,139, Bombardelli *et al.*, 1992) as well as in disease prophylaxis (de Groot and Müller-Goymann, 2016; Rajput *et al.*, 2007; Fernández-Tejada *et al.*, 2014), immunostimulation (Aminin *et al.*, 2016) and even possible cancer treatments (Aminin, Menchinskaya *et al,*. 2015). Historically, many pharmaceutical drugs have originated from traditional medicines used for centuries by indigenous populations (Werner and Muller, 2005). For saponins, recent patents, articles in peer-reviewed journals and numerous active compound discoveries support a similar development model.

Among the 700 saponins isolated from many species of sea cucumbers (Bahrami and Franco, 2015), significant activities have been reported including but not limited to: hemolytic (Baumann *et*

al., 2000; Kalinin *et al*., 1996), antibacterial (Mashjoor and Yousefzadi 2016), antifungal (Shimada, 1969; Yuan, *et al.,* 2008), cytotoxic (Althunibat *et al*., 2013; Tiane *et al.,* 2013), ichthyotoxic (Eeckhaut *et al*., 2015) and anti-tumoral (Moghadam *et al*., 2016) activities. Even as early as 1969, Shimada reported the antifungal activity of the holothurian saponin, holotoxin, and patented the toxin as a cure for athlete's foot disease and commercialized it (Matranga and Muller, 2005). More recent research has demonstrated that *H.scabra* extracts also exhibits anti-parkinsons activity in the model worm *Caenorhabditis elegan* (Chalorak *et al*., 2017).

Paradoxically, the biological roles of saponins in marine animals are still very speculative (Bordbar *et al*., 2011) as are the molecular mechanisms behind these biological activities. Most of the activities of these saponins result from their surface-active properties and interactions with cellular membranes (Vo *et al*., 2017). The ability of the glycosides to form complexes with 5,6-unsaturated sterols of target cell membranes is thought to determine their biological activity including ichthyotoxic action that may protect sea cucumbers against fish predation (Popov 1983; 2003; Eeckhaut *et al*., 2015; Brasseur *et al*., 2016). This complexing reaction leads to the formation of pores, permeabilization of cells and in the case of red blood cells the subsequent loss of haemoglobin in the extracellular medium (Lorent *et al*., 2014b; Eeckhaut *et al*., 2015). Another biological role of the glycosides as reproduction regulators is caused by their ability to increase microviscosity of the oocyte membranes inhibiting Ca^{2+} transport into the cells and thus early oocyte maturation with subsequent synchronization of sea cucumber oogenesis (Kalinin *et al*., 2005). Winter (Winter, 1994) proposed a different mechanism in which the interaction of saponins with the water channel aquaporin results in an increase of the water transport inside the cells inducing the haemolysis of erythrocytes (Gauthier *et al*., 2009). It is evident that although the cytotoxic nature of saponins is well documented, the mechanisms behind their various biological activities remain poorly understood.

Lipid plasma membranes

Throughout the biological world, a 3 nm hydrophobic film is responsible for delimiting individual cells from the environment. Biochemical and biophysical findings have provided detailed models of the composition and structure of plasma membranes, which includes levels of dynamic organization both across the lipid bilayer (lipid asymmetry) and in the lateral dimension (lipid domains) of membranes (van Meer *et al*., 2008; DePierre and Karnovsky, 1973) (Fig 1.6).

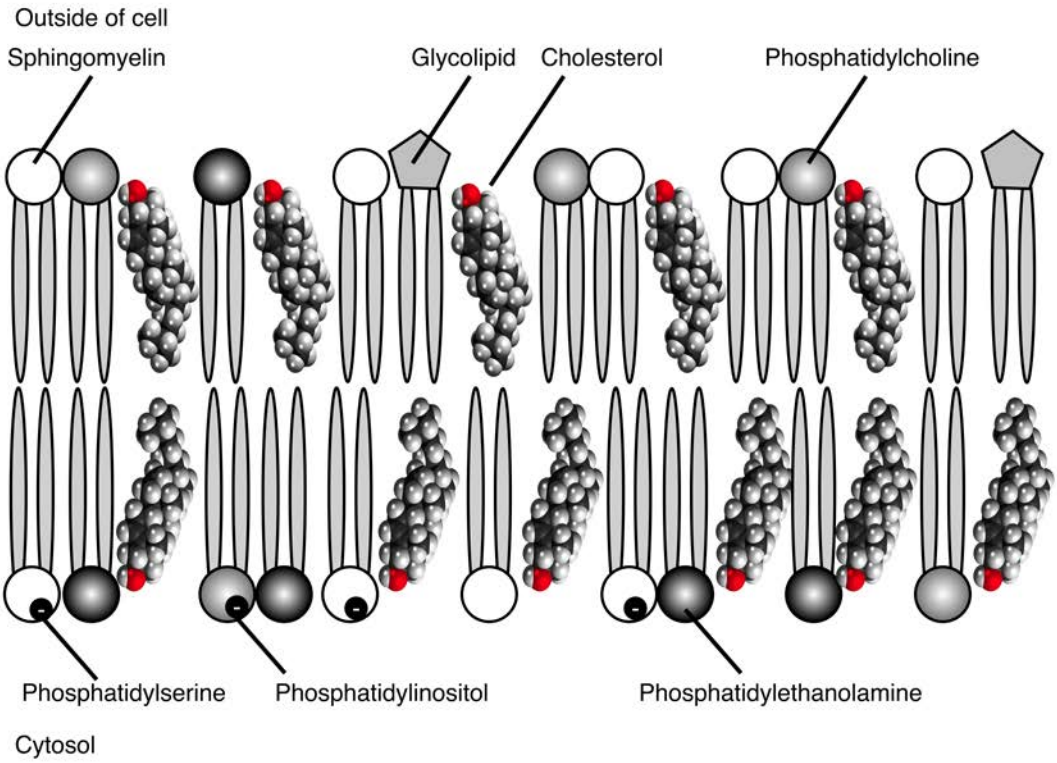

Figure 1.6. Scheme of the phospholipid plasma membrane bilayer, illustrating asymmetric distribution of phospholipids.

Plasma membranes are composed by three main classes of lipids: glycerolipids (mainly phospholipids—PL), sphingolipids and sterols. However, between species or cell types within a species, the lipid composition of membrane can show a high degree of diversity (Deleu *et al*., 2014) (Table 1.2).

Table 1.2. Lipid composition in molar % of different cell membranes in eukaryotic and prokaryotic organisms (adapted from Deleu *et al.*, 2014)

Lipids	Eucaryote cells			Procaryotic cells	
	Human erythrocyte	*S. cereviciae*	*A. thaliana* leaves	*S. aureus* Gram+	*E. coli* Gram -
PC	16	25	17		
PE	15	10	18		82
PE	7	3	3		Traces
PS			4	58	6
CL		~2		42	12
PI	0.5	9	5		
PA	1	5			
SL	14(SM)	10-20	7		
Sterol	46 (Cholesterol)	30-40 (Ergosterol)	46 (Sitosterol)		
Others	0.5				

PC: phosphatidylcholine, PE: phosphatidylethanolamine, PS: phosphatidylserine, PG: phosphatidylglycerol, CL: cardiolipin, PI: phosphatidylinositol, PA: Phosphatidic acid, SL: sphingolipid, SM: sphingomyelin

Phospholipids

The major structural lipids in eukaryotic membranes are glycerophospholipids: such as phosphatidylcholine (PC), phosphatidylethanolamine (PE), phosphatidylserine (PS), and phosphatidylinositol (PI). Their hydrophobic portion is a diacylglycerol (DAG), which contains saturated or cis-unsaturated fatty acyl chains of varying lengths. PC accounts for >50% of the phospholipids in most eukaryotic membranes (Deleu *et al.*, 2014). Phospholipids self-organize spontaneously as a planar bilayer in which each PC has a nearly cylindrical molecular geometry, with the lipidic tails facing each other towards the middle of the membrane and the polar headgroups interfacing with the aqueous phase (Fig.1.6) (Risselada *et al.*, 2008). Whereas all lipids are symmetrically distributed between the two leaflets of the endoplasmic reticulum (ER) membrane bilayer, the Golgi, plasma and endosomal membranes display an asymmetric lipid distribution with sphingomyelin (SM) and glycosphingolipid (GSLs) on the non-cytosolic (lumenal side), with PS and PE enriched in the cytosolic leaflet (Fig.1.6) (van Meer *et al.*, 2008).

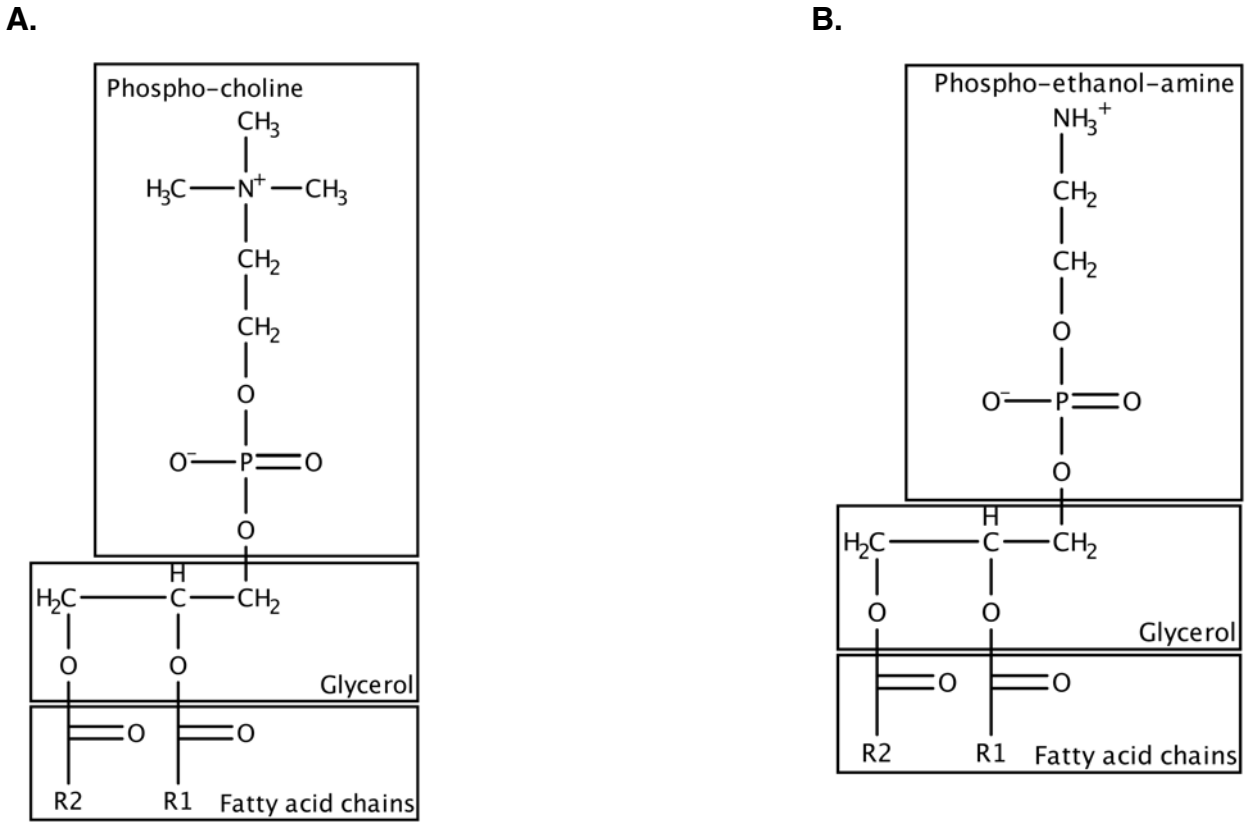

Figure 1.7. Structure of the major phospholipid species in both sea cucumbers and fish. **A**. Phosphatidyl choline composed of a polar phosphocholin group on the glycerol backbone that also bonds with apolar fatty acids that can vary in composition. **B**. phosphatidyl ethanolamine composed of a polar phospho-ethanol-amin group on a glycerol back bone with a polar fatty acid that can vary in composition.

The general composition of phospholipids in sea cucumber and fish appear similar, with the main type of polar heads being PC and PE (Lou *et al*., 2012; Thomas and Patton, 1971) (Fig. 1.7, Table 1.3).

The physical properties of the plasma membrane are determined by its composition of individual phospholipids and therefore by the fatty acids (FA) composing the phospholipids. The degree of unsaturation of the FAs is important in determining the fluidity of the membrane and in providing the correct environment for membrane functions (Dufourc, 2008). In fishes and other poikilotherms the degree of unsaturation of membrane fatty acids is also important in the process of adaptation to different environmental temperatures (Bell *et al*., 1986).

Table 1.3. Composition (%) of the phospholipid lipid fraction of sea cucumber body wall and fish gills (Lou *et al*., 2012; Thomas and Patton, 1971) .

		Sea cucumber	Fish
		Apostichopus japonicus	*Paralabrax maculatofasciatus*
PC	Phosphatidyl choline	58.9	61.8
PE	Phosphatidyl ethanolamine	24.8	17.6
SM	Sphingomyelin	2.1	6.4
PS	Phosphatidyl serine	1.7	9.7
PI	Phosphatidyl Inositol	4.0	5.7
DPG	Diphosphatidyl glycerol	NA	trace
LPC	Lysophosphatidyl choline	NA	NA

Sterols

Sterols are another crucial component of plasma membranes. Sterols are critical for the formation of liquid-ordered membrane states (lipid “rafts”) that play an important role in fundamental biological processes such as signal transduction, cellular sorting, cytoskeleton reorganization, asymmetric growth, and infectious diseases (Deleu *et al*., 2014). According to a recent definition, rafts are small (<200 nm) heterogeneous, highly dynamic, sterol and sphingolipid enriched domains that compartmentalize cellular processes (Risselada and Marine, 2008). Sterols have been proposed as key molecules to maintain membranes in a state of fluidity adequate for function (Dufourc, 2008). While cholesterol (Fig. 1.8 A) is the major sterol of vertebrates, ergosterol plays a key role in fungi, and plants usually possess more complex sterol compositions (Cacas *et al*., 2016).

In mammals the plasma membrane of lung cells have a phospholipid:cholesterol (P:C) ratio of around 3:1 whereas in fish gills the P:C ratio is of 2:1 (Zabelinskii *et al.,* 1995). Fish gills are characterized by an expansive epithelial surface in direct contact with the external environment thus being critical to gas and water exchange. Cholesterol increases the order in lipid bilayers and therefore reduces the transmembrane permeability of water and other small non-electrolytes (Robertson and Hazel, 2008). The elevated cholesterol content in plasma membranes isolated from gills as opposed to other tissues (kidney and liver) (Robertson and Hazel, 2008) suggests that cholesterol appears to provide an advantageous structural mechanism to limit passive water permeability in gill barrier membranes.

However, the composition and functional roles of sterols in marine invertebrate plasma membranes remain obscure. Ever since earlier studies on echinoderm sterols, the most striking feature of the phylum has been the dichotomy between the crinoids, ophiuroids and echinoids which contain Δ^5-sterols (such as cholesterol) like most animals, and the holothuroids and asteroids which contain

majoritarily Δ^7-sterols (Scheuer, 1978). The same dichotomy also appears in the production of saponins, as only the class of holothuroids and asteroids synthesis saponins.

Unfortunately the quantification of the composition of plasma membrane of holothuroids remains unknown. A few studies have investigated the free sterol composition of these organisms (Stonik *et al.*, 1998), revealing a complex diversity of new and rare sterols (Brasseur *et al.*, 2016) compared to most animals. The relative abundance of Δ^7:$\Delta^{9(11)}$:Δ^0:Δ^5 compounds was found to be of ≈4:2:1.5:1. The most abundant Δ7 sterol being 5α-Cholest-7-en-3β-ol (Fig. 1.8 B), at approximately 15% of the free sterol fraction of the body wall extract of *H. scabra*, followed by the $\Delta^{9(11)}$ sterol 4α,14α-dimethyl-5α-cholest-9(11)-en-3β-ol at 13.4% (Fig. 1.8 C) (Stonik *et al.*,1998).

Saponins and lipid membranes

Many sea cucumbers belonging to the family Holothuriidae are more toxic than other species of this class due to a higher content of toxic triterpene glycosides (Elyakov *et al.*, 1973). The toxic effects of these glycosides are thought to be connected to the formation of pores in the cellular membranes as a result of them complexing with membrane Δ^5-sterols (Fig. 1.10).

This complexing reaction starts when saponins integrate into the membrane with their hydrophobic part (aglycone). Within the membrane they form complexes with sterols, which subsequently, driven by interactions of their extra-membranous orientated saccharide residues, accumulate into plaques (Augustin *et al.*, 2011). Sterical interference of these saccharide moieties causes membrane curvature subsequently leading to pore formation (Fig 1.9 A) in the membrane (Armah *et al.*, 1999) or hemitubular protuberances resulting in sterol extraction via vesiculation (Fig. 1.9 B)(Keukens *et al.*, 1995). Alternatively, after membrane integration saponins may migrate towards sphingolipid/ sterol enriched membrane domains (Fig. 1.9 C) prior to complex formation with the incorporated sterols, thereby interfering with specific domain functionalities (Lin and Wang, 2010). Similarly to (Fig 1.9 B), accumulation of saponins in confined membrane domains has further been suggested to cause deconstructive membrane curvature in a dose-dependent manner (Augustin *et al.*, 2011).

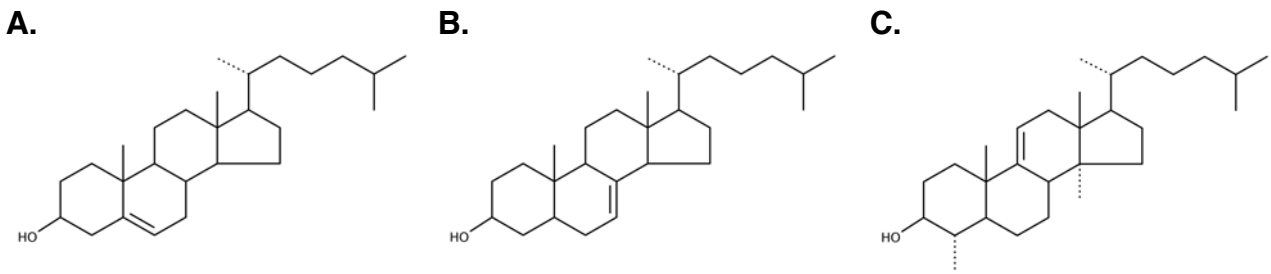

Figure 1.8. A. Structure of cholesterol, the primary sterol present in fish gills. **B.** 5α-Cholest-7-en-3β-ol, the most abundant free sterol of *H. scabra* **C.** 4α,14α-dimethyl-5α-cholest-9(11)-en-3β-ol, the second most abundant free sterol in *H. scabra*. (Stonik *et al.*, 1998)

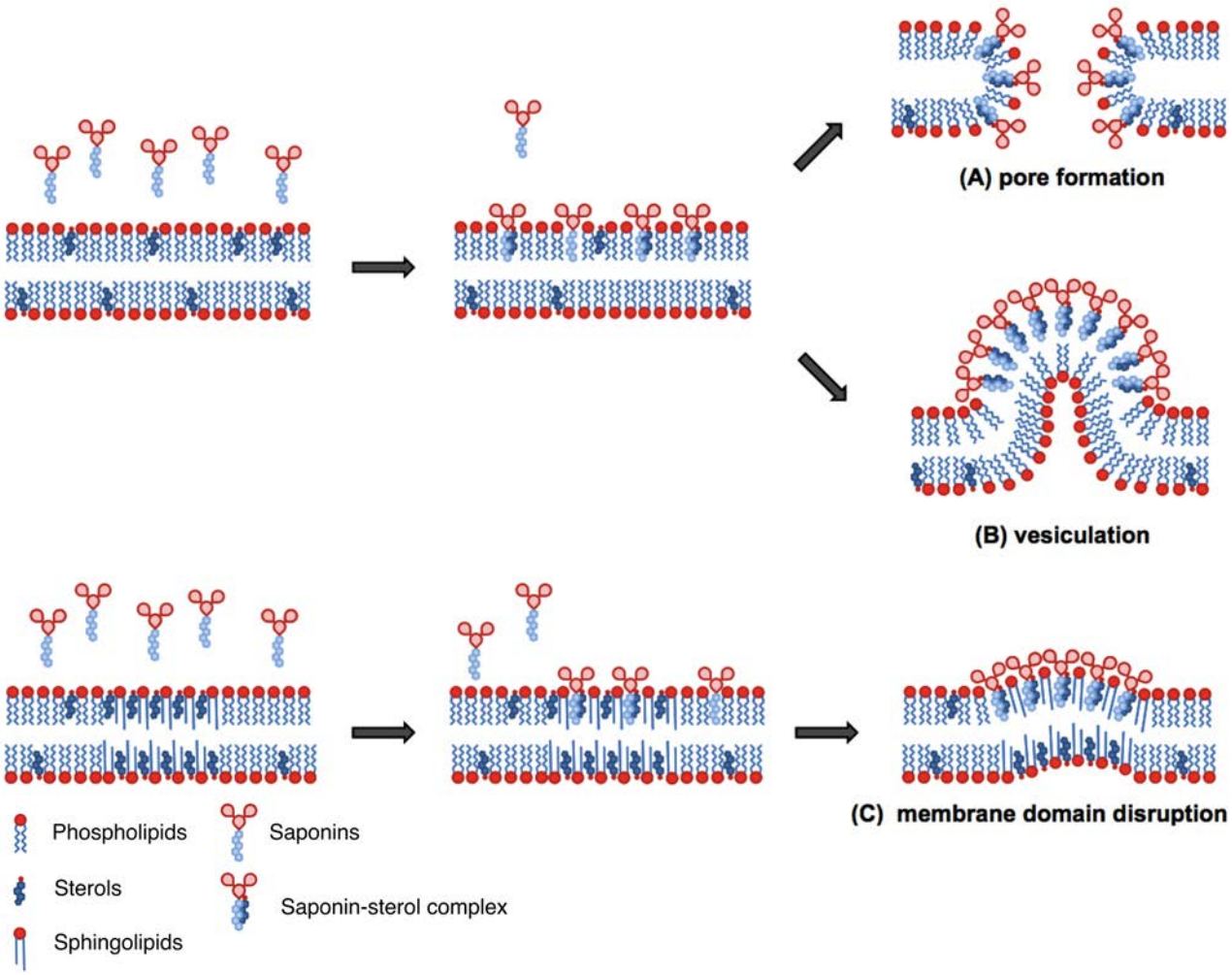

Figure 1.9. Schematic models of the molecular mechanisms of plant saponins activities towards membranes for **A.** Pore formation, **B.** Vesiculation and **C.** Domaine disruption (Augustin *et al.*, 2011).

The observation of pore-like structures and holes in electron microscopy images of membranes and cells treated with saponins (Baumann *et al.*, 2000; Seeman *et al.*, 1973; Augustin *et al.*, 2011) supports the concept of pore formation.

Although interference with the integrity of biological membranes is probably the most abundant effect of saponins, their activities are not limited to this type of action, and not all saponins show significant hemolytic activity (e.g. Chwalek *et al.*, 2006; Gauthier *et al.*, 2009; Nakumura *et al.*, 1979). Several structure–activity relation studies further emphasized that the ability to cause hemolysis often does not correlate with other known activities of saponins such as their antifungal and cytotoxic properties or their applicability as adjuvants (Gauthier *et al.*, 2009; Chwalek *et al.*, 2006; Augustin *et al.*, 2011). Induction of cytotoxicity may in some cases also involve disruption of lipid rafts (Xu *et al.*, 2009). In addition, some saponins have been shown to influence the properties of different types of membrane proteins such as Ca^{2+} channels and Na^{+}–K^{+} ATPases (Chen *et al.*, 2008). However, it is not yet clear, whether these effects are caused by agonistic or antagonistic binding to effector sites and changes in protein topology or as a result from changes in fluidity of the

surrounding membrane layer (Augustin *et al*., 2011). Another intriguing mode of action for some saponins is the ability to bind to glucocorticoid receptors. Glucocorticoids represent a class of steroidal hormones known to be involved in the regulation of a large variety of physiological processes. In mammals, they play an important role in regulation of development, metabolism, neurobiology and apoptosis, etc. (Yudt and Cidlowski, 2002). Due to the structural resemblance of saponin aglycones and steroids, it is therefore not surprising that several pharmacological activities of saponins such as anti-inflammatory (Giner *et al*., 2000) and neuroprotective (Zhang *et al*., 2008) effects as well as induction of adipogenesis (Niu *et al*., 2009) or apoptosis (Jia *et al.,* 2004), are linked to interaction with receptors of glucocorticoid hormones.

There is therefore a lot of leeway for new research into saponins and their functional roles, their biological activities, and the mechanisms behind these.

Sea cucumbers and saponin toxicity

Animals that chemically defend themselves from predation must possess adaptations to circumvent autotoxicity (*i.e*., self-intoxication). Some of these adaptations include, compartmentalization of defensive compounds into specialized structures (*e.g*., glands, vacuoles), modifying or metabolizing defenses into a less toxic form (for storage and/or transport; *e.g*., conversion of pyrrolizidine alkaloids to N-oxides), and molecular changes to receptor or ionchannel sites to prevent substrate-active site bonding (Saporito, 2011).

Older research has attributed sea cucumber immunity to the cytotoxic saponins they produce, to a fundamental difference in sterol composition. By studying the changes in liposomal permeability, with different sterol compositions (including holothuroid sterols) and in the presences of holothuroid saponin, Popov *et al*. (1983), described a difference in membrane activity in function of the sterol composition. The membrane activity decreased in the following order: Cholesterol, total fraction of Δ^5 sterol, total fraction of Δ^7-sterols, Δ^7-sterol xylosides and Δ^5-sterol sulphates. Twenty years later Popov further investigated the stabilizing ability of various holothuroid sterols on PC liposomes as well as the permeability of these sterol infused liposomes in the presence of the holothuroid saponin Cucumaraoside G1 (a strong membrane-lytic holothuroid saponin). The obtained data confirmed the “sterol hypothesis” of the mechanism of resistance of holothuriae to their own glycosides (Popov *et al*., 2003). The saponin lost its ability to permeabilize the liposomes infused with holothuroid sterols. He hypothesized that perhaps the evolutionary replacement of Δ^5-sterols with 5α-Cholest-7-en-3β-ol and 4α,14α-dimethyl-5α-cholest-9(11)-en-3β-ol**,** or other unusual sterols in sea cucumbers, mitigates the lytic action of the saponins they produce (Popov *et al*.,1983). It may also be suggested that a high percentage of toxic saponin in *Holothuria spp.* influences steroidogenesis and stimulates the *de novo* biosynthesis of some unusual sterols.

Objectives and strategy of this thesis

Saponins are a well known and divers class of secondary metabolites in plants and some marine invertebrates. They are amphiphilic molecules composed of a hydrophilic sugar moiety, and a hydrophobic steroid-like moiety known as the aglycone. Saponins are studied for their pharmacological properties such as their antifungal, antimicrobial, and antitumoral activity.

These biological activities are thought to be due to the cytotoxic activity of saponins. The standing view is that saponin interact with cholesterol in plasma membranes, and cause membrane disruption and eventually the formation of pores. Although the permeabilization activity of saponin is well observed, the mechanisms involved remain somewhat obscure. This cytotoxic activity is however a drawback in the development of saponin as a potential pharmaceutical drug.

Holothuroids, or sea cucumbers, produce saponins. It is believed that these invertebrates have evolved saponins as a chemical means of defense against predators, pathogens and spatial competitors. They are immune to the cytotoxic nature of the saponins they produce. This immunity is extremely poorly understood. The standing hypothesis, based purely on observation, is that rare Δ^{7} and $\Delta^{9(11)}$ sterols found in sea cucumbers, that replace cholesterol, mitigate the lytic activity of saponins, however, the molecular mechanism remain obscure.

The complexity of biological plasma membranes makes understanding the biophysical interactions of saponin on ‘real’ plasma membranes very difficult. Therefore, for the purpose of this study, simplified artificial membrane systems, which mimic the natural bilayer lipid membrane, have been designed to mimic both holothuroid plasma membranes, and fish membranes.

The aim of this study was therefore to elucidate the mechanisms behind the immunity of holothuroid to the cytotoxic saponins they produce but also to continue describing on a molecular level the interactions that occur between model plasma membranes and saponins.

This investigation was conducted using complementary biophysical tools, using both *in silico* approaches and an *in vitro* technique.

2. Methodology

Extraction and characterization of *H.scabra* saponins

Sample preparation

Sun dried digestive tubes of *Holothuria scabra* previously collected in Toliara, Madagascar were cut into small pieces. The dry samples were then ground in a grinder (IKA® A11) to obtain a fine powder. Approximately 10 g of the powder was then suspended into 30-40 mL of methanol (70 %), and agitated for 12 hours (overnight). The supernatant was then recovered after centrifugation at 3500 g for 12 minutes.

Saponin extraction

The methanol extracts then underwent a series of liquid/liquid extractions.

All extractions were conducted at a volume:volume ratio in 50 mL separatory funnels. Three non-miscible solvents with increasing polarity were used in succession: n-hexane, dichloromethane, and chloroform. After each extraction the methanol fraction was kept, and the the organic solvent pooled. The sugar moiety of saponins render the molecule more soluble in polar solvents such as methanol, rather than in apolar organic solvents such as n-hexane, dichloromethane and chloroform. However because of their amphiphilic nature the molecules can also be found at the interface, with the apolar fragment of the molecule in the apolar solvent and the polar fragment of the molecule in the polar solvent. It was also therefore important to collect the separation interface when conducting the liquid/liquid extractions. The methanol fraction recuperated after each L/L extraction, corresponded to the inferior fraction for the n-hexane extraction, and the superior fraction for the dicholoromethane and chloroform extraction. These extractions eliminate a maximum of lipophilic components of the holothuroid tissue from the saponins.

After the last liquid/liquid extraction the methanol was evaporated using a rotary evaporator (Heidolph-Laborota 4001) and the dry matter dissolved in 30 mL of ultra pure Milli-Q water.

The saponin rich solution then underwent an isobutanol liquid/liquid (volume:volume) extraction in a 50 mL separatory funnel. This step allows for salts and other water soluble interfering compounds to be removed from the extract. The salts remain in the aqueous fraction, whilst saponins pass into the isobutanol fraction. The inferior aqueous fraction was thrown away and the lighter isobutanol fraction was re-washed a second time with ultra pure Milli-Q water. The isobutanol fraction was then recuperated and evaporated using a rotatory evaporator. The dry matter was re-dissolved in 5 mL of methanol and transferred into 5 Eppendorfs. The concentrated content was then dried using a centrifugal evaporator for 2 hours. The pellet was re-dissolved in 200 µL of water under sonication for 3 minutes , the volumes were pooled into a single Eppendorf and evaporated using the

centrifugal evaporator. The dry mass of the raw saponin mixture was then recorded. The dry samples were conserved in a freezer (-20ºC). Before analysis the dry concentrated saponin samples were re-dissolved in ultra pure Milli-Q water.

Saponin detection

Mass spectrometry was carried out with a Matrix Assisted Lazer Desorption Ionization (MALDI) ion source and Time of Flight (ToF) detection system. This allowed for the detection of saponins and to deduce the structure of the saponins present via known m/Z peaks corresponding to characteristic fragments (Decroo, 2014).

Saponin contents were analyzed on a Water QToF Premier mass spectrometer using MALDI source (MS and MS/MS) in the positive ion mode. The MALDI source consisted of a nitrogen laser operating at 337 nm with a maximum output of 500 mW delivered to the sample in 4ns pulses at 20 Hz repeating rate. The matrix was composed of 1 mL of a 100 mg/mL solution of 2.5-dihydroxybenzoic acid (DHB) in water/acetonitrile (v/v) with 20 µL of N, N-dimethylaniline (DMA). A matrix droplet of 1 µL was spotted on a stainless steel target and air-dried followed by 1 µL of the sample solution. For the single-stage MALDI-MS spectra, the quadrupole (rf-only mode) was set to pass ions between m/z 500 and 2000 and all ions were transmitted into the pusher region of the Time-of-Flight analyzer where they were mass-analyzed with a 1 s integration time. The mass of all the ions was finally measured with the oa-ToF analyzer. Time-of-Flight mass analyses were performed in the reflectron mode at a resolution of about 10 000 (at m/z 1000).

Purification of Scabraside B

Preparative HPLC

A preparative HPLC (Puriflash 4250-250 Interchim) coupled with a UV detector set to 210 nm and 217 nm was used. Separation of the raw extract was conducted on a C18 (Interchim: Uptishpere® Strategy™ C18-2) apolar column with a stationary phase of 15 µm silica particles, in a 250 x 21.2 mm column. A 2 mL sample injection was followed by an isocratic elution of 30% acetonitrile, 70% water (1% Formic acid) with a flow rate of 20 mL/min for 10 minutes, and then the column was washed with 100% ACN. Chromatogram peaks were collected, evaporated, and re-dissolved in 1 mL of water. The fractions were then analyzed by mass spectrometry (as described earlier).

Analytical HPLC - Round 1

The fractions containing saponins (according to the mass spectrometry) from the preparative HPLC were further fractionated by analytical HPLC. An Agilent 1200 series HPLC coupled with a Agilent multi-wavelength UV detector series 1200 set to 210 and 217 nm was used. This HPLC was also equipped with an automatic fraction collector.

Based on the purification techniques used by Han *et al.* (2009) and Wang *et al.* (2014) a 4.6 x 150 mm Zorbax 300SB C18 (3.5 µm) column was used. An injection volume of 20 μL and an elution gradient program (45%-100% MeOH in 10 minutes) was used with a flow rate of 1ml/min and the maximum pressure set to 350 bars. The automatic collector was programmed to detect and collect peaks at predefined times.

Analytical HPLC Round 2

The same Agilent 1200 series HPLC was used for the further fractionation of the promising fractions containing saponins obtained from the first round analytical HPLC. An isocratic elution of 75% methanol was used. The automatic collector was programmed to detect and collect peaks at predefined times.

The studied molecules

Biophysics is in interdisciplinary science that studies the application of physical laws in biological processes. In this study, the physics behind the interactions of saponins and model plasma membranes was investigated.

In this study, two approaches were combined to study these interactions: *in silico* bioinformatic models and *in vitro* experiments using synthesized liposomes to simulate various cell membranes.

However, before being able to describe the interaction, the interacting structures were chosen and defined.

The Lipids

The biophysical study of membranes requires the simplification of the composition of these complex structures. For the *in silico* approaches only the most abundant types of phospholipids in sea cucumbers and fish were tested, according to the literature (Lou *et al.*, 2012; Thomas and Patton, 1971)**:** DPPC: 1,2-dipalmitoyl-*sn*-glycero-3-phosphocholine, DMPC: 1,2-Dimyristoyl-sn-glycero-3-phosphorylcholine and DOPC: 1,2-Dioleoyl-sn-glycero-3-phosphocholine. In addition, three sterols, that are also part of the cell membrane were tested: cholesterol, the major sterol in fish and most animals, and 5α-Cholest-7-en-3β-ol and 4α,14α-dimethyl-5α-cholest-9(11)-en-3β-ol (Figure 1.8 B and C), the two most abundant sterols in *Holothuria scabra* (Han *et al.*, 2009). These same phospholipids and sterols were used for the *in vitro* approach, with the exception of 4α,14α-dimethyl-5α-cholest-9(11)-en-3β-ol, which is not currently commercially available.

The Saponins

For the *in silico* experiments three different holothuroid saponins were investigated. These were chosen based on their abundance in the studied holothuroid species, *H.scabra*, and for their similarities and differences in structure to the only commercially available holothuroid saponin: Frondoside A (Figure 2.1.B).

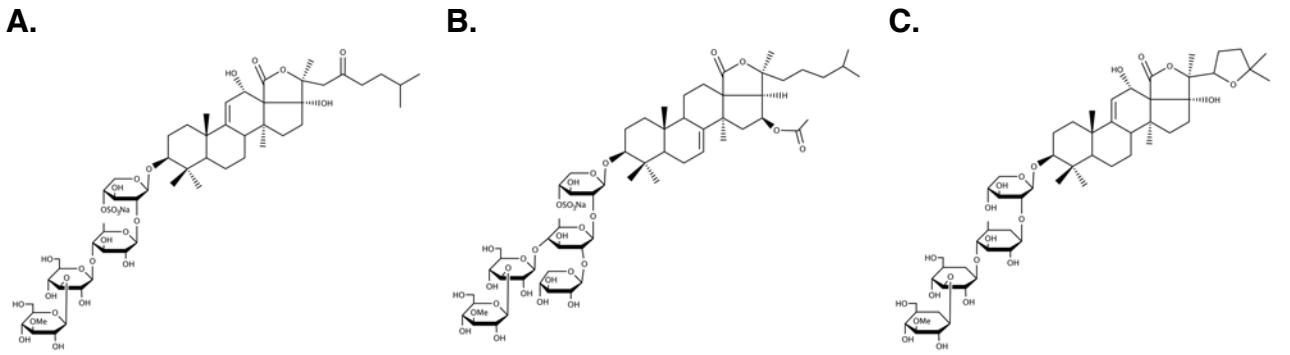

Figure 2.1. Structures of the saponins tested using the *in silico* approach. **A.** Scabraside B (Han et al., 2009), **B.** Frondoside A (Sigma-Aldirch®), **C.** Desholothurine A (Caulier *et al.*, 2013b)

Frondoside A is a sulfated saponin with four saccharide residues, it naturally occurs in the sea cucumber *Cucumaria frondosa* (Park *et al.*, 2014) and is currently commercially available at the Sigma-Aldrich®, and was thus used for the *in vitro* biophysical experiments. Scabraside B is also a sulfated saponin with four saccharide residues, however differences in position as well as the presence of a hydroxyl group instead of an ester group on the aglycone differentiate these two saponins. Finally to investigate the potential role of the sulphate group, a non-sulfated saponin called Desholothurine A was also tested. Both Scabraside B and Desholothurine A are abundant saponins found in *H.scabra* (Caulier *et al.*, 2016).

In silico biophysical experiments

Several *in silico* approaches for describing the interactions between bioactive molecules and membrane lipids have been developed over the years. These can be globally regrouped into two types of experiments: docking experiments and molecular dynamics approaches. The so called "docking" experiments analyze the interaction between molecules (substrate and enzyme, bioactive molecules in interaction with lipids, etc.). In the approach used in this study, a very large number (over 10^7) of positions of lipid molecules around a molecule of interest (saponin) were tested and calculated, mimicking a single leaflet of the lipid bilayer. The Molecular Dynamics approach takes into consideration the dynamic nature of the molecules constituting the molecular system, and the changes that occur overtime during interactions. This approach involves significant computational power and time and was not used for this study.

Structure tree

The first step of the *in silico* experiment was to determine the structure and most likely conformation of the studied saponins in an interfacial environment (such as a lipid membrane). The structure tree technique allows one to model the different possible stable conformations of a molecule. Each conformation is associated with a probability of existence, calculated in considering intra-molecular energies of interaction, using a "home-designed" forcefield (Lins and Brasseur, 1995)*(Equation 2.1).* This force field is applied to bonded and non-bonded atoms to predict the conformation of the molecule. The lowest energy corresponds to the most stable conformation.

$$E_{\text{pot}} = E_{\text{intra}} + E_{\text{inter}} + E_{\text{hydrophobe}} \qquad \textit{Equation 2.1}$$

Where E_{intra} considers the energy from bonded atoms (bond lengths and valence and torsion angles). E_{inter} takes into account the energy of non-bonded atoms (Van der Waals, electrostatic and hydrogen bonding). The hydrophobic energy allows to implicitly to take into account the hydrophobic and/or hydrophilic environment (Lins and Brasseur, 1995).

The structure tree method is based on the analysis of the main rotational axes of the molecule of interest. The angular position of these axes are varied, generating different structures at each cycle (depending on the axes that are chosen). For saponins, 6 axes per cycle were selected, 6 successive cycles were performed, and each cycle kept 3 axes fixed from the previous cycle. The molecule with the least energy obtained after this procedure is assumed as the most stable and therefore the most probable conformation.

Docking Hypermatrix method

The Hypermatrix method is a simple docking method that allows the calculation of the interaction of a bio-molecule with lipids. The molecule of interest (saponins in the case of this study) is fixed at the centre of the system and oriented at the hydrophobic (pho)/hydrophilic (phi) interface using the TAMMO procedure (Brasseur *et al.*, 1987), that takes into account the hydrophilic and hydrophobic centers of the molecule (calculated similarly to a center of mass). The lipid molecules are also oriented at the pho/phi interface and, by a succession of rotations and translations of the lipid around the central molecule, the energy of interaction of over 10^7 positions are calculated (Deleu *et al.*, 2014). This energy of interaction is calculated using the force field described above.

The energy values together with the coordinates of all the positions are stored in a matrix and classified according to decreasing value. The most stable position is used to decide the position of the first lipid. The position of the second lipid is then defined as the next most energetically favorable position stored in the matrix taking into account of the steric and energetic constraints caused by the presence of the first lipid (Deleu *et al.*, 2014). The process ends when the central molecule is completely surrounded with lipids. The interaction energy and its composing terms (E_{VdW}, $E_{electrostatic}$, $E_{H\text{-}bonds}$) provide information on the affinity of the central molecule to its surrounding lipids, and can be compared between molecules. The HM method also calculates the interface surface area occupied by each molecule of the system.

Even though the static nature of this simulation (the structures of the molecules are not modified during the calculation) is a limiting factor, it has shown a very good agreement (less than 5– 10% difference) for the values of the interfacial area either calculated or measured by Langmuir monolayer technique, for different types of molecules (natural molecules, drugs, lipids, lipopeptides), even for molecules differing only by the location of the carbonyl group in a ester bond (Deleu *et al.*, 2014)

IMPALA method

The second *in silico* approach used was the IMPALA method (Ducarme et al, 1998). It uses a membrane model in which the phospholipid molecules (DPPC) are implicitly modeled by an empirical function *C*(*z*) *(Equation 2.2)*. This model assumes that the properties of the implicit membrane are constant in X,Y and only vary along Z. *Z* (in Å) is perpendicular to the plane of the membrane, and its origin is at the bilayer center (Figure 2.2A). *C*(*z*) varies from 1 (completely hydrophilic) to 0 (completely hydrophobic) along the Z axis (Figure 2.2B) (Ducarme *et al.*, 1998). C(z) is given by the following function and can be considered empirically as the water concentration:

$$C(z) = 1 - \frac{1}{1 + e^{\alpha(|z| - z_0)}}$$

Equation 2.2

Where α is a constant equal to 1.99, z_0 is the position of the hydrophilic/hydrophobic interface in the membrane and z is the position in the membrane.

The IMPALA method uses two energy restraints to simulate the interactions between a biomolecule

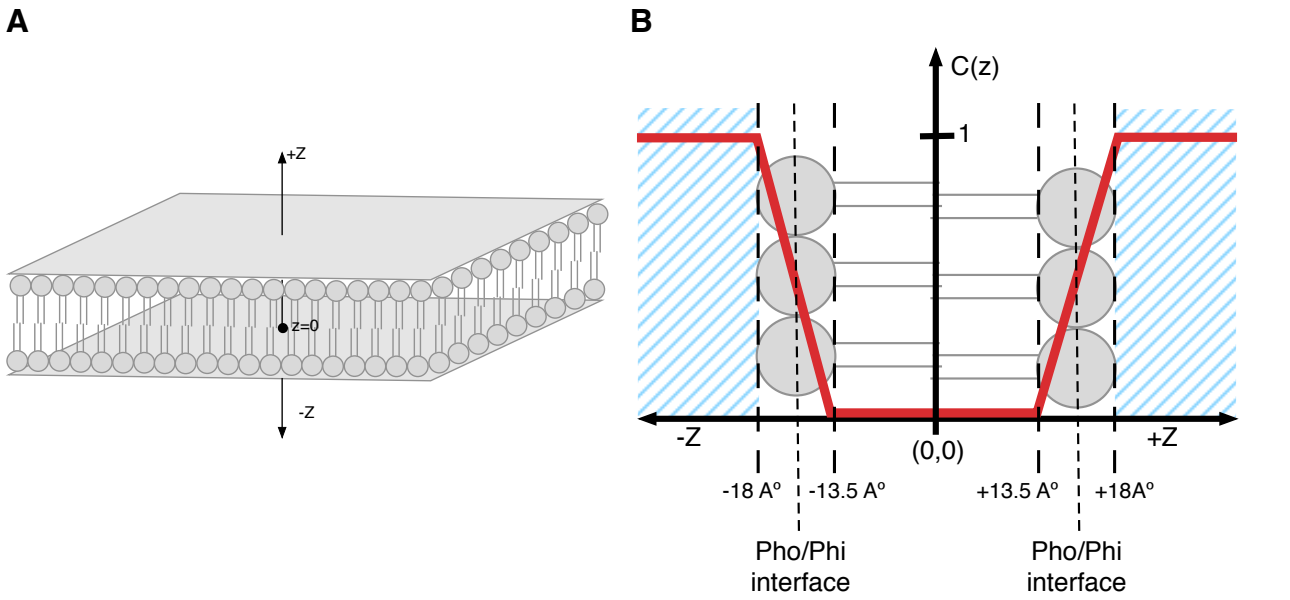

Figure 2.2. Schemes that depict the membrane model described by C(z). **A.** The model considers the planar axes x, and y as constant, and only the z axis varies. **B.** C(z) in function of z. This model implicitly describes the lipid/water interphase found along a Z axis perpendicular to a membrane plane.

and the bilayer. The molecule is systematically translated across the implicit bilayer along the Z axis by 1 Å and rotated 360º at each position $z_{(i)}$ (1000 steps). These restraints, E_{pho} and $E_{lip,}$ are calculated for each atom of the molecule, at each position along the Z axis.

Firstly the hydrophobic restraint (E_{pho}) *(Equation 2.3)*, describes the hydrophobic effect that pushes the hydrophobic atoms of the molecule into the membrane (conversely for hydrophilic atoms). The sign of this restraint is dependent on the hydrophobic/hydrophilic nature of the atom being

considered (positive for hydrophilic, and negative for hydrophobic). The value is function of the solvent-accessible surface.

$$E_{pho} = \sum_{i=1}^{n} S_{(i)} \cdot E_{tr(i)} \cdot C_{(z_i)}$$ *Equation 2.3*

Where n is the total number of atoms, $S_{(i)}$ is the solvent-accessible surface (Å^2) of the atom i, $E_{tr(i)}$ is the transfer energy by surface of individual atoms (kJ.mol.Å^2), and $C_{(zi)}$ is the position of atom i along the bilayer.

Secondly the lipid perturbation restraint (E_{lip}) *(Equation 2.4)* describes the changes in the "integrity" of the lipid bilayer, due to the insertion of a molecule, either hydrophobic or hydrophilic. The interactions between adjacent lipids is disturbed and replaced by weaker interactions when insertion occurs. The value is always positive, and depends mainly on the solvent-accessible surface and the position of the molecule into the implicit membrane:

$$E_{lip} = a_{lip} \sum_{i=1}^{n} S_{(i)} \cdot \left(1 - C_{(z_i)}\right)$$ *Equation 2.4*

Where a_{lip} is an empirical factor fixed at 0.018, n is the total number of atoms, S(i) is the solvent-accessible surface (Å^2) of the atom i, and $C_{(zi)}$ is the position of atom i along the bilayer.

These two restraints are summed to give the total energy of interaction.

The analysis of the IMPALA calculations results therefore in a graph of the total restraint energy values as a function of the penetration of the center of mass of the molecule. This predicts the membrane insertion capability of the molecule and its most likely position within the membrane, ie. if it is likely to be deeply embedded into the membrane or remain superficial.

Big Monolayer

The final in silico calculation conducted is called the Big Monolayer method. This approach is similar in principle to the HM method but increases the number of interacting partners and therefore the total number of molecules in the system. This is a two-step method, in which the first step consists in the calculation of all the one-on-one interaction energies of all the molecular combinations, for example: DPPC/DPPC, DMPC/DPPC, DMPC/DMPC, Saponin/Saponin, Saponin/DPPC, Saponin/DMPC. These calculations are conducted via the same procedure as the Hypermatrix method described earlier. However instead of an energy classification with in the matrix, a statistical Boltzmann energy is determined for each pair of molecules. This considers the maxima of a Maxwell-Boltzmann bell curve distribution as the average interaction energy of the considered pair. This average energy is then used in the second step, which consists in the construction of a grid of n × n molecules (n between 200 and 600), and in the minimization of the system using the values calculated in the first calculation step (Deleu et al., 2014). If n = 600, i.e. a grid of 360,000 molecules, initially positioned at random, is constructed and the energy of the system is calculated. The energy of one molecule is equal to the sum of the interaction energies with its 24 closest neighbors in the grid, i.e. two layers of molecules around the molecule considered (Deleu et al., 2014). Random permutations are then made and the energy of the new configuration calculated. By a Monte Carlo procedure, this new configuration is kept or not, as a function of the energy difference between the previous and current system. For a grid of 360,000 molecules, one calculation step consists in 360,000 permutations; 50,000 to 100,000 steps are carried out. For the molecules at the border of the grid, the molecules at the opposite border are considered as their closest neighbors, therefor avoiding border limits (Deleu et al., 2014). Graphically, each molecule is represented by a colored pixel on the grid. This method allows to visualize preferential interactions and phase separations. This in silico approach has shown good agreement with Atomic Force Microscopy (AFM) experiments using surfactin and DPPC:DOPC (Deleu et al. 2013) and with fluorescence experiments using the saponin α- hederin and a DMPC:Chol system (Lorent et al., 2014a).

For the purpose of the present study, n was set to 200 molecules, and the compositions of the different tested scenarios were derived from the ITC experiments, in order to be able to compare *in vitro* and *in silico* results, in this case the saponin concentration was fixed at 5% (Table 2.1). In addition the same experimental conditions used by Lorent *et al.* (2014a) ie. 67%DMPC, 23% sterol, 10% saponin (in a 200 x 200 grid) were used in order to be able to compare results with his research on the plant saponin α-hedrin and its derivatives.

Each scenario with and with out saponin was repeated 5 times.

Table 2.1. Composition of the different monolayers tested using the Big Monolayer technique, based on the liposome compostions used during the ITC experiments.

	Holothuroid- like membrane	Fish-like membrane
Molecules	Frondo:DMPC:DPPC:Delta 7	Frondo:DPPC:DOPC:Chol
Composition	5:48:19:28	5:48:19:29

Image analysis of the resulting BM colored grids was conducted using the software Fiji (Schindelin *et al.*, 2012). The color threshold parameter were adjusted, and the channels split in order to distinguish the sterol clusters as black particles. The particle analysis tool was then used to determine the surface area of the different particles (Fig. 2.3). Each average was first divided by the total area occupied by sterol, to relativize the data between systems of different composition. In addition because of large differences in variances between compared experiments, the distribution of the mean was normalized using the log of values. A Welch's two sample test was used to compare the mean particle areas of the sterol clusters, using the software R (R Development Core Team, 2011).

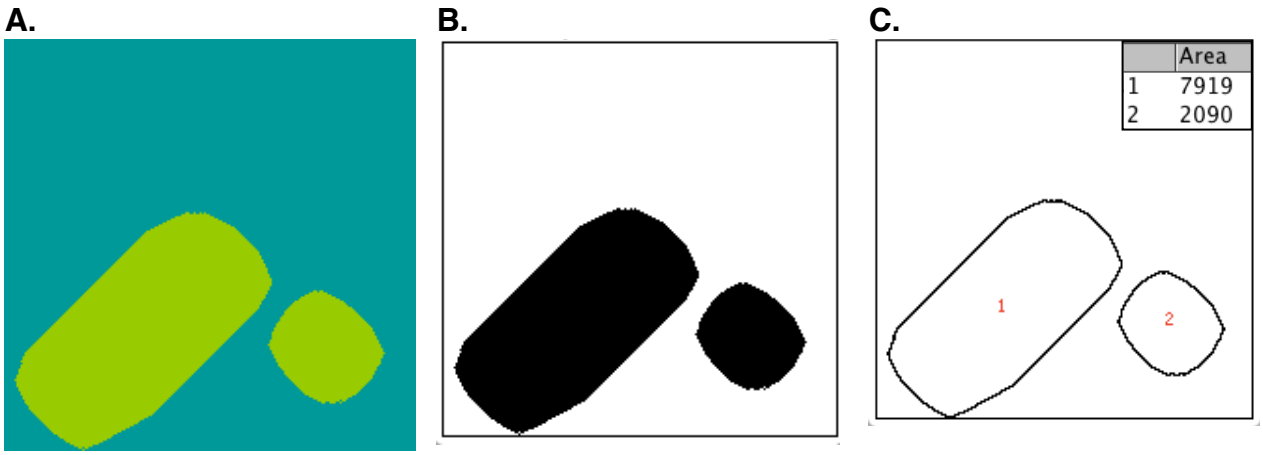

Figure 2.3. Particle size analysis using Fiji. Raw Big monolayer grids **(A)** were converted to black and white, using the color threshold tool **(B)**. The particle analysis tool was used to determine the size of each particle in pixels **(C)**. Phospholipids in teal and sterol in green.

It should be noted that the above *in silico* experiments were conducted in an standard aqueous environment. The salinity was not adjustable, and therefore do not correspond the environmental conditions of the saponin, or the lipid systems of marine organisms.

In vitro biophysical experiment

Isothermal titration calorimetry (ITC)

Isothermal titration calorimetry (ITC) measures the heat released (exothermic reaction) or absorbed (endothermic reaction) when two interacting components are brought together. This is done by determining the power required to maintain a constant temperature in relation to a reference solution (Fig. 2.4). One binding component is titrated into a solution containing the other. The changes in heat energy are recorded over time and allow the evaluation of enthalpy changes due to the interaction between the titrated and titrating solutions. This technique provides a complete thermodynamic description of binding processes (Deleu *et al.*, 2014; Abraham *et al.*, 2005).

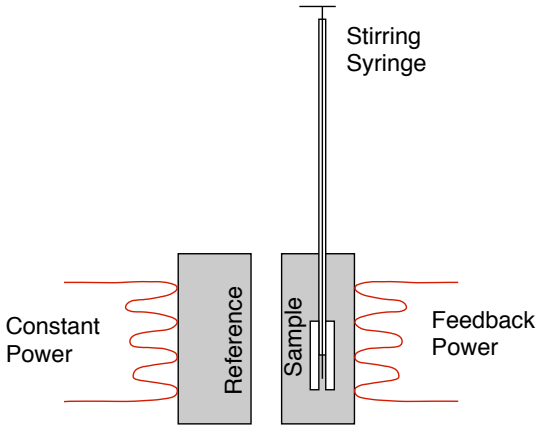

Figure 2.4. Scheme of a MicroCal Isothermal titration calorimeter.

ITC is a method often used when investigating the interaction of bioactive molecules with model plasma membranes (Heerklots *et al.*, 2009). In the present study, a solution of bioactive substance: the holothuroid saponin Frondoside A (Sigma-Aldrich®), was in the measuring cell of the ITC, and a solution of liposomes was in the titrating syringe (Zakanada *et al.*, 2012; Ghai *et al.,* 2011). Liposomes of various compositions mimicking different types of cell plasma membranes (table 2.2) were tested against the holothuroid saponin Frondoside A, as well as against a raw extract of a mix of saponins from the bark of the plant *Quillaja saponaria molina* (VWR®).

Table 2.2. Composition of the different liposomes tested using the *in vitro* biophysical technique called isothermal titration calorimetry.

	Holothuroid membrane 1	Holothuroid membrane 2	Fish like membrane
Lipids	DMPC:DPPC	DMPC:DPPC:Delta 7	DPPC:DOPC:Chol
Composition	75:25	50:20:30	50:20:30

Procedure

Large unilamellar vesicles (LUVs) of approximately 100nm in diameter were prepared by extrusion. In a round-bottom flask covered with aluminum foil, the lipids were weighed to obtain 3 mL of a lipid/ sterol solution with a concentration of 5 mM, and dissolved in 3-5 mL of chloroform:MeOH (2:1). The solvent mix was then evaporated using a rotary evaporator until a dry lipid film covered the bottom of the flask. The flask was then placed in a desiccator overnight to remove any excess solvent. The following day, the lipid film was re-hydrated with 3 mL of buffer (10 mM TRIS, 600 mM NaCl, pH 7.5). The flask was then placed in a water bath set to 37ºC for an hour. The flask was vortexed every 10 minutes.

The lipid solution was then transferred in to a CryoTube®, resistant to liquid Nitrogen. The lipid solution then underwent 5 cycles of freezing in liquid nitrogen and thawing in a water bath at 37ºC. These freeze-thaw cycles cause the organization of the lipids into vesicular forms known as multilamellar liposomes (MLV). The MLV dispersion was then extruded through 15 passages across a membrane with a 100 nm porosity to form unilamellar liposomes (LUV). The size distribution of the liposomes was then determined by dynamic light scattering (DLS) on 500 μL of the solution.

ITC measurements were performed by using a VP-ITC (MicroCal, Northampton, MA). All solutions were thoroughly degassed before use by stirring under vacuum or by ultrasonication. The sample cell (1.4565 mL) was loaded with buffer (blank) or a saponin (plant or holothuroid) solution (15-50 μM) and the reference cell was filled with MilliQ ultra pure water. Titration was carried out at 26 °C using a 300 µL syringe filled with the LUV suspension at 5 mM. The solution in the sample cell was stirred at 305 rpm during the experiments. A titration experiment consisted of consecutive injections of 10 µL of the LUV suspension. Each injection took 10 s and a delay of 360 s was applied between each successive injection to allow steady state to be attained. Data were processed using the software provided by the manufacturer (ORIGIN 7, Originlab, Northampton, USA).

Determination of the Thermodynamic Parameters

As the titration advances and the binding sites become saturated, the heat flux progressively decrease to zero. After i injections of liposomes the concentration of bonded saponins in the measuring cell is $n_{D,b}^{(i)} \cdot C_{D,b}^{(i)}$ and the accumulated heat is calculated using the cumulative model described by Heerklotz and Seelig (2000), using the following equation:

$$\sum_{k=1}^{i} \delta h_k = n_{D,b}^{(i)} \cdot \Delta H_D^{w \to b} = \Delta H_D^{w \to b} \cdot V_{cell} \cdot C_{D,b}^{(i)} = \Delta H_D^{w \to b} \cdot V_{cell} \cdot C_D^0 \cdot \frac{KC_L^0}{1 + KC_L^0} \qquad \textit{Equation 2.5}$$

Where δh_k is the heat produced following each injection (corresponds to the area of each peak on the heat flow = f(time) plot), $\Delta H_D^{w \to b}$ is the molar enthalpy change corresponding to the transfer of a saponin molecule from the aqueous phase (w) to the bilayer membrane (b) (µcal/mmol), V_{cell} is the

volume of the calorimeter sample cell (1.4565 x 10^{-3} L), C_D^0 and C_L^0 are the concentrations of saponin and of lipids in the calorimeter sample cell, respectively (mmol L^{-1}), and K is the binding constant.

K and $\Delta H_D^{w\to b}$ can be evaluated simultaneously by a fit of the measured cumulative heat as a function of C_L^0.

The corresponding free Gibbs energy $\Delta G_D^{w\to b}$ and the reaction entropy $\Delta S_D^{w\to b}$ were then calculated by the equations:

$$\Delta G_D^{w\to b} = -RT\ln\left(KC_w\right) = \Delta H_D^{w\to b} - T\Delta S_D^{w\to b} \qquad \text{Equation 2.6}$$

With R= 8.31 $Jmol^{-1}K^{-1}$, C_w= 55.5 M, and T the temperature in Kelvin

These thermodynamic parameters, (ΔH, ΔG, TΔS, and K) describe the reaction taking place in the measuring cell. The free energy of Gibbs (ΔG), in Joules (J), informs on the favorability of the occurring reaction, if it is negative the reaction is spontaneous and therefore favorable, if ΔG>0 the reaction is not spontaneous and therefore disfavored. The absolute values of the Enthalpy (ΔH) and the entropy (TΔS) can be compared, and reveal the nature of the interactions occurring. Van der Waals interactions are enthalpy-driven processes with minor favorable or unfavorable entropies of interaction (IΔHI > ITΔSI). However, hydrophobic interactions are entropy-driven, where the entropy of the interaction is large and positive whereas the enthalpy of the process is small (IΔHI < ITΔSI). Other intermolecular interactions, such as hydrogen bonding and electrostatic interactions could also be contributing to the interaction (Du *et al.*, 2016; Wang *et al.*, 2010; Du *et al.*, 2016).

3. Results

Saponin Purification

The mass spectra of the saponin mixture present in the raw extract of *Holothuria scabra* digestive tubes, contained at least 4 known saponins (Fig. 3.1). The saponin Scabraside B and Scabraside A are both sulfated saponins, whereas Desholothurine A and Holothurinoside C are not (Fig. 1.5).

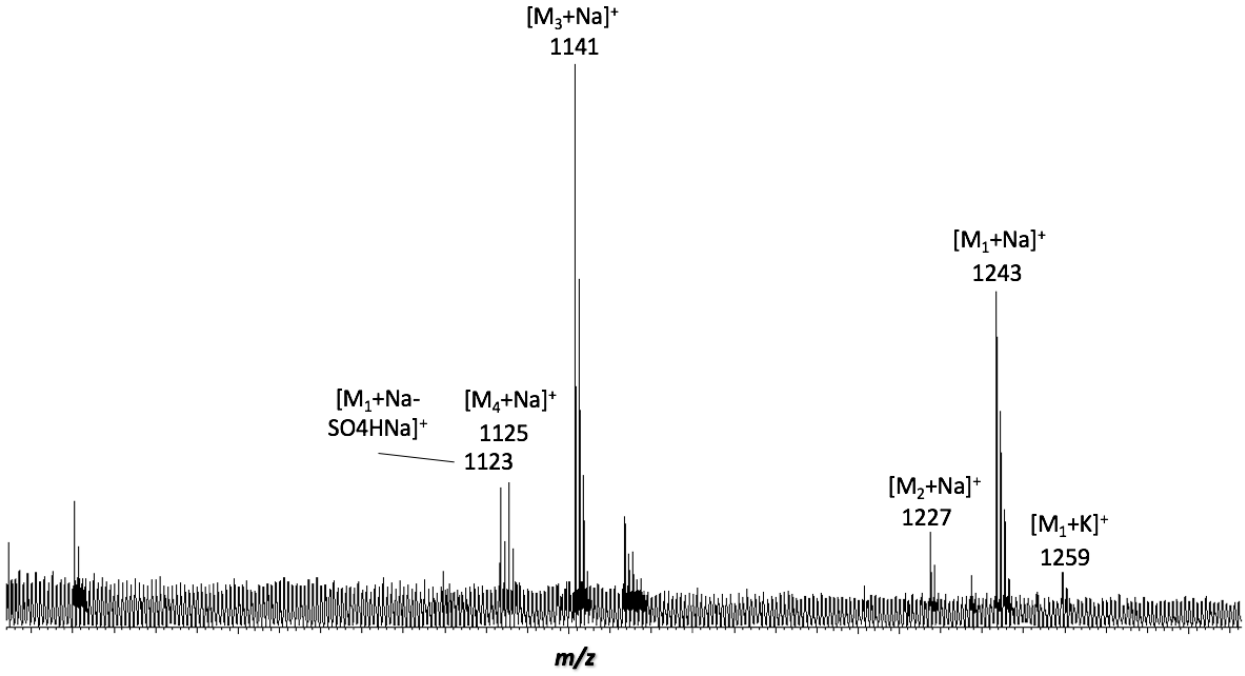

Figure 3.1. Mass spectra of the raw extract of the digestive tubes of *Holothuria scabra*. M1: Scabraside B, M2: Scabraside A, M3: Desholothurine A, M4: Holothurinoside C. Non-annotated peaks correspond to the matrix polymer and/or plastic polymers.

The separation of this raw mixture by preparative HPLC led to a chromatogram with four distinct peaks (Fig. 3.2). The mass spectra of the fractions corresponding to each of these peaks revealed that although the first peak was intense it did not harbor any saponins, however the three other peaks did (Fig. 3.3) .

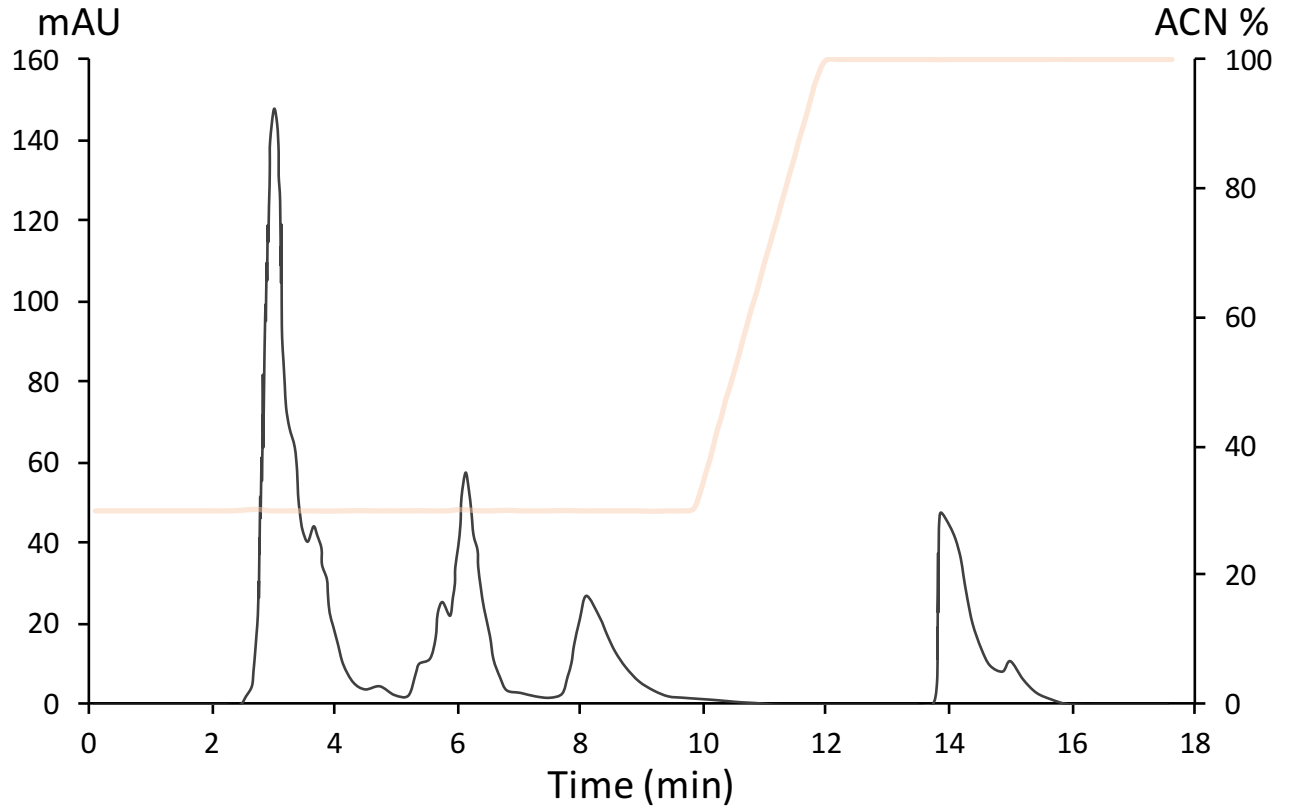

Figure 3.2. Chromatogram of the separation of the raw extract of *H.scabra* by preparative HPLC using a C18 (15µm) 250 x 21.2 mm column. Four peaks were collected for further analysis and fractionation. An isocratic elution over 10 minutes was followed by column washing at 100% ACN (Orange line).

Peak 2 contained the original mixture of the raw extract, but also a lot of background noice. Peak 3 had a reduced mixture of the two non-sulfated saponins: Desholothurine A and Holothurinoside C (Fig. 3.3). And finally the last peak that exited the column upon increasing the Acetonitrile concentration to 100%, had a mixture of the sulfated saponin Scabraside B, and Desholothurine A. This fourth peak had little background noice and was therefore chosen for further fractionation (Fig. 3.4). It was concentrated and stored as a dry pellet.

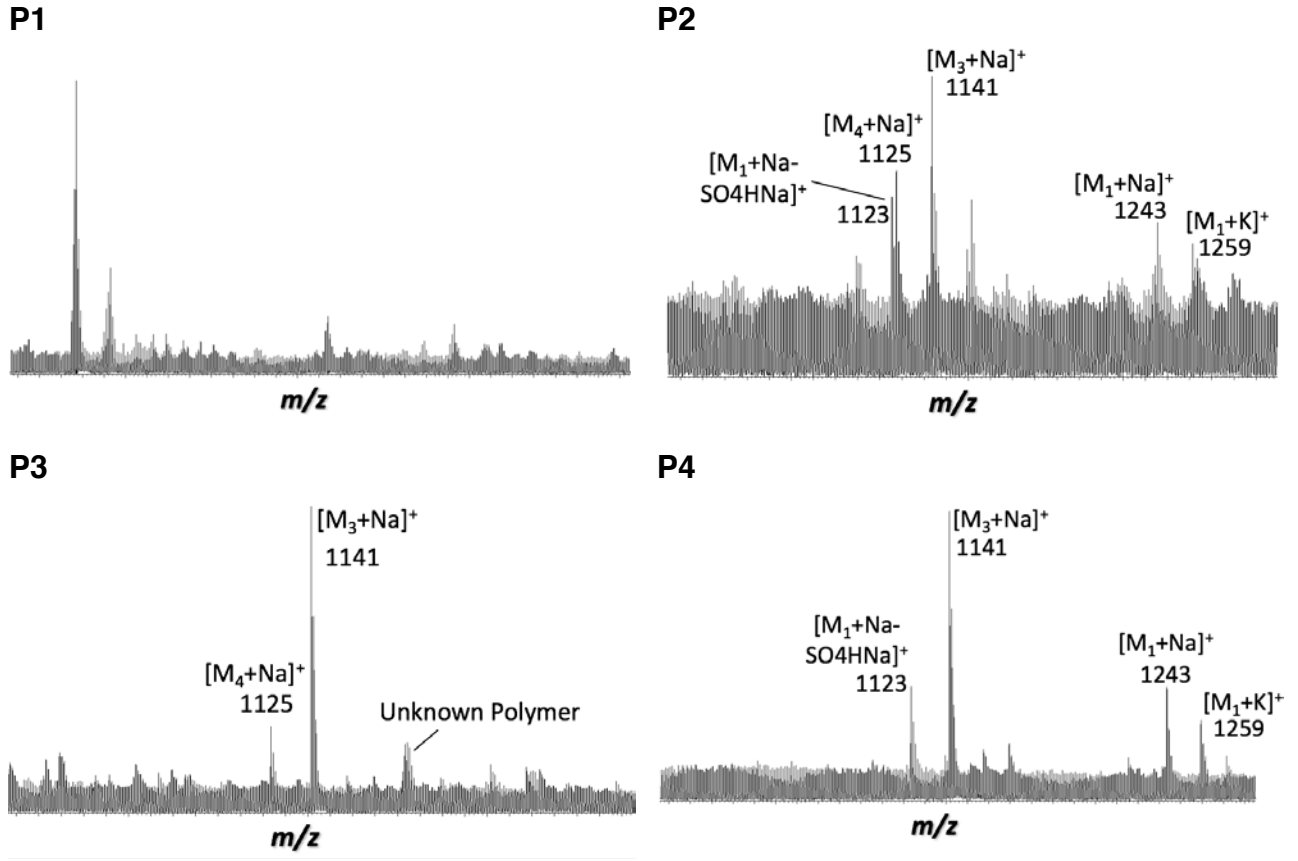

Figure 3.3. Mass spectra of the four collected peaks (**P1, P2, P3, P4**) of the first fractionation of the raw *H. scabra* extract by preparative HPLC (Fig. 3.2). M1: Scabraside B, M2: Scabraside A, M3: Desholothurine A, M4: Holothurinoside C. Non-annotated peaks correspond to the matrix polymer and/or plastic polymers.

Further fractionation of this 4th peak was conducted by analytical HPLC. The first set of runs (conducted the 09/05/2017) resulted in a chromatogram with two fractions (Fig. 3.4 A), the first of which consisted of several co-eluted compounds (Fig. 3.5). Eight runs were conduct and the collected fractions pooled and concentrated for further analysis.

Mass spectrometry of these revealed that only the first “compound” peak contained saponins, and that it in fact contained a large mixture of saponins (Fig. 3.5).

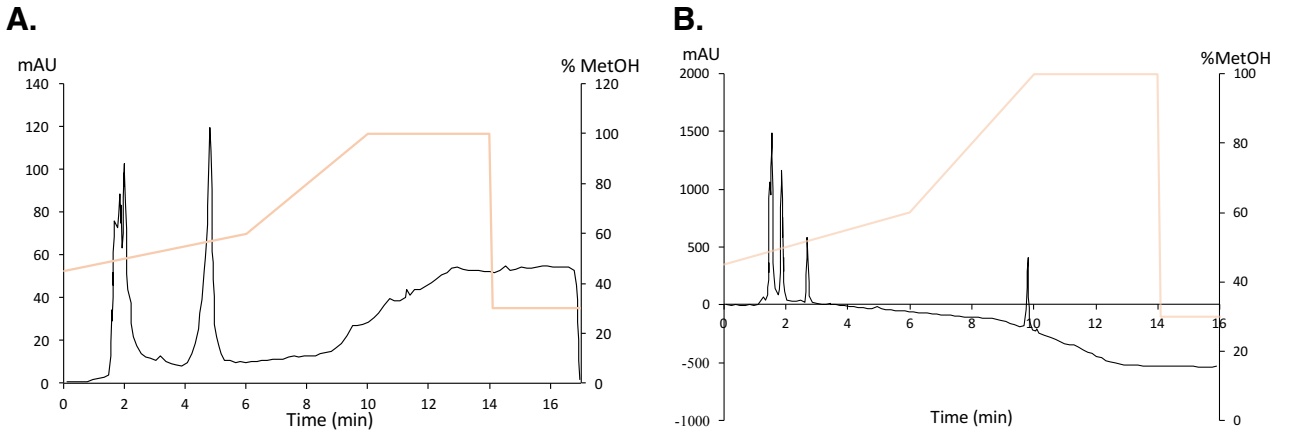

Figure 3.4. Chromatograms of the fractionation of the fourth peak of the preparative HPLC step (Figure 3.2). **A.** Experiment conducted on the 9th of May using sample produced on the 29th of March. **B.** Exactly the same experimental conditions and sample as experiment A, but conducted on the 23rd of June. An analytical HPLC was used with a Zorbax 300SB C18 column, with a methanol gradient elution (Orange line).

However when the same experiment was conducted on June 23rd (more than a month later), on the same sample, the resulting chromatogram was very different (Fig. 3.4). The collected fractions of 5 runs were pooled and concentrated for further analysis.

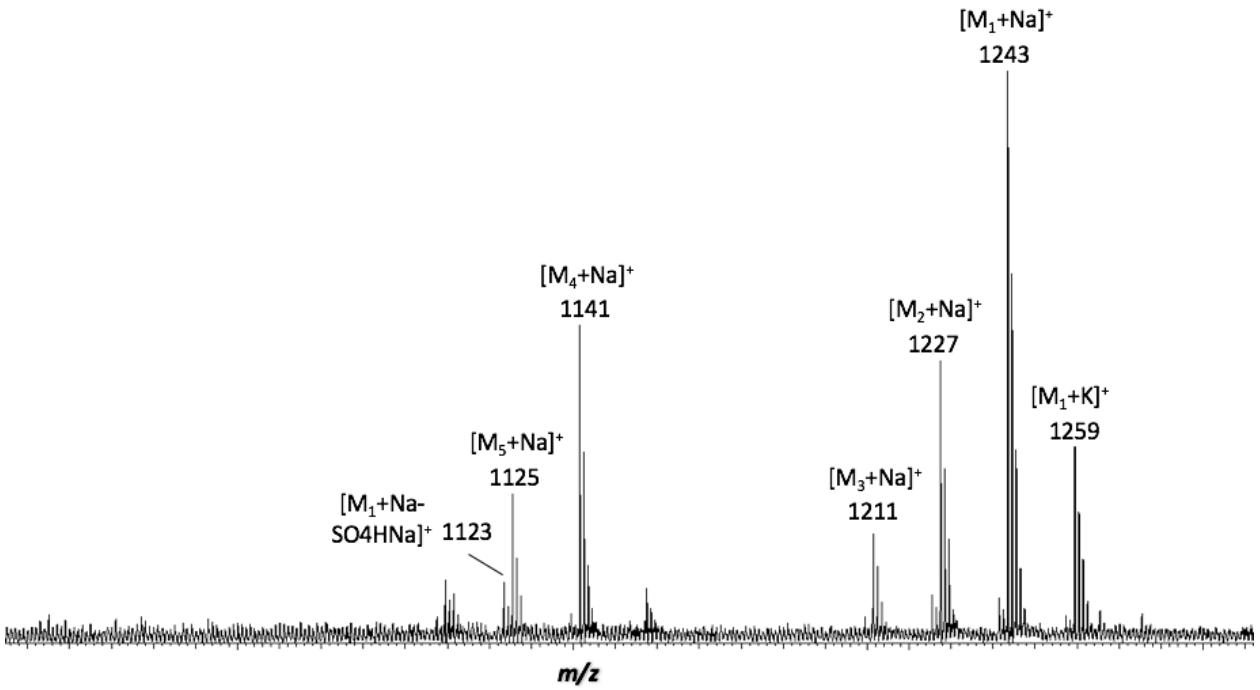

Figure 3.5. Mass spectra of the first peak of the chromatogram of figure 3.4 A. M1: Scabraside B, M2: Scabraside A, M3: An unknown saponin, with the molecular formula: $C_{54}H_{85}O_{25}Na_2S$, M4: Desholothurine, M5: Holothurinoside C. Non-annotated peaks correspond to the matrix polymer and/or plastic polymers.

In this second trial, mass spectrometry analysis were not able to detect any saponins in any of the 4 peaks collected. Due to the inconsistencies in the chromatograms over time, and to time constraints, the objective of purifying a single saponin was abandoned.

In silico biophysical experiments

Structure tree

The structure tree calculations were conducted based on the structural formula of the three studied sterols (Fig. 3.6) and the three studied saponins (Fig.3.7). The calculations resulted in stable 3D structural conformations of the three sterols (Fig. 3.6) and the three saponins studied (Fig. 3.7).

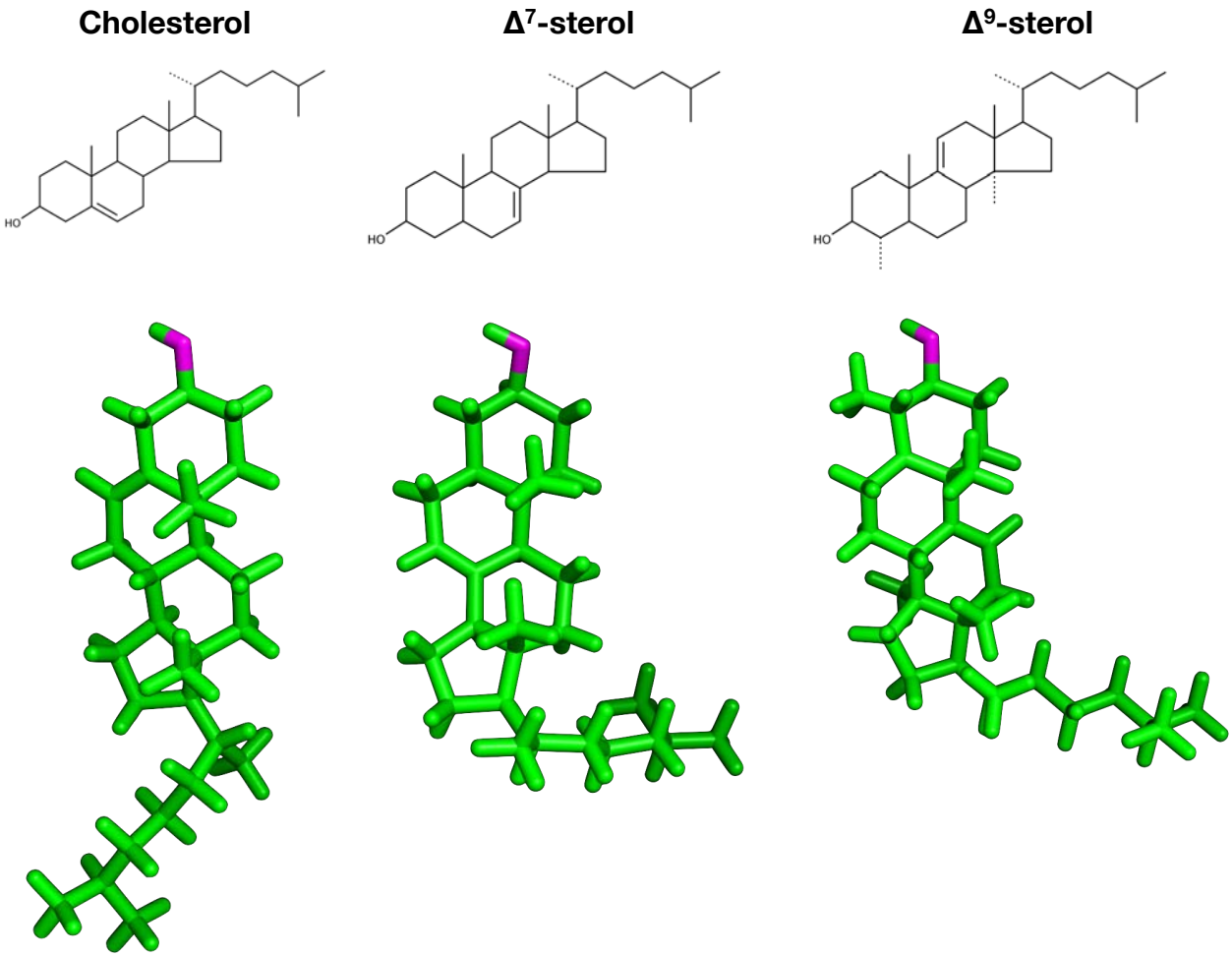

Figure 3.6. Structural formula and 3D conformation of the three sterols tested during the *in silico* experiments. Δ7 sterol: 5α-Cholest-7-en-3β-ol and Δ9 sterol: 4α,14α-dimethyl-5α-cholest-9(11)-en-3β-ol. Green corresponds to Carbon and Hydrogen atoms, and magenta indicates the position of the hydroxyl group.

The 3D conformations of the different sterols were very different. The Δ^7 and $\Delta^{9(11)}$ double bond caused a bend in the molecule generating an "L" shaped sterol. The Δ^7 and $\Delta^{9(11)}$ sterols are therefore shorter and wider compared to the Δ^5 cholesterol that is relatively elongated.

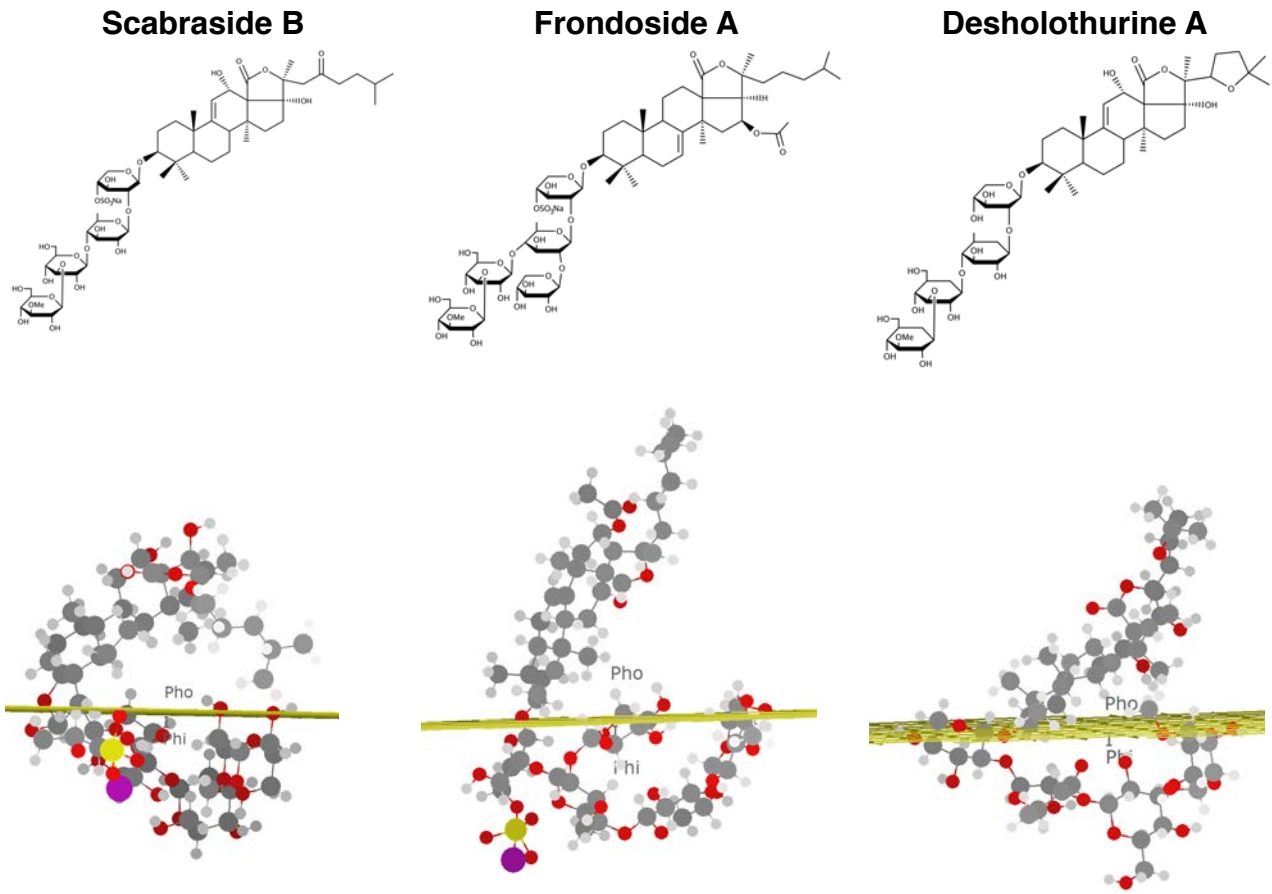

Figure 3.7. Structural formula (top panel) and 3D structures (bottom panel) of the 3 saponins used for the *in silico* biophysical experiments. The plane separating the hydrophobic (Pho) and hydrophilic (Phi) moieties are presented as a yellow gridded structure and were determined by the TAMMO procedure. Carbons atoms are dark grey, Hydrogen light grey, oxygen atoms are red, Sulfur yellow and Sodium purple.

The 3D structures of the saponins revealed that Scabraside B has a more spherical 3D conformation than Desholothurine A and Frondoside A.

Hypermatrix method

These 3 saponins were then tested against the 6 different membrane lipids, using the Hypermatrix method, this resulted in both 3D models (Fig. 3.8), and data on the energies of interaction.

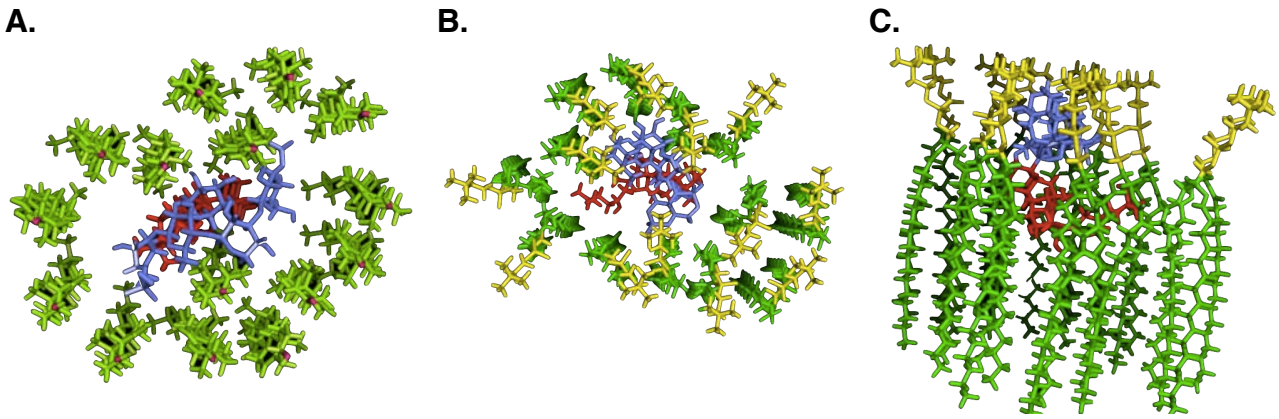

Figure 3.8. Model generated by the Hypermatrix method. **A.** Birds eye view 3D model of Scrabraside B (Apolar in red, Polar in Blue) surrounded by Cholesterol (green). **B** and **C.** Birds eye view and side view respectively of the 3D representation of Scrabraside B (Apolar in red, Polar in Blue) surrounded by DPPC (Yellow: polar head group; green: Apolar fatty acid tails).

The visualization of the 3D models illustrates the spacial disposition of the lipids around the central saponin, *i.e.* whether the lipids were in close proximity, or more distant to the saponin molecule. Interactions with phospholipids (Fig. 3.8B) seemed to be in closer proximity than those with sterols (Fig. 3.8A).

In these molecular assemblies, the energies of interaction between a central molecule and its surrounding lipids (Fig. 3.9) were calculated, in addition to the energies of interaction between the surrounding lipids themselves (Fig 3.10).

The major component of the energy of interaction between the central saponin and the different kinds of lipids tested was the apolar component that takes into account hydrophobic and Van der Waals interactions (Fig. 3.9). The energy values for the interaction between a central saponin and phospholipids were more negative (therefore more favorable) than those with sterols. Amongst the different sterols, interactions with cholesterol were more negative than those with Δ^9 and Δ^7 sterols, suggesting a more favorable interaction. If differences in energy were significantly different between lipids (Two-way ANOVA without replication, $p=1.877\ 10^7$), there was no significant differences between the different kinds of saponins (Two-way ANOVA without replication, $p = 0.1987$)(Table 3.1).

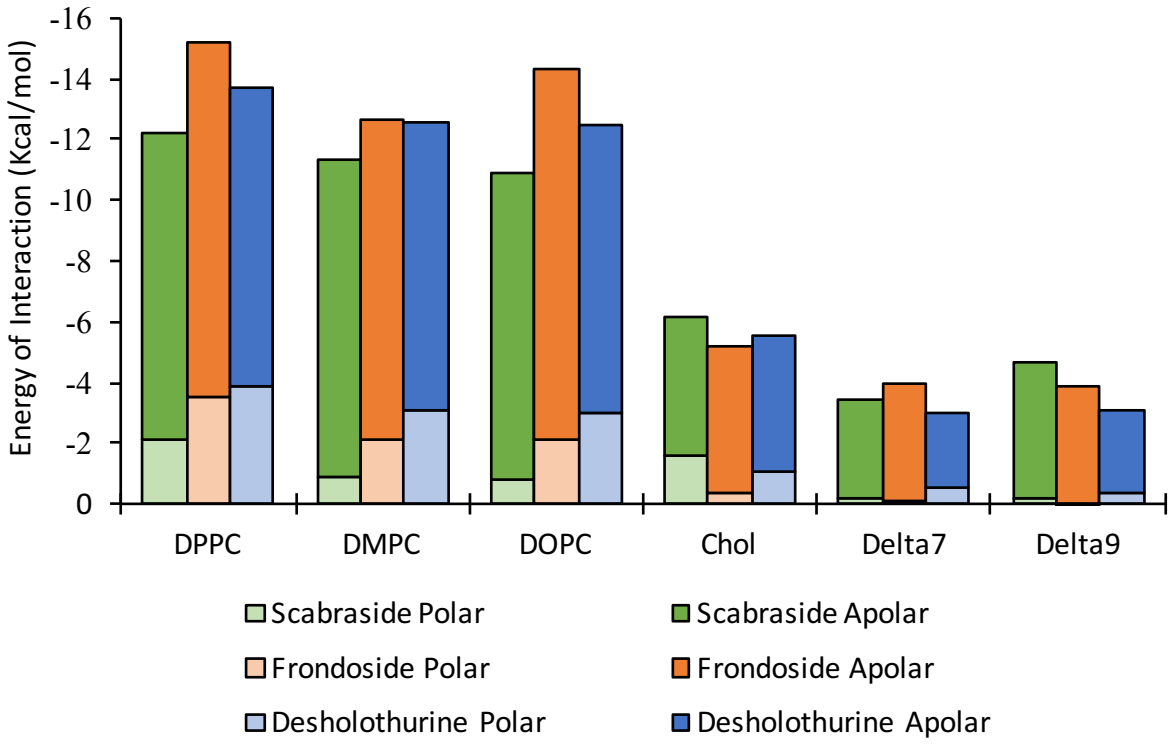

Figure 3.9. Energy of interactions between a central saponin and different membrane lipids. The different components of the total energy of interaction are represented by pale colors for apolar interactions, and darker colors for polar interactions. The Different bars illustrate the interactions of the different lipids with Scabraside B in green, Frondoside A in orange, and Desholothurine A in blue.

Table 3.1. Results from a two-way ANOVA without replication analysis on the data obtained from the hypermatrix method, represented graphically in figure 3.9.

Source of variation	Degrees of Freedom	Sum Squared	Mean Squared	F-value	P-value
Lipid	5	335.94	67.188	69.9678	$1.877\ 10^{7}$
Saponin	2	3.66	1.832	1.9075	0.1987
Residuals	10	9.60	0.960		

In addition to the energies of interaction between the central saponin and its surrounding lipids, the energies of interaction of the surrounding lipids with themselves were also investigated (Fig. 3.10). A significant difference in energy was observed between the different types of lipid systems ($p=3.413\ 10^{-8}$), phospholipid lipid systems were more energetically stable than purely sterol systems. In addition a significant difference between intra-lipid interaction energies was observed between systems with a saponin present as the central molecule and those with no saponin (p=0.01484) (Table. 3.2). Intra-lipid interactions were therefore generally more favorable in the presence of a saponin. In other words, the presence of a saponin in the lipid system, made the system more energetically stable. When considering the magnitude of scale between lipid-lipid interactions (Fig.

3.10) and the saponin-lipid interaction (Fig. 3.9), the saponin-lipid interaction are more negative and therefore more energetically favorable.

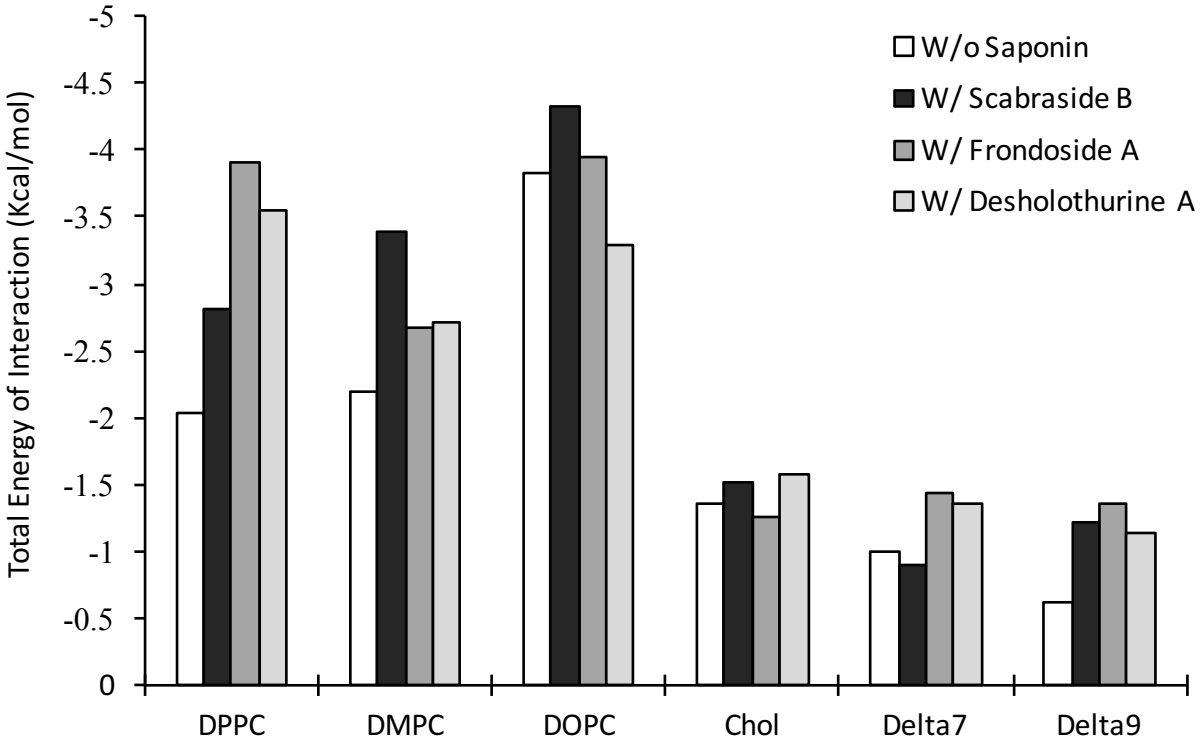

Figure 3.10. Total energy of interaction between lipids of monolayer systems tested using the Hypermatrix method. Lipid systems were modeled with the presence of a saponin (Scabraside B, Frondoside A, or Desholothurine A) as the central molecule, and without a saponin present.

Table 3.2. Results from a two-way ANOVA without replication analysis on the data obtained from the hypermatrix method, represented graphically in figure 3.10. Data used was simplified into the presence of saponin (yes or no) in the system.

Source of variation	Degrees of Freedom	Sum Squared	Mean Squared	F-value	P-value
Lipid	5	26.6883	5.3377	33.1787	$3.413\ 10^{-8}$
Presence of Saponin	1	1.1820	1.1820	7.3473	0.01484
Residuals	17	2.7349	0.1609		

The Hypermatrix method also indicated the interfacial area of the different molecules modeled (Table 3.3), as well as the entire monolayer system created (Table 3.4). Although cholesterol and 5α-Cholest-7-en-3β-ol (Δ^7) have the same molecular mass and differ only by the placement of a double bond, there is a significant difference in their individual interfacial area: the 2 holothuroid sterols were around 75 $Å^2$ while cholesterol was only 51 $Å^2$. The saponins occupy about twice the interfacial area as the molecules of phospholipids.

Table 3.3. Molecular formula and mass of the different molecules studied during the *in silico* experiments. The area of each molecule was determined at the water/lipid interface using the Hypermatrix simulation.

	Molecular Formula	Molecular mass (g/mole)	Interface area (A^{o2})
Phospholipids			
DPPC	$C_{40}H_{80}NO_8P$	734.0	59.1
DMPC	$C_{36}H_{72}NO_8P$	677.9	61.0
DOPC	$C_{44}H_{84}NO_8P$	786.1	59.0
Sterols			
Cholesterol	$C_{27}H_{46}O$	382.7	51.0
5α-Cholest-7-en-3β-ol	$C_{27}H_{46}O$	386.7	78.0
4α,14α-dimethyl-5α-cholest-9(11)-en-3β-ol	$C_{29}H_{50}O$	414.7	76.0
Saponins			
Frondoside A	$C_{60}H_{95}O_{29}SNa$	1335.4	125.0
Scabraside B	$C_{54}H_{85}O_{27}SNa$	1221.3	105.0
Desholothurine A	$C_{54}H_{86}O_{23}$	1103.2	124.0

The total system interfacial surface area describes to a certain degree the “compactness” of the system consisting of a central molecule completely surrounded by a monolayer of lipids. This area ranged from 732 -842 $Å^2$ for the phospholipid-saponin systems, and from 763-905 $Å^2$ for there sterol-saponin systems. The systems with cholesterol were more compact than those with the holothuroid sterols (Table 3.4).

Table 3.4. Total system interfacial surface area ($Å^2$) of the molecular systems generated by the Hypermatrix experiments conducted between the 3 studied saponins and the 6 different membrane lipids.

	Scabraside B	Frondoside A	Desholothurine A
DPPC	842	805	742
DMPC	793	842	753
DOPC	837	732	767
Cholesterol	763	771	786
Δ7 sterol	825	843	806
Δ9 sterol	882	839	905

IMPALA method

The IMPALA *in silico* approach showed small but significant differences in energy profiles of the center of mass of the 3 tested saponins (Fig. 3.12). These differences are highlighted in figure 3.11 showing the different saponin molecules positioned in relation to the membrane interfaces. Frondoside A had its apolar aglycone deep inside the bilayer, whereas Scabraside B had few atoms in contact with the hydrophobic core of the bilayer, and had most of its mass well above the membrane/water interface. Desholothurine had most of its mass in contact with the polar heads of the phospholipids.

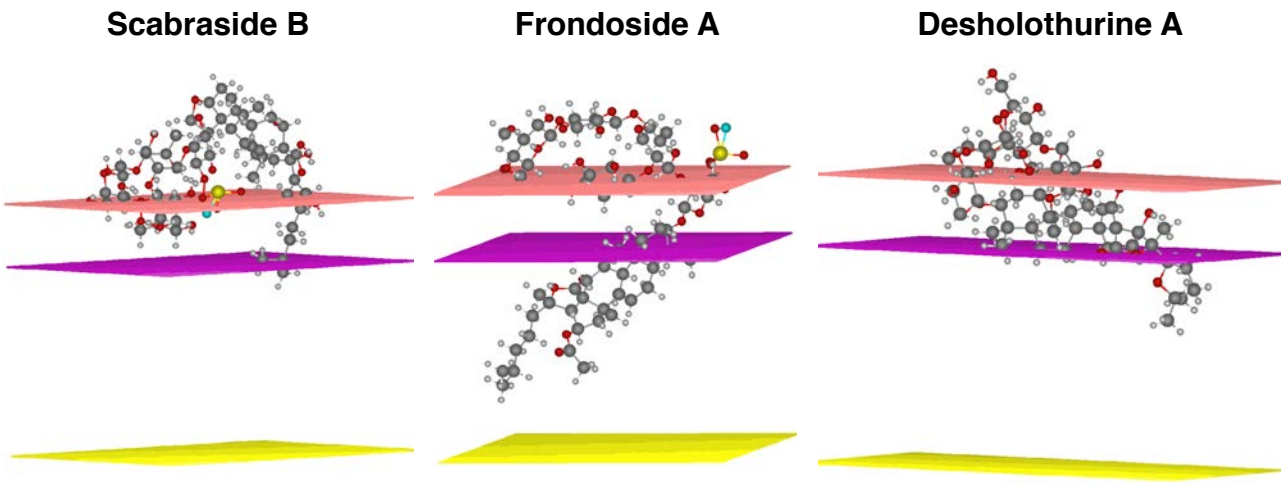

Figure 3.11. IMPALA simulation of the most stable position of the three saponins tested across a lipid bilayer. The different planar surfaces represent the water/membrane interface (pink), the hydrophilic head/hydrophobic tail interface of the phospholipid bilayer (purple), and the center of the bilayer (yellow). Carbons atoms are dark grey, Hydrogen light grey, Oxygen atoms are red, Sulfur yellow and Sodium purple.

Because of the symmetry of the simulated plasma membrane, the energy profiles are symmetrical around the middle of the membrane (Fig.3.12). For Scabraside B and Frondoside A the profiles showed a minimum interaction energy near the surface of the membranes at ± 21Å and ± 19Å respectively, with their center of mass in the aqueous environment.

Another minimum at ± 17Å was observed, with a significant increase in energy from -12 to -5 kcal/mol for Scabraside B. Frondoside A also demonstrated a second energy minimum at ± 16Å but that was only slightly less stable than the first as the energy went from -14 to -13 kcal/mol. The profile of Desholothurine A was slightly different in that the first minimum at ± 22Å was less stable than the second minimum at ± 18Å, which is at the membrane/water interface (Fig. 3.12).

Positive interaction energies were observed for all three molecules at the hydrophobic center of the bilayer, suggesting that the saponin would not be able to cross the bilayer, as would be expected for amphiphilic molecules. Frondoside A and Scabraside B had more positive energies than Desholothurine A at the hydrophobic core of the bilayer.

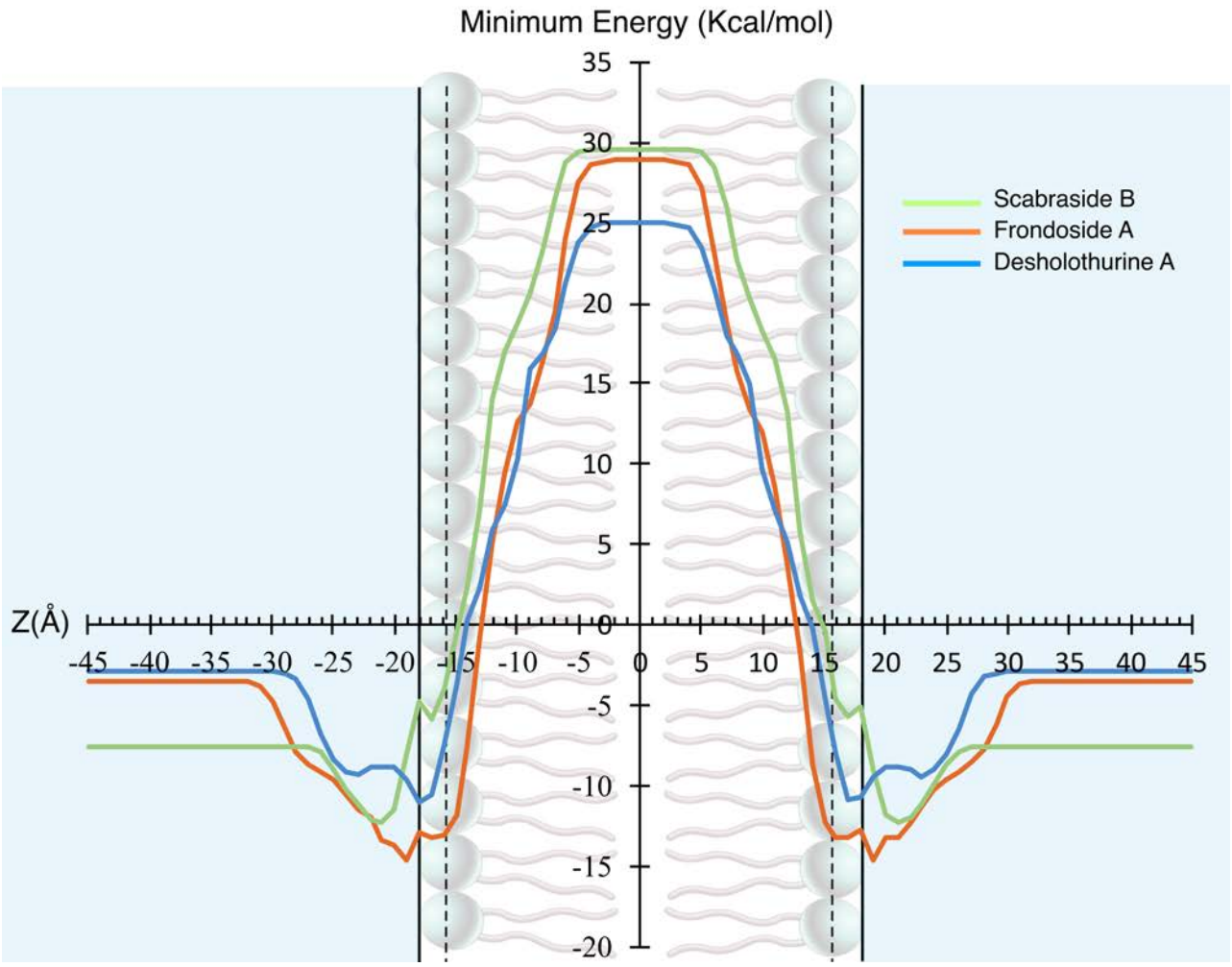

Figure 3.12. Energy profile of Frondoside A , Scabraside B, and Desholothurine A as the molecule traverses an implicit plasma membrane using the IMPALA method. The X-axis corresponds to the position along an axis traversing a plasma membrane of 36 Å thick. The dotted line at ± 15.75 corresponds to the interface between the hydrophobic and hydrophilic parts of the phospholipid bilayer.

Big Monolayer

The big monolayer technique was used to investigate the behavior of the sterols and saponins in a phospholipid system. This first step of the technique summarized all the Hypermatrix energies of all the interaction pairs by calculating a Boltzmann energy (Table 3.5). The second step of the big monolayer uses this matrix (Table. 3.5) to conduct the simulations described below. The more negative the energy the more favorable the interaction.

Table 3.5. Boltzmann energy of interaction matrix (Kcal/mol) calculated during the first step of the Big Monolayer technique, and used for the simulations of the second step.

	Cholesterol	Delta7	DMPC	DOPC	DPPC	Frondoside A
Cholesterol	-47.51	-60.98	-37.99	-34.80	-27.86	-58.19
Delta7	-60.98	-60.95	-63.35	-18.16	-44.80	-57.87
DMPC	-37.99	-63.35	-39.87	-21.09	-30.67	-60.55
DOPC	-34.80	-18.16	-21.09	-36.85	-49.73	-60.52
DPPC	-27.86	-44.80	-30.67	-49.73	-34.24	-60.81
Frondoside A	-58.19	-57.87	-60.55	-60.52	-60.81	-67.17

The first experiment conducted used the same conditions as Lorent *et al.* (2014a) and the behavior of cholesterol and the Δ7 sterol were compared (Fig. 3.13 A and B). Welch's unequal variances T-test determined that there were not significant differences in the relative mean particle size (sterol cluster size) between the systems A and B (Welch two sample test, df = 6.2355, p-value = 0.3741). Although these binary systems are not realistic on a biological standpoint, they provide a "control" simulation to compare subsequent simulations with.

The addition of the saponin Frondoside A to the DMPC:Chol system (Fig. 3.13 C) resulted in very similar changes in cholesterol domain form and size as seen upon the addition of the plant saponin α-Hedrin (Lorent *et al.,* 2014) (FIg. 3.13 D). There was a significant difference in the relative mean particle size between the "control" cholesterol system and the system with Frondoside A (Fig. 3.13 A and C) (Welch two sample test, df = 6.826, p-value = 0.02113). The domaine size seemed to increased with the addition of the saponin, and became more globular.

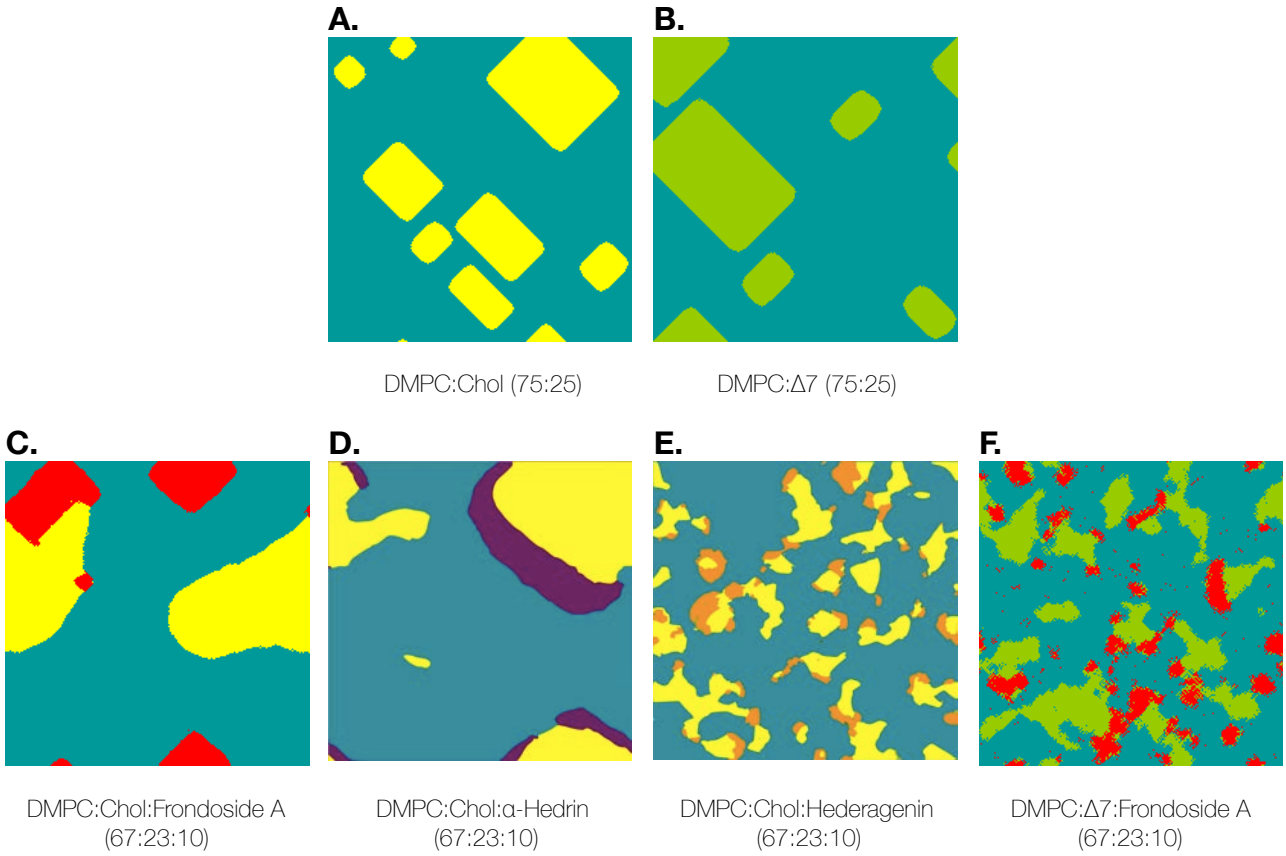

Figure 3.13. Stable structure of BigMonolayer grids (200x200 pixels) resulting from minimization of the total energy of the systems through a large numbers of permutation among the molecules of the system. Each molecule occupies one pixel of the double torus simulation world. Experimental conditions (relative composition of the monolayer) are similar to that used by Lorent *et al.*, 2014 and Deleu *et al.*, 2014. Cholesterol in yellow, DMPC in teal, Frondoside A in red, Δ^7-sterol in green, α-Hedrin in purple, and Hederagenin in orange.
Panel D and E are adapted from Lorent *et al.* (2014).

In contrast, the addition of Frondoside A to the Δ^7 system resulted in the fragmentation of the large sterol domains, into scattered irregularly shaped clusters of Δ^7-sterol often associated with the saponin (Fig. 3.13F). There was a highly significant difference in the relative mean cluster size between the Δ^7 system with and without Frondoside A (Welch two sample test, df = 4.9905, p-value = 2.885e-06) (Fig. 3.13 B and F). This fragmented sterol profile, is similar to the experiment conducted by Lorent *et al.* (2014), using Hederagenin, a sugar-less derivative of the the plant saponin α-Hederin (Fig. 3.13 E).

A significant difference in relative mean size was detected between the two sterol systems in the presence of Frondoside A (Fig. 3.13 C and F) (Welch two sample test, df = 4.9905, p-value = 2.885e-06).

Experiments were also conduct using the same liposome compositions as those used during the ITC experiment (see Table 2.2). The top panel of figure 3.14 illustrates these compositions with out the presence of any saponin, i.e. before injection. On a visual analysis, a difference is observable in the size of the sterol domains. The cholesterol formed relatively small clusters that were often

surrounded with DOPC (Fig. 3.14 top left panel). In contrast the Δ7-Sterol formed a very large domain. The introduction of 5% of Frondoside A into the holothuroid-like lipid system resulted in a fragmentation of the giant sterol domain. In addition the saponin did not to seem to have a greater association either the Δ7 sterol nor the PLs (Fig. 3.14 right panel).

However the addition of 5% of Frondoside A into the fish-like lipid system (Fig. 3.14 left panel), resulted in no visibly outstanding changes in cholesterol cluster form nor size. The saponin was often associated with the cholesterol.

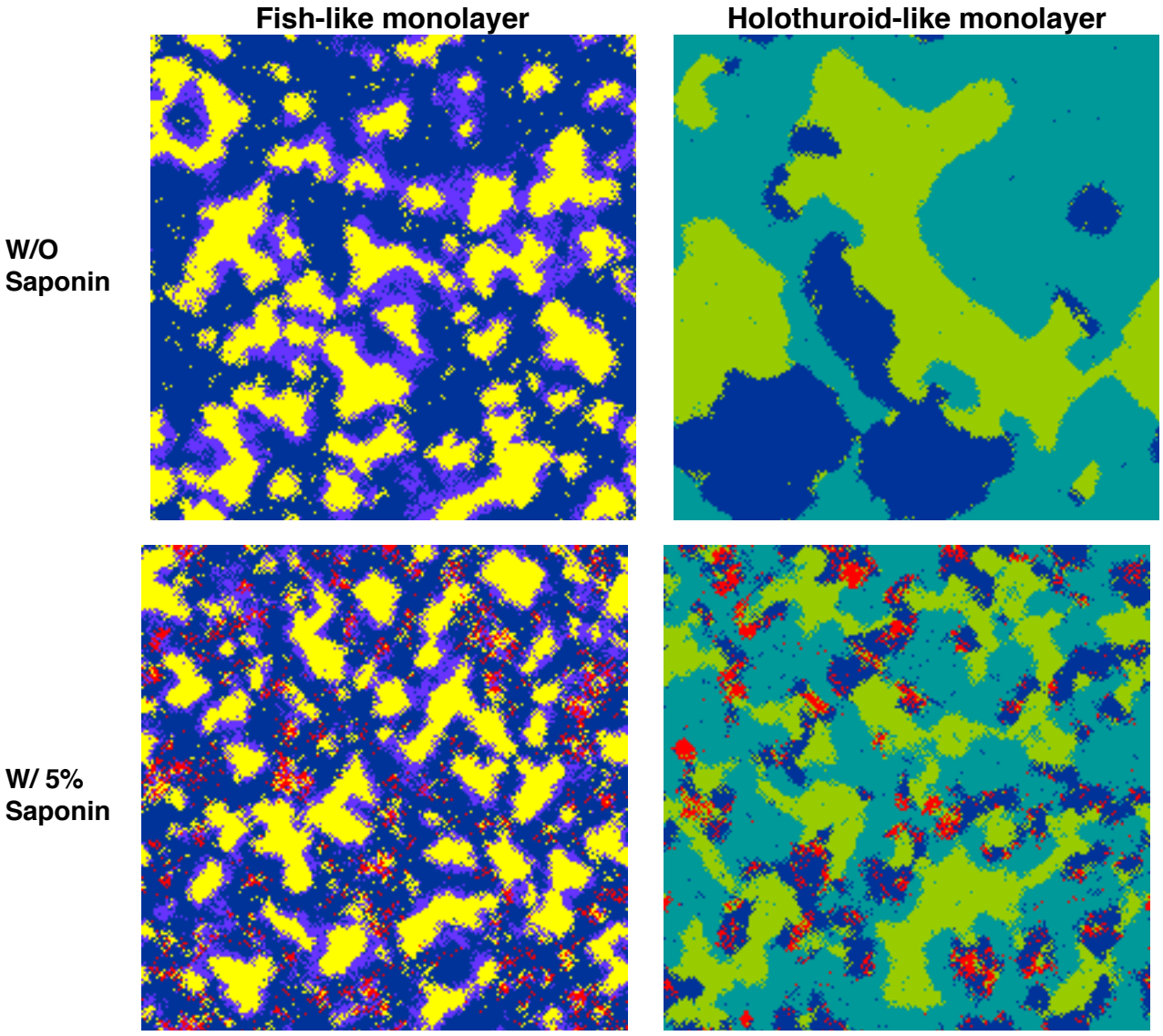

Figure 3.14. Stable structure of BigMonolayer grids (200x200 pixels) resulting from minimization of the total energy of the systems through a large numbers of permutation among the molecules of the system. Each molecule occupies one pixel of the double torus simulation world.
Top panel: Simulation with out Frondoside A. **Left:** DPPC:DOPC:Chol (50:20:30); **Right:** DMPC:DPPC:Δ^7-sterol.
Bottom panel: Simulations with the presence of 5% of Frondoside A. **Left:** Frondo:DPPC:DOPC:Chol (5:48:19:28); **Right:** Frondo:DMPC:DPPC:Delta7 (5:48:19:28).
DPPC in navy blue ; DOPC in violet ; DMPC in teal ; Δ^7-sterol in green; cholesterol in yellow, and Frondoside A in red.

In vitro biophysical experiments

Isothermal titration calorimetry

ITC experiments were conducted on three liposomes compositions using 2 surfactant types, plant derived saponin (purified extract from the bark of *Quillaja saponaria*) and the holothuroid saponin: Frondoside A.

Each experiment was performed in duplicates. In addition, two types of blanks were carried out and subtracted from the raw thermograms to reveal the actual interaction thermogram. It was observed that the blank experiment conducted with buffer in the measuring cell and liposomes suspension progressively added to the system with a syringe resulted in systematic negative peaks whereas the blank experiment conducted with Frondoside A in the measuring cell and buffer in the syringe resulted in systematic positive peaks. No such trend was observed with the *Quillaja saponaria* derived saponin mix.

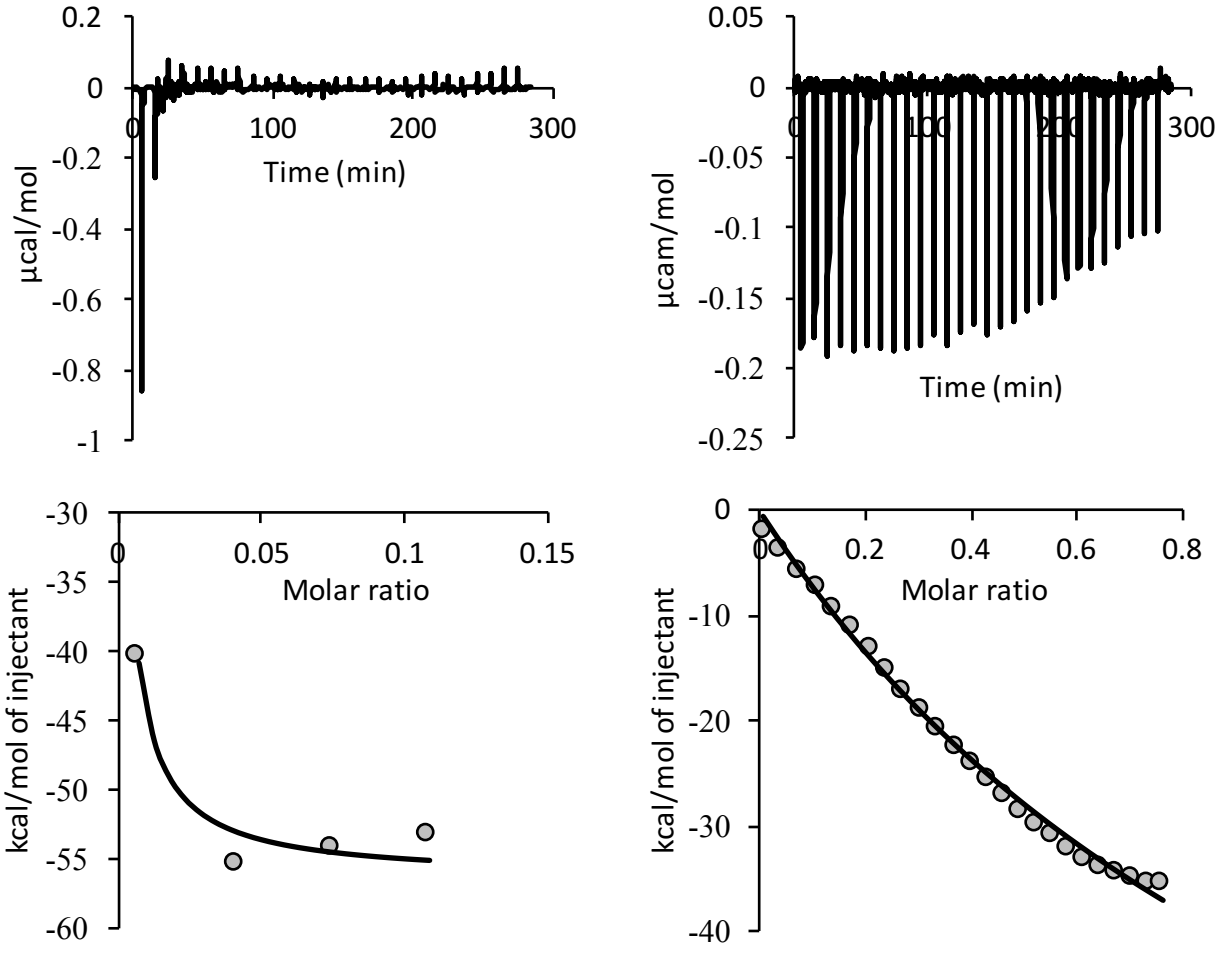

Figure 3.15. Raw thermograms (top panel) and cumulated molar enthalpy (bottom panel) of ITC experiments conducted with fish like DPPC:DOPC:Chol (5:2:3) liposomes and Frondoside A (17µM) (left panel) or raw saponin extract from *Quillaja saponaria* (right panel) (25µM).

The experiments conducted with fish like liposomes; DPPC:DOPC:Chol (5:2:3) resulted in negative peaks decreasing over time (Fig. 3.15). The rates of change were very different between the experiments conducted with the plant saponins and the holothuroid Frondoside A.

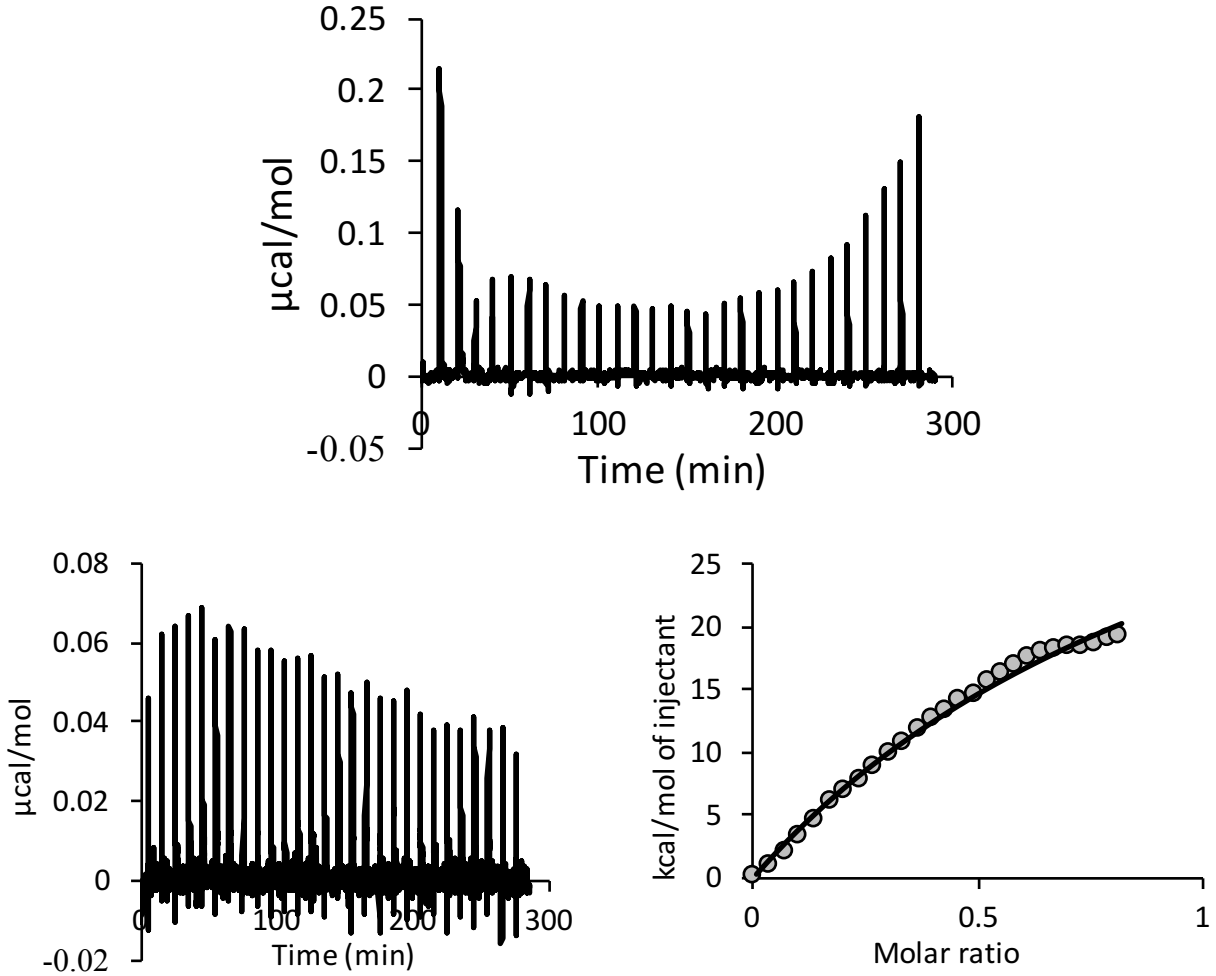

Figure 3.16. Top panel: Raw thermograms of ITC experiment conducted with holothuroid like DMPC:DPPC:Δ^7-sterol (5:2:3) liposomes with 17 µM of Frondoside A **Bottom panel:** Raw thermogram and cumulated molar enthalpy of the ITC experiment of holothuroid like DMPC:DPPC:Δ^7-sterol liposomes (5:2:3) with 50 µM of raw saponin extract from *Quillaja saponaria*.

Experiments conducted with holothuroid like liposomes; DMPC:DPPC:Δ^7 sterol, resulted in very different profiles compared to the fish-like liposomes. The titration resulted in positive peaks that decreased over time (Fig. 3.16). However, an unexpected, and untreatable profile was obtained for the titration of holothuroid liposomes into Frondoside A, this same odd profile was obtained in all three repetitions. An initial decrease was observed and then a wave like heat profile until an eventual increasing heat profile (Fig. 3.16 top panel).

Finally experiments conducted with DPPC:DMPC (3:1) liposomes with no sterols, resulted in similar thermogram profiles to the experiment with the holothuroid liposomes (Fig. 3.16), with positive peaks decreasing in size overtime (Fig. 3.17). However the rate of change was different between the plant saponins and the holothuroid saponin.

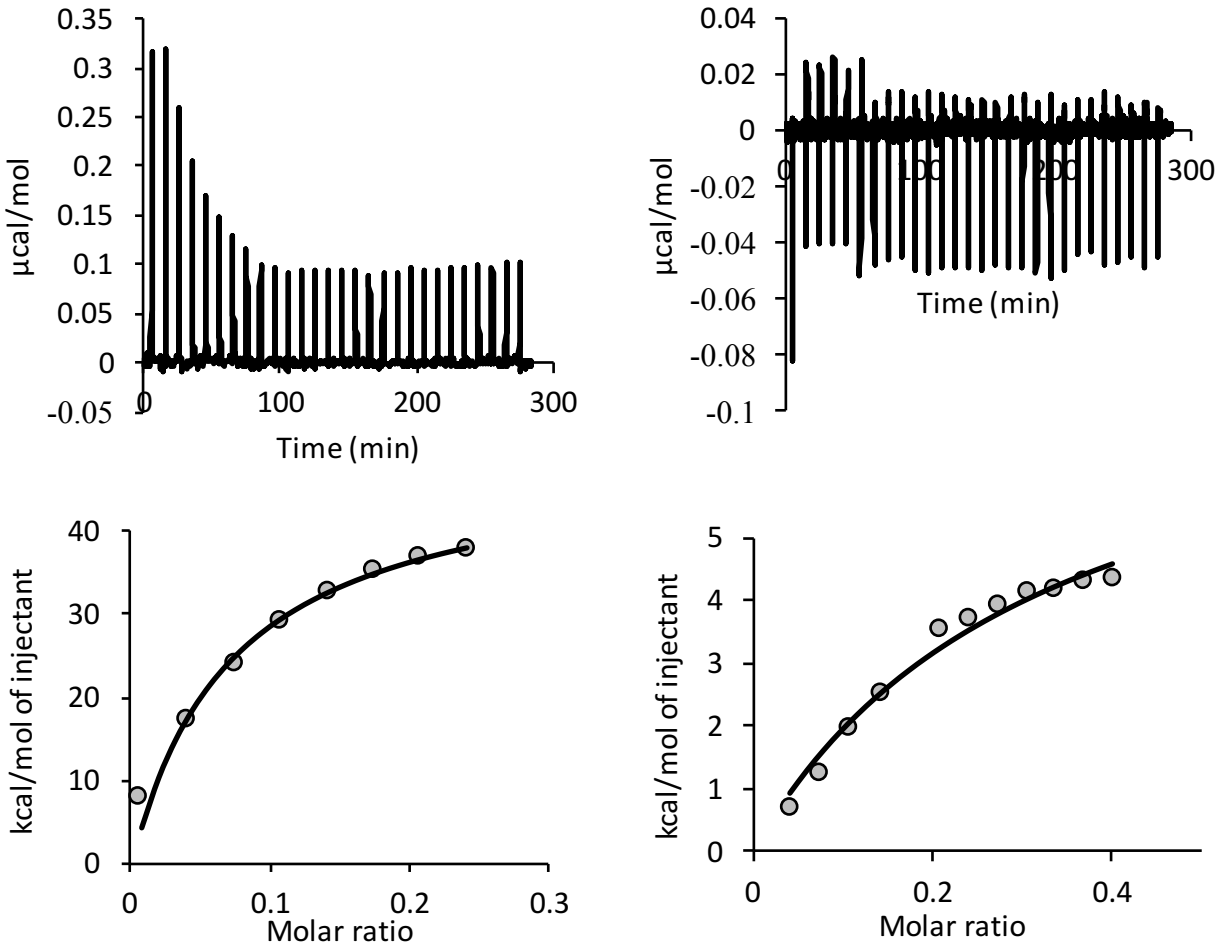

Figure 3.17. Raw thermograms (top panel) and cumulated molar enthalpy (bottom panel). Of ITC experiments conducted with DMPC:DPPC (3:1) liposomes and 20 µM of Frondoside A (left panel) or 50µM of raw saponin extract from *Quillaja saponaria* (right panel).

For all the tested modalities with the exception of holothuroid-like liposomes wish Frondoside A, the thermodynamic characteristics of the occurring interactions were calculated (Table 3.4; Fig. 3.18). The binding constants were significantly different between the experiments with the plant saponins and Frondoside A. The highest binding constant was obtained for fish liposomes (DPPC:DOPC:Chol) with Frondoside A (K=469.59±123.01 mM^{-1}). Binding constants of experiments involving the plant saponin extracted from *Quillaja saponaria*, were of the order of magnitude of 1 mM^{-1}, and were similar for the different liposomes. However, experiments with the holothuroid saponin Frondoside A, were in the order of magnitude of 500 mM^{-1} with fish-like liposomes and 40 mM^{-1} with holothuroid liposomes without sterol (Table 3.6). Although large variabilities were observed in some instances, values were always of the same order of magnitude, within a tested modality.

Table 3.6. Average binding constants (K) in mM^{-1} and standard deviations of ITC experiments conducted with Frondoside A and raw saponin extract from *Quillaja saponaria* bark.

	Fish Liposomes	Holothuroid Liposomes (W/o sterol)	Holothuroid Liposomes (W/ sterol)
Plant saponins	1.01 ±0.32	1.81±1.73	0.82±0.01
Frondoside A	469.59±123.01	37.39±33.55	NA

The free Gibbs energy of the different experiments were negative for all the tested modalities (Fig 3.18C). These energy values were more negative for the experiments with Frondoside A, than those with the plant saponin. The enthalpy values for the different experiments varied, and were negative for interactions with fish like liposomes and positive for interactions with holothuroid liposomes (with and with out sterol) (Fig. 3.18A). Finally the entropy values were greater than the absolute values of the respective enthalpies. In addition the entropy component of interactions with Frondoside A were greater than those with plant saponins (Fig. 3.18B).

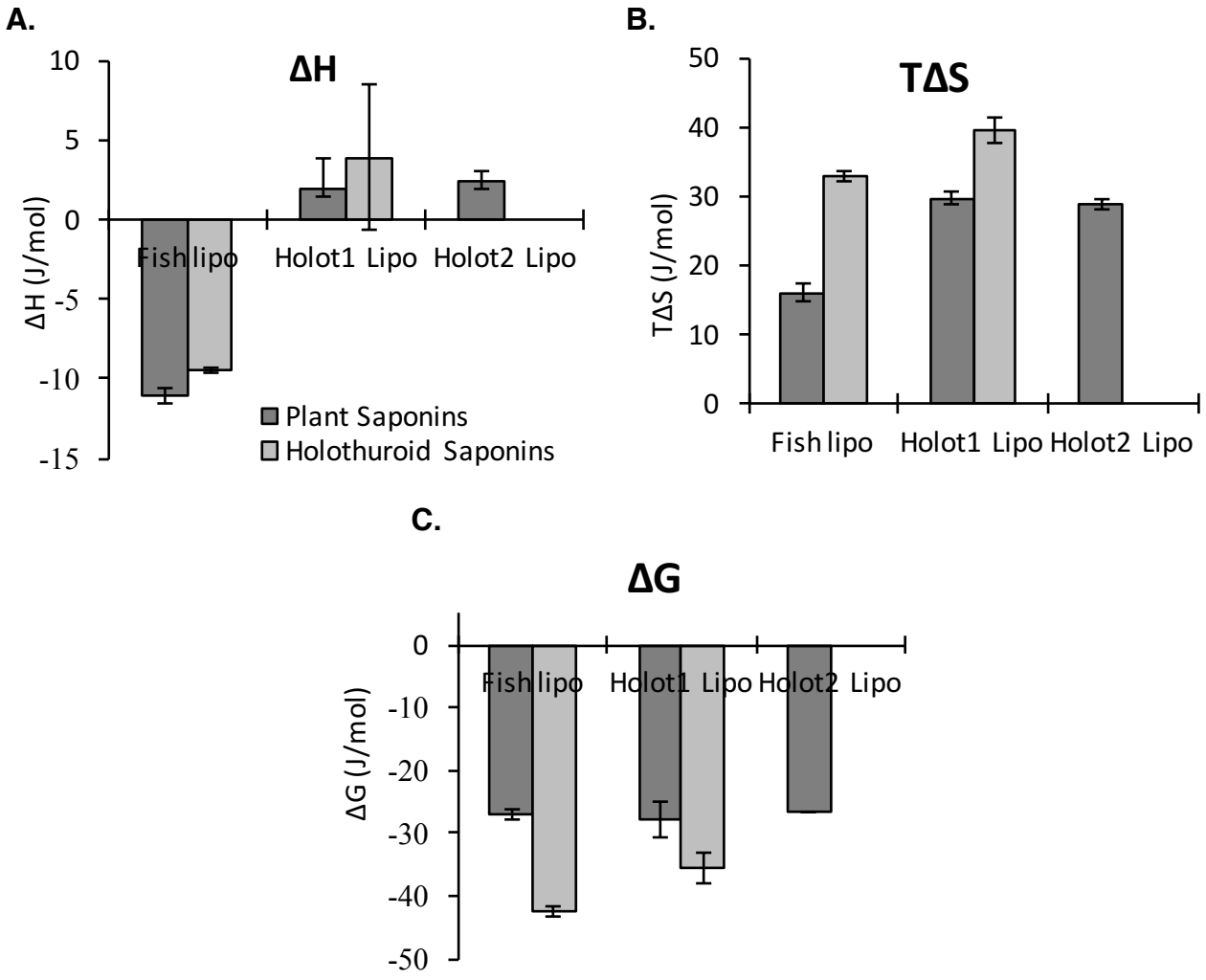

Figure 3.18. Graphic representation of the thermodynamic values (**A.** Enthalpy **B.** Entropy **C.** Free Gibbs Energy) associated with the different ITC experiments conducted using raw *Q.saponaria saponin* extract and Frondoside A an holothuroid saponin against different liposomes: Fish lipos: DPPC:DOPC:Chol (5:2:3), Holot1 Lipos: DMPC:DPPC (3:1), Holot2 Lipos: DMPC:DPPC: Δ^7 sterol (5:2:3).

4. Discussion

Extraction, purification and characterization of saponin in *H.scabra*

The mass spectra of the raw extract of sun-dried digestive tubes of *Holothuria scabra* revealed that 4 saponins were present, all of which have been previously described in this species. However to the best of my knowledge this is the first time that the saponin profile of the digestive system of *H.scabra* has been described. Previous studies on the saponin profile of the body wall and the conditioned water of this species have revealed similar saponin profiles (Table 4.1).

Table 4.1. Saponins previously described in *H. scabra*.

Digestive tubes (Present study)	Conditioned water (Caulier *et al.*, 2013a)	Bodywall (Caulier et al., 2013b)
Holothurinoside C	Holothurinoside C	Holothurinoside C
Scabrasie A	Scabraside A	Scabrasie A
Scabraside B	Scabraside B	Scabraside B
Desholothurine A	Holothurin A2	Desholothurine A
		Pervicoside C
		Holothurinoside G

* a volume of water that a sea cucumber has been left in for a given amount of time

Unfortunately the methodology of purification and isolation of a single saponin followed in this study was unsuccessful, or incomplete and not very efficient. It would seem that saponins have little affinity for C18 columns, as they exit the column soon after injection and poorly separated (coelution). Although this has been the standard column for LC/MS protocols for saponin isomer separation, it appeared that this column was less than ideal for the separation of different saponins. An ion exchange resin would be a better approach to separating these large amphiphilic molecules (Han *et al.*, 2009). Han's method uses a DA101 resin (Mitsubishi Chemical) designed for large molecules. It is a weak basic anion exchange resin that consists of dimethylamine functional groups. This kind of resin would be a better choice particularly for separating sulfated saponins, as the sulfate group is ionic in nature and typically associated with a sodium ion. A saponin solution would therefore interact more with the anion exchanging nature of the DA101 resin than a C18 column.

One of the reasons why the purification process was halted, was due to observed inconsistencies in replications over time. As illustrated in figure 3.4, HPLC separations conducted on "fresh" and one month old *H.scabra* extract solutions resulted in very different chromatograms. Although parallels can be drawn between the two chromatograms (multiple intense peaks early on in the elution), they were considered too different to continue the purification process. Some sort of sample degradation

took place between the first preparative experiments on 9 May 2017 and the second experiment on 23 June 2017. It should also be noted that between these two HPLC experiments we experienced very hot weather in Belgium, and the sample was being stored in aqueous solution in the HPLC injecting tray. It is also bizarre that the first chromatogram resulted in an interesting MS spectra (Fig. 3.5) whereas for the second nothing was detectable. This could be due to a significant degradation of saponin in the fractions due to thermal degradation of the initial sample, although the chromatogram still illustrated that something was absorbing at 210 nm, which is characteristic of holothuroid saponins, and uncommon amongst other molecule classes. It could have also been a problem of saponin concentration, and that the pooling of 5 runs instead of 8 runs was insufficient for detection. Although this also seems unlikely due to the high sensitivity of MALDI-ToF as a detector. The inconsistencies therefore remain difficult to explain. Further investigation needs to be conducted to develop better methods of saponin extraction, separation and purification.

Membrane-saponin interactions

Apolar interactions

The analysis of the data from the Hypermatrix, IMPALA simulations and ITC experiments suggest that the interactions that occur between saponins and membrane lipids were mostly apolar in nature.

An apolar interaction implies that the interactions between the lipids and the saponin were taking place between the apolar moieties of the two structures. Apolar interactions are defined as being due to a hydrophobic effect (Du *et al.*, 2016). The hydrophobic effect means that there is release of disordered water upon the aggregation of the two apolar moieties causing an increase in environmental entropy ($T\Delta S>0$) (Ben-Amotz *et al.*, 2008). This was first evidenced through the results obtained by the Hypermatrix calculations (Fig. 3.9), where the major component of all the studied interactions between saponins and membranes lipids was the apolar component. In addition the entropy-producing nature of these apolar interactions was observed in all ITC experiments as the entropic component of the free Gibbs energy was larger than the absolute value of the enthalpy component (Fig. 3.18).

The apolar nature of the interaction between saponins and lipids was further evidenced by the results of the IMPALA experiment (Fig. 3.11 and 3.12). Frondoside A had its aglycone moiety deep inside the apolar core of the lipid bilayer, reinforcing its hydrophobic interactions with the apolar tails of the phospholipids and rendering the complex the most stable.

Influence of saponin structure

The three saponins studied in the *in silico* biophysical experiments had similar structural formulas (Fig. 3.7). The lateral chain found on the C20 of the aglycone differed slightly for each of the three saponins studied (Fig. 3.7 and Fig. 4.1). Although this chain seemed to be important for the 3D conformation, the structural formula found in the literature for the same molecule name was

sometimes variable. For example, the Scabraside B molecule described by (Caulier *et al.*, (2013a) had a furan like pentane structure on the C20, whereas the Scabraside B molecule described by Han *et al.* (2009) has a 5-methyl-2-hexanone structure on the C20. Because Han *et al.* (2009) provided NMR justification for his structure description, this structure was used for the *in silico* experiments. More attention should be taken into account in future studies on the structural formula and stereo-chemistry of novel compounds.

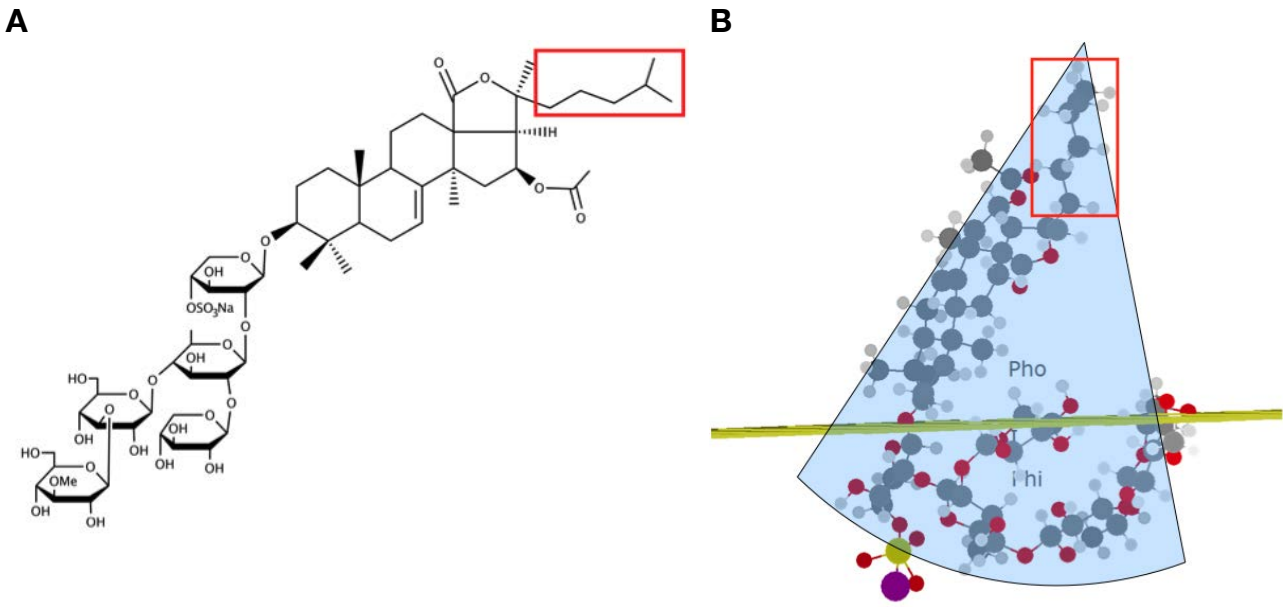

Figure 4.1. **A.** Structural formula of Frondoside A illustrating the position of the C20 lateral chain (red box) **B.** Illustration of the conical shape of Frondoside A. The yellow plane separates the hydrophobic and hydrophilic moieties of the molecule, the red boxes indicates the position go the C20 lateral chain.

The different 3D structures obtained from the structure tree minimization step resulted in different spatial configurations for the three saponins (Fig. 3.7). Scabraside B had a more spherical shape, most likely due to its higher density of oxygen in both its hydrophilic and the hydrophobic moiety compared to its non-sulfated counterpoint Desholothurine A, and to Frondoside A. In comparison Frondoside A and Desholothuine A both have more conical shapes, with a shallow, wide hydrophilic oligosaccharide moiety, and an elongated hydrophobic moiety (Fig. 4.1B). This conical shape has been previously related to the saponins ability to induce membrane curvature and pore formation (Lorent *et al.*, 2013). It is hypothesized that the glycoside residues could act like "umbrellas" shielding the cholesterol from water, and thereby enhancing the hydrophobic interaction between the saponin and the sterol and inhibiting polar interactions of the phospholipid heads with the sterol hydroxyl groups (Fig. 4.2). It is proposed that the interaction of a cone shaped saponin with cholesterol and an asymmetric lateral distribution of the saponin, induces curvature stress, resulting in membrane permeabilization and pore formation (Lorent *et al.,* 2013).

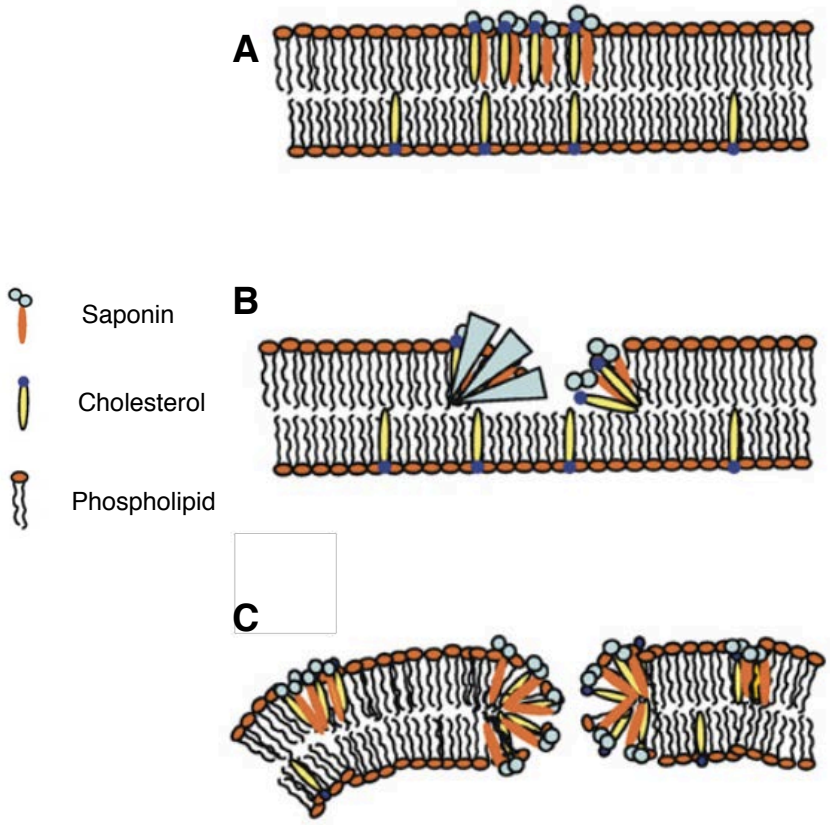

Figure 4.2. Model proposed for the interaction of saponin with lipid membranes**. *A.*** Interaction between saponins and cholesterol leads to the formation of regions with a higher saponin/ cholesterol concentration. **B.** Increase of spontaneous curvature in a transbilayer direction due to the sugar moiety of the saponin in these regions leads to permeabilization. **C.** The pore is stabilized by the sugar moieties pointing to the exterior of the membrane and reducing line tension, and a slight negative curvature in the direction of the membrane plane. The grey triangle illustrate the conical shape of saponin. Figure adapted from *Lorent et al.*, (2013).

This 3D conical structure of the saponin could perhaps explain the differences in membrane binding affinity and interaction thermodynamics observed during the ITC experiments. The two tested saponin solutions had very different magnitudes of binding constants to fish-like liposomes (DPPC:DOPC:Chol; 50:20:30), with Frondoside A having a binding constant of a magnitude of 500 mM^{-1}, whilst the saponin extract from *Quillaja saponaria* bark was only of 1-2 mM^{-1}. To compare, the plant derived surfactant Hexadecylbetainate chloride demonstrated a biding constant of 195 mM^{-1} for Sphingomyelin/cholesterol (50:50) liposomes (Zakanda *et al.*, 2012).

It is difficult to pinpoint the cause of the differences observed between these two saponins, as the *Q. saponaria* extract is a raw mixture of saponins. However it should be noted that the majority of the saponins in this mixture have 2 sugar substitutes, on opposing sides of the aglycone (Fig. 4.3) (Nyberg *et al.*, 2000), possibly rendering the hydrophobic/hydrophilic interface less distinguishable than that of Frondoside A, therefore inhibiting strong hydrophobic interactions.

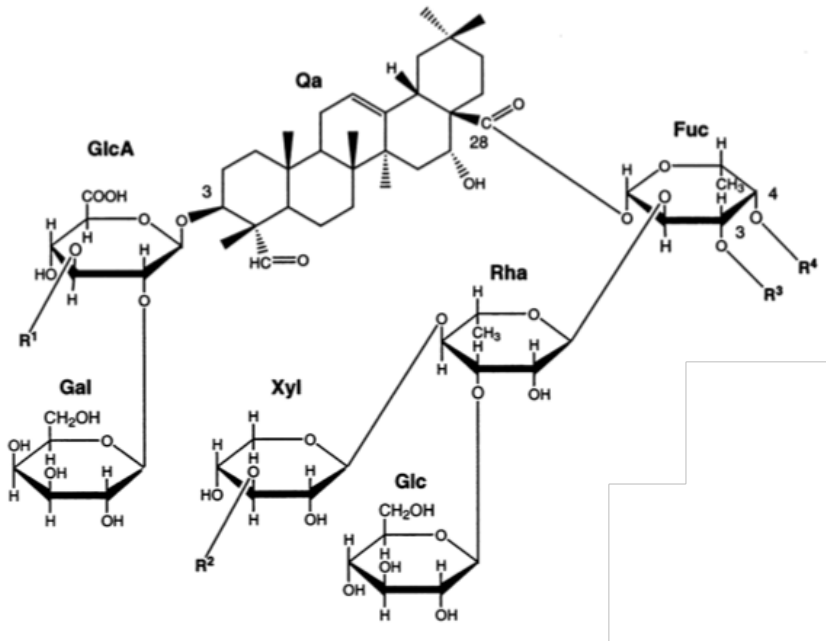

Figure 4.3. Backbone structure of saponins isolated from *Q.saponaria* (Nyberg *et al.*, 2000).

The influence of the saponin structure on membrane interactions was also investigated through the use of the HM method. The three saponins investigated differed in molar mass, atomic composition, and in 3D conformation (Table. 3.3; Fig. 3.7). However, no significant differences were observed in their interaction energies with lipids (Fig. 3.9), or in terms of their effect on monolayer lipid systems (Fig. 3.10). Previous studies have investigated structural diversity of saponins in function of their cytolytic activity, and have highlighted the hemolytic potency of saponins with a sulfate group attached at position 4 of the first xylose of the sugar moiety (Kalinin *et al.*, 1996), such as in Frondoside A and Scabraside B. However, a favorable interaction with sulfated saponin with the tested membrane lipids was not observed in the HM data obtained in the present study (Fig. 3.9). The lack of difference could be due to the limited PLs investigated in the present study. Other lipids, perhaps such as sphingomyelin could be more involved in the interaction and/or insertion of these molecules making them more potent.

The HM data suggested that the three tested saponins did not differ in their interaction affinity with the different monolayers of lipids, however differences in penetration were observed using the IMPALA method that was used to predict the insertion of the saponin into a model membrane. Similar energetic profiles for the two sulfated saponins, Scabraside B and Frondoside A, when traversing a DPPC bilayer were observed (Fig. 3.12), but due to the elongated structure of Frondoside A compared to the spheric shape of Scabraside B, the molecular models were quite different (Fig. 3.11).

Frondoside A had its aglycone moiety deep inside the apolar core of the lipid bilayer, reinforcing hydrophobic interactions with the apolar tails of the phospholipids, and had few atoms in contact with the polar heads of the PLs, rendering the molecule the most stable in the membrane among the three tested saponins.

In contrast Desholothurine A had a more horizontal position vis-a-vis the bilayer planes (Fig. 3.11), with a large part of its structure in contact with the polar heads of the PLs and Scabraside B, had very little contact with the PLs compared to the 2 other saponins with most of the spherical molecule located above the membrane/water interface (Fig. 3.11).

Since this does not agree with the fact that sulfated saponin are more cytotoxic, it cannot be assumed that the potency of a saponin is due to its ability to traverse a DPPC model membrane.

Overall the amphiphilic nature of saponins clearly inhibits these molecules from passively traversing a phospholipid bilayer. In addition the 3D cone-like structure of these molecule seem to play a role in reinforcing their interaction with PLs. This implies that the cytotoxic nature of this class of molecules is not due to a penetration action like certain biomolecules such as the wide spectrum drug ciprofloxacin that is most stable in the hydrophobic core of a DPPC model membrane (Bensikaddour *et al.*, 2008), but to a mechanism of membrane disruption that takes place at the water/membrane interface of the membrane.

Influence of sterol type

Membrane binding

Previous studies have consistently emphasized the necessity of cholesterol in saponin-membrane interactions (Bangham and Horne, 1962; Popov *et al.*, 2003; Augustin *et al.,* 2011), and have described this interaction as the “spontaneous formation of sterol-saponin complexes” possibly as a result of the observed lack of activity of saponins with cholesterol depleted liposomes. However, the results obtained from the Hypmermatrix calculation determined that saponin interactions are more energetically favorable with phospholipids than with sterols. In addition lipid monolayers (both phospholipid and sterol) were more energetically stable when saponin was the central molecule than in the absence of saponin (Fig. 3.9). It can not be assumed that saponins initially bind with PLs and not sterols, due to the docking (pre-fixed position) of the saponin amongst the PL monolayer in the HM procedure. However the HM results do suggest that the interactions of saponin with PLs are more favorable than those with sterols.

The ITC experiments with sterol-free liposomes resulted in thermograms with positive peaks, indicating that an endothermic reaction was taking place (Fig. 3.18). An endothermic reaction is characterized by the disruption of energetically favorable non-covalent interactions (Du *et al.*, 2016). This indicates that even though no cholesterol was present in the liposomes, saponins were disturbing the hydrophobic interactions of the PLs of the liposomes.

These results coupled with the observation of a similar reduction of the surface potential between liposomes with and with out cholesterol in the presence of the plant saponin α-hederin (Lorent *et al.*, 2013) suggest that saponin membrane binding is independent of cholesterol and that PLs may play an important role in the initial binding. The reduction in surface potential is caused by the incorporation of saponins into the membrane, and was measured in this study by the variation of the binding affinity of a fluorescent probe to the lipid surface (Domenech *et al.,* 2010), as a result of the membrane disruption.

It is therefore possible to conclude and corroborate more recent hypotheses, first proposed by Brain *et al.* (1990) suggesting that saponins bind spontaneously to phospholipids and do so independently of the presence of cholesterol (Augustin *et al.*, 2011; Lorent *et al*., 2013; 2014a, 2014b).

Membrane activity

The cytotoxic nature of Frondoside A is well documented (Kalinin *et al.,* 1996; Avilov *et al.*, 2007), and its potency against cancer cells has caused a rise in interest in this saponin (Aminin *et al.*, 2016; Moghadam *et al.,* 2016, Lorent *et al.*, 2016).

Understanding the molecular mechanism involved in this cytotoxic activity is critical and could be exploited for therapeutic applications in the future (Lorent *et al.,* 2013). It is also critical for understanding how holothuroids use saponins as a chemical means of defense against predators, pathogens and competitors, and how they manage to not be affected by the cytotoxicity of these metabolites.

Although permeability assays were not conducted in the present study, the results from the BM and ITC experiments confirmed previous findings that conclude that the presence of cholesterol is essential for a strong membrane activity. The ITC experiments of the interaction of Frondoside A with fish-like liposomes (*i.e.* containing cholesterol) resulted in a reaction that took place very rapidly making the processing of the thermogram very difficult, as saponin depletion occurred after only 3-4 injections (Fig. 3.16 left panel). The negative heat fluxes correspond to the release of heat due to an exothermic process that is characterized by the formation of energetically favorable non-covalent interactions between atoms (Du *et al*., 2016). The negative enthalpies therefore likely resulted from the formation of energetically favorable hydrophobic associations of saponin with cholesterol, these interactions also induce an increase in compactness in surrounding lipids, further favoring hydrophobic interactions. The interaction was also characterized by a negative free Gibbs energy, characteristic of a spontaneous reaction. The very large binding constant (400 mM^{-1}) observed for the binding of Frondoside A to fish-like liposomes, was 2x those of that of the plant derived surfactant hexadecylbetainate chloride to sphingomyelin:cholesterol (50:50) liposomes (195 mM^{-1}) (Zakanda *et al*., 2012).

The BM simulations were long calculations that allowed for the visualization of model monolayers with known lipid compositions at their most energetically stable configuration. In order to compare results with the literature, experimental conditions were replicated from Lorent *et al.* (2014a), who used α-Hederin, a plant saponin, and some of its derivatives. Frondoside A had a similar (not significantly different) effect on DMPC:Chol (75:25) systems to α-Hederin, resulting in the sequestration of cholesterol into larger domains (Fig. 3.13 C and D). Extensive experimental evidence observed and described by Lorent *et al.* (2013) concluded that this ability to induce domain aggregation generates curvature stress, which in turn causes membrane permeabilization and pore formation (Lorent *et al.*, 2013).

These results support the current hypothesis that the cytotoxic nature of saponins is due to the following sequence of events: (i) cholesterol-independent binding to the membrane, this step occurs spontaneously, driven by the lipophilic character of the aglycone; (ii) saponins then assemble into 1:1-complexes with membrane sterols (iii) saponin-sterol complexes accumulate into matrices or plaques by processes whose driving force is not currently understood (iv) finally as a consequence of such accumulation, the sterical properties of saponin induce curvature stress, resulting in membrane permeabilization and pore formation, as well as budding and the formation of a new lipid phase containing cholesterol, saponin, and phospholipids (Augustin *et al.*, 2011; Lorent *et al.*, 2013, 2014a).

Behavior of Δ7 Vs. cholesterol

Although cholesterol and the Δ^7-sterol are similar on paper, a 3D rendering of the molecules revealed that the slight differences in the 2D structure of the molecules had dramatic effects on their 3D conformation (Fig. 3.6). The Δ^7 bond of 5α-Cholest-7-en-3β-ol, resulted in the uplift of the aliphatic chain to an almost 90º angle. This fundamental difference in structure, was most certainly the cause for the differences observed in HM, BM and ITC experiments.

The differing structure of the sterols, resulted in different interacting behaviors and probably mechanisms with phospholipids and the saponin Frondoside A. This was observed in the results of the preliminary Hypermatrix calculations conducted to quantify the interactions necessary for the Big Monolayer experiment (Table. 3.5). This calculated Boltzmann energy for each interacting pair also allowed for the visualization of the nature of PL-sterol interactions being used for the simulation step. As the cholesterol interacted with phospholipids with its Beta face, the Δ^7 holothuroid sterol on the other hand were interacting with their alpha face (Fig.4.4).

To the best of my knowledge this is the first time that an holothuroid sterol has been modeled and its behavior simulated vis-a-vis phospholipids.

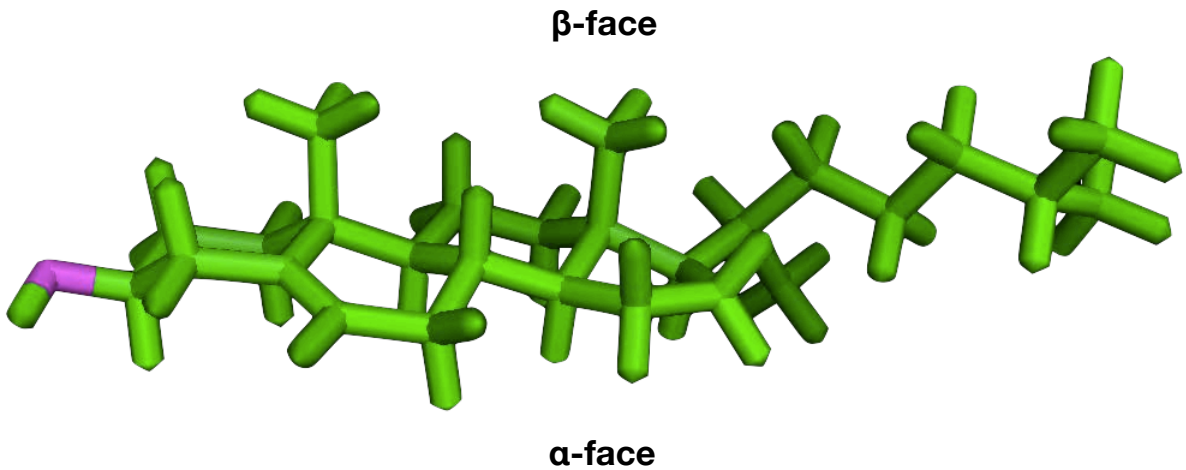

Figure 4.4. 3D representation of cholesterol, with an emphasis on the position of the β and α face of the sterol. The magenta atom indicates the position of the hydroxyl group.

The HM calculations revealed that interactions were more energetically favorable with cholesterol than with the Δ^7-sterol (Fig.3.9). This was also illustrated by the 3D models of the interacting molecules (difficult to depict in 2D figures). The HM models with a central saponin molecule surrounded by cholesterol were more "compact" than those surrounded by the holothuroid sterols, where 3 cholesterols were in close proximity to the central saponin. Models with the Δ^7 sterol surrounding the saponin were a lot less compact due to the steric hindrance of the "L" shaped sterol. In these systems only one sterol was in direct proximity to the central saponin, and the rest were more isolated, and had their aliphatic "foot" pointing outwards, away from the central molecule. This compactness was also detectable when regarding the different total system surface areas (Table 3.4). Although the HM method doesn't inform us of the permeabilizing potential of the saponin vis-a-vis a liposome, it does suggest the same differences in affinity between the saponin and the different sterols as Popov *et al.* (1983). In an investigation of the membrane-lytic action of a holothuroid saponin on egg yolk PC liposomes infused with cholesterol, and the same Δ^7 and Δ^9-sterols studied in the present study, holothuroid saponins were not able to permeabilize phospholipid membranes containing the holothuroid sterols (Popov *et al.* 2003).

Differing ITC results for lipid systems containing cholesterol, and systems containing the rare Δ^7 holothuroid sterol: 5α-Cholest-7-en-3β-ol were obtained. If the interactions of saponins with fish-like liposomes were exothermic the interactions of the same saponin with holothuroid-like liposomes were endothermic. This indicates that the interaction of saponins with fish-like liposomes were causing the formation of energetically favorable non-covalent interactions, possibly due to the hydrophobic interactions of the saponins aglycone with cholesterol and the apolar core of the lipid bilayer. In contrast the endothermic interactions of saponin with holothuroid-like liposomes suggest the disruption of energetically favorable non-covalent interactions. This maybe due to the disruption or rearrangement of the lipid bilayer that could correspond to the fragmentation of the large sterol domains, as seen in the BM results on a monolayer of the same composition (Fig.3.13).

The BM simulations regarding the influence of sterol type on saponin-lipid interaction were very revealing (Fig. 3.13). Firstly it was noted that Δ^7-sterols behave quite similarly to cholesterol in a simple binary system with DMPC (Fig. 3.13 A and B), although these are not realistic systems, it does allow for a "control" simulation. Once Frondoside A was added to the systems, the resulting sterol distribution and domain size were significantly different. The addition of Frondoside A to cholesterol resulted in the sequestration of the cholesterol into larger domains, similarly to the observed effect of the plant saponin α-Hederin (Fig.3.13 C and D). However, in great contrast to this domain expansion, the addition of Frondoside A to the Δ^7-sterols resulted in the creation of numerous small irregular clusters.

This fragmented sterol profile observed in membranes composed of DMPC, Δ^7-sterol and saponin were very similar to that observed for a system of DMPC, cholesterol and a sugar-less α-Hederin derivative, called Hederagenin (Fig.3.13 E). *In vitro* experiments (Lorent *et al.,* (2014) showed that Hederagenin:

1) did not significantly increase cell death regardless of the cholesterol content.

2) did not cause the release of calcein regardless of the cholesterol content, the time, or the hederagenin/lipid molar ratio.
3) was unable to induce permeation of FITC-dextran (4 kDa) even after 24 h of incubation.
4) induced neither membrane deformation nor reduction in the size of the Giant unilamellar Vesicles (GUVs), but sometimes it induced the formation of intravesicular buds.
5) did not cause any pore formation.

In brief, removing the sugar from the saponin made the saponin much less active against model plasma membranes.

It is already known and demonstrated that Frondoside A is cytotoxic (Kalinin *et al.,* 1996; Avilov *et al*., 2007), and has similar cytotoxic activities to α-Hederin (Lorent *et al.*, 2016). Frondoside A could therefore not be the cause for the divergent sterol behavior observed between figure 3.13 C and F *i.e*. the agglomeration of cholesterol domains, and the fragmentation of Δ^7-sterol domains. The Δ^7-sterol was thus responsible for the change in behavior of Frondoside A. It can be hypothesized that Δ^7-sterol somehow inhibits the "sterol-agglomerating" activity of Frondoside A.

Explaining the "bizarre" thermogram

The bizarre thermodynamic phenomena occurring in figure 3.16, as holothuroid liposomes are titrated into a frondoside A solution were perplexing, and mathematically impossible to treat and extract thermodynamic data from. However, the heat flow profiles were identical in all 3 replicates, decreasing the likelihood of an experimental error or equipment failure and suggesting the occurrence of a new phenomenon in the measuring cell.

The results from the BM simulation have indeed highlighted a significant difference in behavior between cholesterol and Frondoside A, and Δ^7-sterol and Frondoside A. As illustrated in figure 3.14, a concentration of 5% of saponin was sufficient for fragmenting the Δ^7-sterol domains.

The following series of events can be hypothesized:

Before the injection of the holothuroid-like liposomes into the saponin solution, the liposomes are dotted with sterol domains (Fig. 3.14, top right panel). However upon arrival into the saponin solution, similarly to the fish-like liposome experiment, the saponins spontaneously bind the PLs, and there is a depletion of saponin in solution in the measuring cell. However, the wave like heat flux variations that occurred after liposome saturation could be due to the rearrangement and energy minimization of the liposomes that have integrated saponin. This minimization resulted in the same small sterol clusters observed in the BM simulations (Fig. 3.14, bottom right panel). New incoming liposomes no longer interacted with saponins as there has been complete depletion of the saponin solution beforehand. However, once the saponin-free liposome concentration reaches a certain threshold in the measuring cell, a phenomena of agglomeration between liposomes occuors. This results in the increasing heat flux trend seen towards the end of the ITC reaction after each new injection (Fig. 4.4).

This hypothesis remains so far purely speculative, and based heavily on results from an *in silico* experiment that has not been validated using *in vitro* techniques for Δ^7-sterols. The following

should therefore be considered with caution. It would seem that Δ^7-sterols have a high affinity for themselves and can cause significant phase separation (Fig. 3.13 and 3.14). Large domains of a liquid ordered phase, enriched in the sterol could cause the compression of the PLs (DPPC) of the liquid ordered phase that is depleted of sterol. This compression leads to the formation of thicker membrane zones and can cause curvature stress, and may cause membrane rupture (Lorent *et al.*, 2013).

Therefore what was observed in the BM experiments, but also in the ITC results suggests that the saponin-Δ^7-sterol pair may be an adaptation required for holothuroid membranes to inhibit the "sterol-agglomerating" activity of saponin. It should be emphasized that this is an interpretation that needs to be validated and tested.

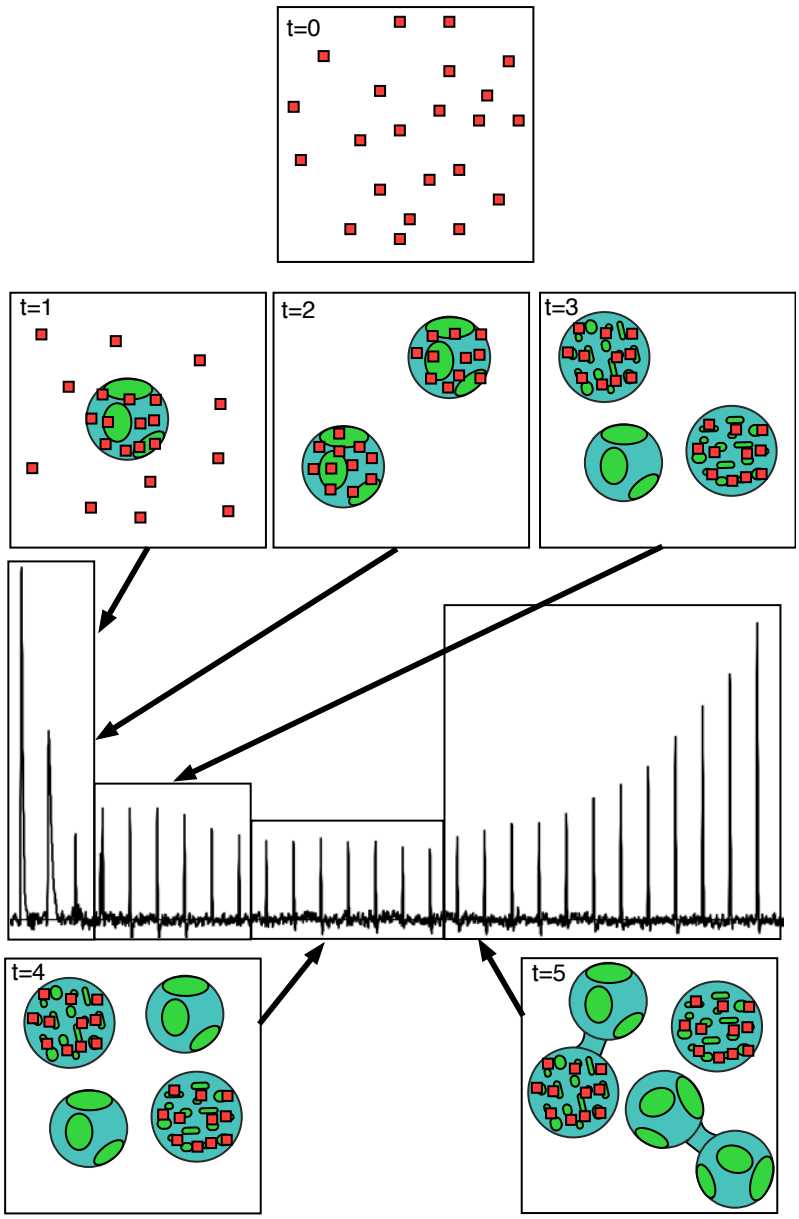

Figure. 4.5. Proposed interaction mechanism to describe the strange ITC thermogram of the titration of a 5mM solution of holothuroid like liposomes (DMPC:DPPC:Δ7; 50:20:30) into a 17μM solution of the holothuroid saponin Frondoside A. t=0; t=1 saponins spontaneously bind the PLs, and there is a depletion of saponins in solution in the measuring cell t=2. t=3 A dynamic phenomena, perhaps due to saponins causing the breakup of sterol domains into smaller domains. t=4 the titration of liposomes continues, but no reaction occurs due to depletion of saponins, the heat flow corresponds to the heat of dilution. t=5 after a threshold concentration of liposomes in the measuring cell, they aggregate.

5. Conclusion

Although it has long been accepted that holothuroid immunity to the potent cytotoxic saponins they produce is due to their rare membrane sterols, the molecular reasoning behind this has never been described let alone considered.

The present study has described the structural differences of these sterols compared to the mammalian membrane sterol cholesterol. The interactions of these sterols have been investigated in relation to phospholipid monolayer systems resembling those of liposomes used in *in vitro* experiments. In addition fish-like and holothuroid-like lipid systems were investigated under the addition of the saponin Frondoside A, both by *in silico*, and *in vitro* means. I have interpreted these findings, and have suggested the following hypothesis: Sea cucumbers may require the presence of their saponins, in order to inhibit the formation of large disruptive sterol domains. It would seem that the Δ^7-sterol inhibits the “sterol-agglomerating” activity of saponins.

This hypothesis remains speculative and will need further investigation in future research. The first test to be conducted will be an examination of the permeabilization of the two types of liposomes (fish-like and holothuroid-like) in the presence of Frondoside A. This consists of following the changes of fluorescence of a solution of liposomes encapsulating calcein at a self quenching concentration. The leakage and therefore dilution of calcein, causes an increase fluorescence (Deleu *et al.*, 2014), allowing to monitor the permeabilization of the liposomes, or lack there of in the presence of Frondoside A. Similar experimental conditions could be used as Lorent *et al.*, (2014a), who studied the affect of α-Hederin on liposomes containing cholesterol, ergosterol, and stigmasterol, the major sterols of mammals, fungi, and plants, respectively.

There is a whole panoply of biophysical *in vitro* experiments that could be conducted with these liposomes and this holothuroid saponin, to complete the comprehension of the mechanisms behind holothuroids immunity agains saponins. However the limiting factor is the price of the holothuroid saponin, it is therefore crucial to develop an adapted method for extracting and purifying saponin from a sustainable source for continuing this investigation

In addition to completing the *in vitro* aspect of this investigation, more advanced *in silico* experiments could be conducted. The use of molecular dynamics could allow for a better comprehension of how membrane-saponin interactions are initiated. To predict the how and the where of the initial steps of a saponin approaching a bilayer membrane.

6. Cited References

Abraham, T., Lewis, R.N.A.H., Hodges, R.S. & McElhaney, R.N. (2005) Isothermal Titration Calorimetry Studies of the Binding of the Antimicrobial Peptide Gramicidin S to Phospholipid Bilayer Membranes. Biochemistry. 44 (33), pp. 11279–11285.

Al-Wahaibi, M.K. & Claereboudt, M.R. (2017) Extraocular vision in the sea urchin *Diadema setosum*. Marine and Freshwater Behaviour and Physiology. pp. 1–10.

Althunibat, O., Ridzwan, B., Taher, M., Daud, J., Jauhari Arief Ichwan, S. & Qaralleh, H. (2013) Antioxidant and cytotoxic properties of two sea cucumbers, *Holothuria edulis* (Lesson) and *Stichopus horrens* (Selenka). Acta Biologica Hungarica. 64 (1), pp. 10–20.

Aminin, D., Menchinskaya, E., Pisliagin, E., Silchenko, A., Avilov, S. & Kalinin, V. (2015) Anticancer Activity of Sea Cucumber Triterpene Glycosides. Marine Drugs. 13 (3), pp. 1202–1223.

Aminin, D., Pislyagin, E., Astashev, M., Es'kov, A., Kozhemyako, V., Avilov, S., Zelepuga, E., Yurchenko, E., Kaluzhskiy, L., Kozlovskaya, E., Ivanov, A. & Stonik, V. (2016) Glycosides from edible sea cucumbers stimulate macrophages via purinergic receptors. Scientific Reports. pp. 1–11.

Armah, C.N., Mackie, A.R., Roy, C., Price, K., Osbourn, A.E., Bowyer, P. & Ladha, S. (1998) The Membrane-Permeabilizing Effect of Avenacin A-1 Involves the Reorganization of Bilayer Cholesterol. Biophysical Journal. 76pp. 281–290.

Augustin, J.R.M., Kuzina, V., Andersen, S.B. & Bak, S. (2011) Molecular activities, biosynthesis and evolution of triterpenoid saponins. Phytochemistry. 72 (6), pp. 435–457.

Avilov, S.A., Kalinin, V.I., Silchenko, A.S., Aminin, D.L., Agafonova, I.G., Stonik, V.A., Collin, P.D. & Woodward, C. (2007) Process for isolating sea cucumber saponin Frondoside A, and immunomodulatory methods of use. (11/145,580) pp. 1–18.

Bahrami, Y. & Franco, C. (2016) Acetylated Triterpene Glycosides and Their Biological Activity from Holothuroidea Reported in the Past Six Decades. Marine Drugs. 14 (8), pp. 147–38.

Bahrami, Y. & Franco, C. (2015) Structure Elucidation of New Acetylated Saponins, Lessoniosides A, B, C, D, and E, and Non-Acetylated Saponins, Lessoniosides F and G, from the Viscera of the Sea Cucumber *Holothuria lessoni*. Marine Drugs. 13 (1), pp. 597–617.

.Bangham, A.D. & Horne, R.W. (1962) Action of saponin on biological cell membranes. Nature. 196pp. 952–953.

Baumann, E., Stoya, G., Völkner, A., Richter, W., Lemke, C. & Linss, W. (2000) Hemolysis of human erythrocytes with saponin affects the membrane structure. Acta Histochemica. 102 (1), pp. 21–35.

Bell, M.V., Henderson, R.J. & Sargent, J.R. (1986) The Role of Polyunsaturated Fatty Acids in Fish. Comp. Biochem Physiol. 83B (4), pp. 711–719.

Ben-Amotz, D. & Underwood, R. (2008) Unraveling Water's Entropic Mysteries: A Unified View of Non-polar, Polar, and Ionic Hydration. Accounts of Chemical Research. 41 (8), pp. 957–967.

Bensikaddour, H., Fa, N., Burton, I., Deleu, M., Lins, L., Schanck, A., Brasseur, R., Dufrêne, Y.F., Goormaghtigh, E. & Mingeot-Leclercq, M.-P. (2008) Characterization of the Interactions between Fluoroquinolone Antibiotics and Lipids: a Multi-technique Approach. Biophysical Journal. 94 (8), pp. 3035–3046.

Berenbaum, M.R. (1995) The chemistry of defense: Theory and practice. Proceedings of the National Academy of Sciences. 92pp. 2–8.

Blunt, J.W., Copp, B.R., Keyzers, R.A., Munro, M.H.G. & Prinsep, M.R. (2015) Marine natural products. Natural Product Reports. 32pp. 116–211.

Bombardelli, E., Patri, G. & Pozzi, R. (1992) Complexes of sapoins and their aglycons with phospholipids and pharmaeutical and cosmetic compositions containing them. (643,791) pp. 1–3.

Bondoc, K.G.V., Lee, H., Cruz, L.J., Lebrilla, C.B. & Juinio-Meñez, M.A. (2013) Chemical fingerprinting and phylogenetic mapping of saponin congeners from three tropical holothurian sea cucumbers. Comparative Biochemistry and Physiology, Part B. 166 (3-4), pp. 182–193.

Bordbar, S., Anwar, F. & Saari, N. (2011) High-Value Components and Bioactives from Sea Cucumbers for Functional Foods—A Review. Marine Drugs. 9 (12), pp. 1761–1805.

Bourlat, S.J., Juliusdottir, T., Lowe, C.J., Freeman, R., Aronowicz, J., Kirschner, M., Lander, E.S., Thorndyke, M., Nakano, H., Kohn, A.B., Heyland, A., Moroz, L.L., Copley, R.R. & Telford, M.J. (2006) Deuterostome phylogeny reveals monophyletic chordates and the new phylum Xenoturbellida. Nature. 444 (7115), pp. 85–88.

Brain, K., Hadgraft, J. & Al-Shatalebi, M. (1990) Membrane Modification in Activity of Plant Moluscicides. Planta Medica. 56pp. 663.

Brasseur, L., Parmentier, E., Caulier, G., Vanderplanck, M., Michez, D., Flammang, P., Gerbaux, P., Lognay, G. & Eeckhaut, I. (2016) Mechanisms involved in pearlfish resistance to holothuroid toxins. Marine Biology. pp. 1–14.

Brasseur, R., Killian, J.A., De Kruijff, B., Ruysschaert, J.M. (1987) Conformational analysis of gramicidin–gramicidin interactions at the air/water interface suggests that gramicidin aggregates into tube-like structures similar as found in the gramicidin-induced hexagonal HII phase. Biochim. Biophys. Acta 903, pp.11–17.

Bruhn, T., Schaller, C., Schulze, C., Sanchez-Rodriguez, J., Dannmeier, C., Ravens, U., Heubach, J.F., Eckardt, K., Schmidtmayer, J., Schmidt, H., Aneiros, A., Wachter, E. & Béress, L. (2001) Isolation and characterisation of five neurotoxic and cardiotoxic polypeptides from the sea anemone. Toxicon. 39pp. 693–702.

Cacas, J.-L., Buré, C., Grosjean, K., Gerbeau-Pissot, P., Lherminier, J., Rombouts, Y., Maes, E., Bossard, C., Gronnier, J., Furt, F., Fouillen, L., Germain, V., Bayer, E., Cluzet, S., et al. (2016) Revisiting Plant Plasma Membrane Lipids in Tobacco: A Focus on Sphingolipids. PLANT PHYSIOLOGY. 170 (1), pp. 367–384.

Caulier, G., Van Dyck, S., Gerbaux, P., Eeckhaut, I. & Flammang, P. (2011) Review of saponin diversity in sea cucumbers belonging to the family Holothuriidae. SPC Beche-de-mer Information Bulletin. 31pp. 48–54.

Caulier, G., Flammang, P., Gerbaux, P. & Eeckhaut, I. (2013a) When a repellent becomes an attractant: harmful saponins are kairomones attracting the symbiotic Harlequin crab. Scientific Reports. 3pp. 1–6.

Caulier, G., Guilla, Flammang, P., Rakotorioa, P., Gerbaux, P., Demeyer, M. & Eeckhaut, I. (2013b) Preservation of the bioactive saponins of Holothuria scabra through the processing of trepang. 54pp. 685–690.

Caulier, G., Mezali, K., Soualili, D.L., Decroo, C., Demeyer, M., Eeckhaut, I., Gerbaux, P. & Flammang, P. (2016) Chemical characterization of saponins contained in the body wall and the Cuvierian tubules of the sea cucumber *Holothuria* (Platyperona) *sanctori* (Delle Chiaje, 1823). Biochemical Systematics and Ecology. 68 (C), pp. 119–127.

Chalorak, P., Jattujan, P., Nobsathian, S., Poomtong, T., Sobhon, P. & Meemon, K. (2017) Holothuria scabra extracts exhibit anti-Parkinson potential in C. elegans: A model for anti-Parkinson testing. Nutritional Neuroscience. 6 (3), pp. 1–12.

Chen, R.J., Chung, T.-Y., Li, F.-Y., Lin, N.-H. & Tzen, J.T. (2008) Effect of sugar positions in ginsenosides and their inhibitory potency on Na+/K+-ATPase activity. Acta Pharmacologica Sinica. 30 (1), pp. 61–69.

Chwalek, M., Lalun, N., Bobichon, H., Plé, K. & Voutquenne-Nazabadioko, L. (2006) Structure–activity relationships of some hederagenin diglycosides: Haemolysis, cytotoxicity and apoptosis induction. Biochimica et Biophysica Acta (BBA) - General Subjects. 1760 (9), pp. 1418–1427.

Conand, C. (1979) Beche-de-mer in New Caledonia; weight loss and shrinkage during processing in three species of holothurians. SPC Fisheries Newsletter, 19: 14-17.

Conand, C. (2004) Present status of world sea cucumber resources and utilisation : an international overview. In: Advances in sea cucumber aquaculture and management. (A. Lovatelli, C. Conand, S. Purcell, S. Uthicke, J.-F. Hamel & A. Mercier eds), pp. 13-23. FAO Fisheries Technical Paper No. 463. Rome.

Coppard, S.E. & Campbell, A.C. (2004) Taxonomic significance of spine morphology in the echinoid genera Diadema and Echinothrix. Invertebrate Biology. 123 (4), pp. 357–371.

Coulon, P. & Jangoux, M. (1993) Feeding rate and sediment reworking by the holothuroid *Holothuria tubulosa* (Echinodermata) in a Mediterranean seagrass bed off Ischia Island, Italy. Marine Ecology Progress Series. 92pp. 201–204.

Cuypers, E., Yanagihara, A., Karlsson, E. & Tytgat, J. (2006) Jellyfish and other cnidarian envenomations cause pain by affecting TRPV1 channels. FEBS Letters. 580 (24), pp. 5728–5732.

Decroo, C. (2014) Etude des saponines d'*Holothuria forskali* par spectrométrie de masse: Diversité moléculaire et distribution inter-organe. Masters thesis. University of Mons.

de Groot, C. & Müller-Goymann, C. (2016) Saponin Interactions with Model Membrane Systems – Langmuir Monolayer Studies, Hemolysis and Formation of ISCOMs. Planta Medica. 82 (18), pp. 1496–1512.

Deleu, M., Lorent, J., Lins, L., Brasseur, R., Braun, N., Kirat, El, K., Nylander, T., Dufrêne, Y.F. & Mingeot-Leclercq, M.-P. (2013) Effects of surfactin on membrane models displaying lipid phase separation. BBA - Biomembranes. 1828 (2), pp. 801–815.

Deleu, M., Crowet, J.-M., Nasir, M.N. & Lins, L. (2014) Complementary biophysical tools to investigate lipid specificity in the interaction between bioactive molecules and the plasma membrane: A review. BBA - Biomembranes. 1838 (12), pp. 3171–3190.

Demeyer, M., De Winter, J., Caulier, G., Eeckhaut, I., Flammang, P. & Gerbaux, P. (2014) Molecular diversity and body distribution of saponins in the sea star *Asterias rubens* by mass spectrometry. Comparative Biochemistry and Physiology, Part B. 168 (C), pp. 1–11.

Demeyer, M., Wisztorski, M., Decroo, C., De Winter, J., Caulier, G., Hennebert, E., Eeckhaut, I., Fournier, I., Flammang, P. & Gerbaux, P. (2015) Inter- and intra-organ spatial distributions of sea star saponins by MALDI imaging. Analytical and Bioanalytical Chemistry. 407 (29), pp. 8813–8824.

DePierre, J.W. & Karnovsky, M.L. (1973) Plasma membranes of mammalian cells. The Journal of Cell Biology. 56pp. 275–303.

Dewi, A., Cheney, K., Urquhart, H., Blanchfield, J. & Garson, M. (2016) The Sequestration of Oxy-Polybrominated Diphenyl Ethers in the Nudibranchs *Miamira magnifica* and *Miamira miamirana*. Marine Drugs. 14 (12), pp. 198–198.

Dobretsov, S., Al-Wahaibi, A.S.M., Lai, D., Al-Sabahi, J., Claereboudt, M., Proksch, P. & Soussi, B. (2015) Inhibition of bacterial fouling by soft coral natural products. International Biodeterioration & Biodegradation. 98 (C), pp. 53–58.

Domenech, Ò., Dufrêne, Y.F., Van Bambeke, F., Tukens, P.M. & Mingeot-Leclercq, M.-P. (2010) Interactions of oritavancin, a new semi-synthetic lipoglycopeptide, with lipids extracted from *Staphylococcus aureus*. BBA - Biomembranes. 1798 (10), pp. 1876–1885.

Du, X., Li, Y., Xia, Y.-L., Ai, S.-M., Liang, J., Sang, P., Ji, X.-L. & Liu, S.-Q. (2016) Insights into Protein–Ligand Interactions: Mechanisms, Models, and Methods. International Journal of Molecular Sciences. 17 (2), pp. 144–34.

Ducarme, P., Rahman, M. & Brasseur, R. (1998) IMPALA: A Simple Restraint Field to Simulate the Biological Membrane in Molecular Structure Studies. Proteins Structure, Function and Genetics. 30pp. 357–371.

Dufourc, E.J. (2008) Sterols and membrane dynamics. Journal of Chemical Biology. 1 (1-4), pp. 63–77.

Ebel, R. (2010) Terpenes from Marine-Derived Fungi. Marine Drugs. 8 (8), pp. 2340–2368.

Eeckhaut, I., Caulier, G., Brasseur, L., Flammang, P., Gerbaux, P. & Parmentier, E. (2015) Effects of Holothuroid Ichtyotoxic Saponins on the Gills of Free-Living Fishes and Symbiotic Pearlfishes. 228pp. 253–265.

Elyakov, G.B., Stonik, V.A., Levina, E.V., Slanke, V.P., Kuznetsoza, T.A. & Levin, V.S. (1972) Glycosiddes of marine invertebrates- A comparative study of the glycoside fractions of pacific sea cucumbers. 44Bpp. 325–336.

Fernández-Tejada, A., Chea, E.K., George, C., Pillarsetty, N., Gardner, J.R., Livingston, P.O., Ragupathi, G., Lewis, J.S., Tan, D.S. & Gin, D.Y. (2014) Development of a minimal saponin vaccine adjuvant based on QS-21. Nature Chemistry. 6 (7), pp. 635–643.

Ferrari, M.C.O., Wisenden, B.D. & Chivers, D.P. (2010) Chemical ecology of predator–prey interactions in aquatic ecosystems: a review and prospectusThe present review is one in the special series of reviews on animal–plant interactions. Canadian Journal of Zoology. 88 (7), pp. 698–724.

Flammang, P. (2002) Biomechanics of Adhesion in Sea Cucumber Cuvierian Tubules (Echinodermata, Holothuroidea). Integrative and Comparative Biology. 42 (6), pp. 1107–1115.

Friedman, M. (2006) Potato Glycoalkaloids and Metabolites: Roles in the Plant and in the Diet. Journal of Agricultural and Food Chemistry. 54 (23), pp. 8655–8681.

Friess, S.L., Durant, R.C. & Chanley, J.D. (2002) Further studies on biological actions of steroidal saponins produced by poisonous echinoderms. pp. 1–12.

Fürstenberg-Hägg, J., Zagrobelny, M., Jørgensen, K., Vogel, H., Møller, B.L. & Bak, S. (2014) Chemical Defense Balanced by Sequestration and *De Novo* Biosynthesis in a Lepidopteran Specialist Emmanuel Gaquerel (ed.). PLOS ONE. 9 (10), pp. e108745–e108749.

Gauthier, C., Legault, J., Girard-Lalancette, K., Mshvildadze, V. & Pichette, A. (2009) Haemolytic activity, cytotoxicity and membrane cell permeabilization of semi-synthetic and natural lupane- and oleanane-type saponins. Bioorganic & Medicinal Chemistry. 17 (5), pp. 2002–2008.

Genta-Jouve, G., Boughanem, C., Ocaña, O., Pérez, T. & Thomas, O.P. (2015) Eryloside W, a triterpenoid saponin from the sponge *Dictyonella marsilii*. Phytochemistry Letters. 13pp. 252–255.

Gershenzon, J. & Dudareva, N. (2007) The function of terpene natural products in the natural world. Nature Chemical Biology. 3 (7), pp. 408–414.

Ghai, R., Falconer, R.J. & Collins, B.M. (2011) Applications of isothermal titration calorimetry in pure and applied research-survey of the literature from 2010. Journal of Molecular Recognition. 25 (1), pp. 32–52.

Giner, R.-M., Villalba, M.-L., Recio, M.-C., Manez, S., Cerda-Nicolas, M. & Rios, J.-L. (2000) Anti-inflammatory glycoterpenoids from Scrophularia auriculata. European Journal of Pharmacology. 389pp. 243–252.

Goodheart, J.A. & Bely, A.E. (2016) Sequestration of nematocysts by divergent cnidarian predators: mechanism, function, and evolution. Invertebrate Biology. 136 (1), pp. 75–91.

Hamel, J.-F., Conand, C., Pawson, D.L. & Mercier, A. (2001) The sea cucumber *Holothuria scabra* (Holothuroidea: Echinodermata): Its biology and exploitation as Beche-de-mer. In: Advances in Marine Biology Volume 41. Advances in Marine Biology. Elsevier. pp. pp. 129–223. doi:10.1016/S0065-2881(01)41003-0.

Han, H., Yi, Y., Xu, Q., La, M. & Zhang, H. (2009) Two New Cytotoxic Triterpene Glycosides from the Sea Cucumber Holothuria scabra. Planta Medica. 75 (15), pp. 1608–1612.

Hay, M.E. (1996) Marine chemical ecology: what's known and what's next? Journal of experimental marine ecology. 200pp. 103–134.

He, R., Wakimoto, T., Takeshige, Y., Egami, Y., Kenmoku, H., Ito, T., Wang, B., Asakawa, Y. & Abe, I. (2012) Porphyrins from a metagenomic library of the marine sponge *Discodermia calyx*. Molecular BioSystems. 8 (9), pp. 2334–2335.

Heerklotz, H. & Seelig, J. (2000) Titration calorimetry of surfactant-membrane partitioning and membrane solubilization. Biochimica et Biophysica Acta. 1508pp. 69–85.

Heerklotz, H., Tsamaloukas, A.D. & Keller, S. (2009) Monitoring detergent-mediated solubilization and reconstitution of lipid membranes by isothermal titration calorimetry. Nature Protocols. 4 (5), pp. 686–697.

Ivanchina, N.V., Kicha, A.A., Malyarenko, T.V., Kalinovsky, A.I., Dmitrenok, P.S. & Stonik, V.A. (2013) Biosynthesis of polar steroids from the Far Eastern starfish *Patiria* (=Asterina) *pectinifera*. Cholesterol and cholesterol sulfate are converted into polyhydroxylated sterols and monoglycoside asterosaponin P1 in feeding experiments. Steroids. 78 (12-13), pp. 1183–1191.

Iyengar, E.V. & Harvell, C.D. (2001) Predator deterrence of early developmental stages of temperate lecithotrophic asteroids and holothuroids. Journal of Experimental Marine Biology and Ecology. 264pp. 171–188.

Jia, W.W.G., Bu, X., Philips, D., Yan, H., Liu, G., Chen, X., Bush, J.A. & Li, G. (2004) Rh2, a compound extracted from ginseng, hypersensitizes multidrug-resistant tumor cells to chemotherapy. Canadian Journal of Physiology and Pharmacology. 82 (7), pp. 431–437.

Jouiaei, M., Yanagihara, A., Madio, B., Nevalainen, T., Alewood, P. & Fry, B. (2015) Ancient Venom Systems: A Review on Cnidaria Toxins. Toxins. 7 (6), pp. 2251–2271.

Kalinin, V.I., Aminin, D.L., Avilov, S.A., Silchenko, A.S. & Stonik, V.A. (2008) Triterpene glycosides from sea cucucmbers (holothurioidea, echinodermata). Biological activities and functions. Studies in Natural Products Chemistry. 35 (C), pp. 135–196.

Kalinin, V.I., Prokofieva, N.G., Likhatskaya, G.N., Schentsova, E.B., Agafonova, I.G., Avilov, S.A. & Drozdova, O.A. (1996) Hemolytic activities of triterpene glycosides from the holothurian order dendrochirotida: some trends in the evolution of this group of toxins. Toxicon. 34 (4), pp. 475–483.

Kalinin, V.I., Silchenko, A.S., Avilov, S.A., Stonik, V.A. & Smirnov, A.V. (2005) Sea Cucumbers Triterpene Glycosides, the Recent Progress in Structural Elucidation and Chemotaxonomy. Phytochemistry Reviews. 4 (2-3), pp. 221–236.

Kerr, R.G. & Chen, Z. (1995) In vivo and in vitro biosynthsis of saponins in sea cucmbers. 58 (2), pp. 172–176.

Keukens, E., de Vrije, T., van den Boom, C., de Waard, P., Plasman, H., Thiel, F., Chupin, V., Jongen, W. & Ben de Kruijff (1995) Molecular basis of glycoalkaloid induced membrane disruption. Biochimica et Biophysica Acta. 1240pp. 216–228.

Kim, S.-K. & Wijesekara, I. (2010) Development and biological activities of marine-derived bioactive peptides: A review. Journal of Functional Foods. 2 (1), pp. 1–9.

König, G.M., Kehraus, S., Seibert, S.F., Abdel-Lateff, A. & Müller, D. (2005) Natural Products from Marine Organisms and Their Associated Microbes. ChemBioChem. 7 (2), pp. 229–238.

Krug, P.J. (2006) Defense of Benthic Invertebrates Against Surface Colonization by Larvae: A Chemical Arms Race. In: Nobuhiro Fusetani & Anthony S Clare (eds.). Antifouling Compounds. Marine Molecular Biotechnology. Berlin/Heidelberg: Springer-Verlag. pp. pp. 1–53. doi:10.1007/3-5403-0016-3_1.

Kubanek, J., Whalen, K., Engel, S., Kelly, S., Henkel, T., Fenical, W. & Pawlik, J. (2002) Multiple defensive roles for triterpene glycosides from two Caribbean sponges. Oecologia. 131 (1), pp. 125–136.

Kuramoto, M., Arimoto, H. & Uemura, D. (2004) Bioactive Alkaloids from the Sea: A Review. Marine Drugs. 2pp. 39–54.

Lee, C.-C., Hsieh, H.J., Hsieh, C.-H. & Hwang, D.-F. (2014) Spine venom of crown-of-thorns starfish (Acanthaster planci) induces antiproliferation and apoptosis of human melanoma cells (A375.S2). Toxicon. 91 (C), pp. 126–134.

Lin, F. & Wang, R. (2009) Hemolytic mechanism of dioscin proposed by molecular dynamics simulations. Journal of Molecular Modeling. 16 (1), pp. 107–118.

Lins, L. & Brasseur, R. (1995) The hydrophobic effect in protein folding. The FASEB Journal. 9pp. 535–540.

Loh, T.L. & Pawlik, J.R. (2014) Chemical defenses and resource trade-offs structure sponge communities on Caribbean coral reefs. Proceedings of the National Academy of Sciences. 111 (11), pp. 4151–4156.

Lorent, J., Le Duff, C.S., Quetin-Leclercq, J. & Mingeot-Leclercq, M.-P. (2013) Induction of Highly Curved Structures in Relation to Membrane Permeabilization and Budding by the Triterpenoid Saponins, - and -Hederin. The Journal of Biological Chemistry. 288 (20), pp. 14000–14017.

Lorent, J., Lins, L., Domenech, Ò., Quetin-Leclercq, J., Brasseur, R. & Mingeot-Leclercq, M.-P. (2014a) Domain Formation and Permeabilization Induced by the Saponin α-Hederin and Its Aglycone Hederagenin in a Cholesterol-Containing Bilayer. Langmuir. 30 (16), pp. 4556–4569.

Lorent, J.H., Quetin-Leclercq, J. & Mingeot-Leclercq, M.-P. (2014b) The amphiphilic nature of saponins and their effects on artificial and biological membranes and potential consequences for red blood and cancer cells. Org. Biomol. Chem. 12 (44), pp. 8803–8822.

Lorent, J., Léonard, C., Abouzi, M., Akabi, F., Quetin-Leclercq, J. & Mingeot-Leclercq, M.-P. (2016) α-Hederin Induces Apoptosis, Membrane Permeabilization and Morphologic Changes in Two Cancer Cell Lines Through a Cholesterol-Dependent Mechanism. Planta Medica. 82 (18), pp. 1532–1539.

Lorente, A., Makowski, K., Albericio, F. & Alvarez, M. (2014) Bioactive Marine Polyketides as Potential and Promising Drugs. Ann Mar Biol Res. 1 (1), pp. 1003.

Lou, Q.-M., Wang, Y.-M., Liu, X.-F. & Xue, C.-H. (2012) Lipid profile and fatty acid compositions in bady wall of Apostichopus japonicus (Selenka). Journal of Food Biochemistry. 36 (3), pp. 317–321.

Mackie, A.M., Singh, H.T. & Owen, J.M. (1976) Studies on the distribution, biosynthesis and function of steroidal saponins in echinoderms. Comp. Biochem Physiol. 56Bpp. 9–14.

MacTavish, T., Stenton-Dozey, J., Vopel, K. & Savage, C. (2012) Deposit-Feeding Sea Cucumbers Enhance Mineralization and Nutrient Cycling in Organically-Enriched Coastal Sediments Martin Solan (ed.). PLOS ONE. 7 (11), pp. e50031–11.

Mashjoor, S. & Yousefzadi, M. (2017) Holothurians antifungal and antibacterial activity to human pathogens in the Persian Gulf. Journal de Mycologie Medicale. 27 (1), pp. 46–56.

Matranga, V., Muller, W.E.G.(2005) Echinodermata. ed. Berlin: Springer, pp.251- 284

Moghadam, F.D., Baharara, J., Balanezhad, S.Z., Jalali, M. & Amini, E. (2016) Effect of Holothuria leucospilota extract saponin on maturation of mice oocyte and granulosa cells. Research in Pharmaceutical Sciences. 11 (2), pp. 130–137.

Moses, T., Papadopoulou, K.K. & Osbourn, A. (2014) Metabolic and functional diversity of saponins, biosynthetic intermediates and semi-synthetic derivatives. Critical Reviews in Biochemistry and Molecular Biology. 49 (6), pp. 439–462.

Moureaux, C., Pérez-Huerta, A., Compère, P., Zhu, W., Leloup, T., Cusack, M. & Dubois, P. (2010) Structure, composition and mechanical relations to function in sea urchin spine. Journal of Structural Biology. 170 (1), pp. 41–49.

Nakagawa, H. & Kimura, A. (1982) Partial purification and characterization of a toxic substance from pedicellariae of the sea urchin Toxopneustes pileolus. Japan Journal of Pharmacology. 32pp. 966–968.

Nakamura, T., Inoue, K., Nojima, S., Sankawa, U., Shoji, J., Kawasaki, T. & Shimata, S. (1979) Interaction of saponins with red blood cells as well as with the phosphatidylcholine liposomal membranes. J.Parm. Dyn. 2pp. 374–382.

Niu, C.-S., Yeh, C.-H., Yeh, M.-F. & Cheng, J.-T. (2008) Increase of Adipogenesis by Ginsenoside (Rh2) in 3T3-L1 Cell via an Activation of Glucocorticoid Receptor. Hormone and Metabolic Research. 41 (04), pp. 271–276.

Nyberg, N.T., Kenne, L., Rönnberg, B. & Sundquist, B.G. (2000) Separation and structural analysis of some saponins from Quillaja saponaria Molina. Carbohydrate Research. 323pp. 87–97.

Obermann, D., Bickmeyer, U. & Wägele, H. (2012) Incorporated nematocysts in Aeolidiella stephanieae (Gastropoda, Opisthobranchia, Aeolidoidea) mature by acidification shown by the pH sensitive fluorescing alkaloid Ageladine A. Toxicon. 60 (6), pp. 1108–1116.

Park, J.-I. & Kwak, H.-R.B.A.J.-Y. (2014) Relationships between chemical structures and functions of triterpene glycosides isolated from sea cucumbers. pp. 1–14.

Pawlik, J.R. (1993) Marine invertebrate chemical defenses. Chemical Reviews. 93 (5), pp. 1911–1922.

Petschenka, G. & Agrawal, A.A. (2015) Milkweed butterfly resistance to plant toxins is linked to sequestration, not coping with a toxic diet. Proceedings of the Royal Society B: Biological Sciences. 282 (1818), pp. 20151865–20151869.

Popov, A.M. (2003) Comparative Study of Effects of Various Sterols and Triterpenoids on Permeability of Model Lipid Membranes. Journal of Evolutionary Biochemistry and Physiology. 39 (3), pp. 314–320.

Popov, A.M., Kalinovskaya, N.I., Kuznetsova, T.A., Agafonova, I.G. & Anisimov, M.M. (1983) Sterols and membranotropic activity of triterpene glycosides. pp. 1–4.

Proksch, P. (1994) Defensive roles for secondary metabolites from marine sponges and spong-feeding nudibranchs. Toxicon. 32 (6), pp. 639–655.

Purcell, S.W., Ngaluafe, P., Foale, S.J., Cocks, N., Cullis, B.R. & Lalavanua, W. (2016) Multiple Factors Affect Socioeconomics and Wellbeing of Artisanal Sea Cucumber Fishers Sebastian C A Ferse (ed.). PLOS ONE. 11 (12), pp. e0165633–20.

R Development Core Team (2011). R: A Language and Environment for Statistical Computing. Vienna, Austria : the R Foundation for Statistical Computing. ISBN: 3-900051-07-0. Available online at http://www.R-project.org, consulted on 9 Aug 2017.

Rajput, Z.I., Hu, S.-H., Xiao, C.-W. & Arijo, A.G. (2007) Adjuvant effects of saponins on animal immune responses. Journal of Zhejiang University SCIENCE B. 8 (3), pp. 153–161.

Risselada, H.J. & Marrink, S.J. (2008) The molecular face of lipid rafts in model membranes. PNAS. 105 (45), pp. 17367–17372.

Robertson, J.C. & Hazel, J.R. (1995) Cholesterol content of trout plasma membranes varies with acclimation temperature. Am J Physiol Regul Integr Comp Physiol. 269 (5), pp. R1113.

Saporito, R.A., Donnelly, M.A., Spande, T.F. & Garraffo, H.M. (2011) A review of chemical ecology in poison frogs. Chemoecology. 22 (3), pp. 159–168.

Scheuer, P.J. (1978) Marine Natural Products, Volume II. ed. New York: Academic Press, Inc. pp.105-109. [online] https://books.google.be/books?hl=fr&id=qMN25FQbK20C&dq=Scheuer%2C+1978&q=dichotomy#v=onepage&q&f=false

Schindelin, J., Arganda-Carreras, I., Frise, E., Kaynig, V., Longair, M., Pietzsch, T., Preibisch, S., Schmid, B., Tinevez, J.-Y., White, D.J., Hartenstein, V., Eliceiri, K. & Cardona, A. (2012) Fiji: an open-source platform for biological-image analysis. Nature Methods. 9 (7), pp. 676–682.

Seeman, P., Cheng, D. & Iles, G.H. (1973) Structure of membrane holes in osmotic and saponin hemolysis. The Journal of Cell Biology. 56pp. 519–527.

Shimada, S. (1969) Antifungal Steroid Glycoside from Sea Cucumber. Science. 163pp. 1462.

Schindelin, J., Arganda-Carreras, I., Frise, E., Kaynig, V., Longair, M., Pietzsch, T., Preibisch, S., Schmid, B., Tinevez, J.-Y., White, D.J., Hartenstein, V., Eliceiri, K. & Cardona, A. (2012) Fiji: an open-source platform for biological-image analysis. Nature Methods. 9 (7), pp. 676–682.

Stonik, V.A. & Tachibana, K. (1988) Secondary Metabolites from Echinoderms as Chemotaxonomic Markers. In: Paul J Scheuer (ed.). Bioorganic Marine Chemistry. Berlin, Heidelberg: Springer Berlin Heidelberg. pp. pp. 43–86. doi:10.1007/978-3-642-48346-2.

Stonik, V.A., Ponomarenko, L.P., Makarieva, T.N., Boguslavsky, V.M., Dmitrenok, A.S., Fedorov, S.N. & Strobikin, S.A. (1998) Free sterol compositions from the sea cucumbers Pseudostichopus trachus, Holothuria (Microtele) nobilis, Holothuria scabra, Trochostoma orientale and Bathyplotes natans. Comparative Biochemistry and Physiology Part B: Biochemistry and Molecular Biology. 120pp. 337–347.

Suput, D. (2009) In vivo effects of cnidarian toxins and venoms. Toxicon. 54 (8), pp. 1190–1200.

Thimmappa, R., Geisler, K., Louveau, T., O'Maille, P. & Osbourn, A. (2014) Triterpene Biosynthesis in Plants. Annual Review of Plant Biology. 65 (1), pp. 225–257.

Thomas, A.J. & Patton, S. (1971) Phospholipids of Fish Gills. Lipids. 7 (1), pp. 76–78.

Tian, X., Tang, H., Lin, H., Cheng, G., Wang, S. & Zhang, X. (2013) Saponins: the Potential Chemotherapeutic Agents in Pursuing New Anti-glioblastoma Drugs. Mini-Reviews in Medicinal Chemistry. 13 (12), pp. 1709–1724.

Van Dyck, S., Caulier, G., Todesco, M., Gerbaux, P., Fournier, I., Wisztorski, M. & Flammang, P. (2011) The triterpene glycosides of Holothuria forskali: usefulness and efficiency as a chemical defense mechanism against predatory fish. Journal of Experimental Biology. 214 (8), pp. 1347–1356.

Van Dyck, S., Gerbaux, P. & Flammang, P. (2010) Qualitative and Quantitative Saponin Contents in Five Sea Cucumbers from the Indian Ocean. Marine Drugs. 8 (1), pp. 173–189.

Van Dyck, S., Gerbaux, P. & Flammang, P. (2009) Elucidation of molecular diversity and body distribution of saponins in the sea cucumber Holothuria forskali (Echinodermata) by mass spectrometry. Comparative Biochemistry and Physiology, Part B. 152 (2), pp. 124–134.

van Meer, G., Voelker, D.R. & Feigenson, G.W. (2008) Membrane lipids: where they are and how they behave. Nature Reviews Molecular Cell Biology. 9 (2), pp. 112–124.

Vandenspiegel, D., Jangoux, M. & Flammang, P. (2000) Maintaining the Line of Defense: Regeneration of Cuvierian Tubules in the Sea Cucumber Holothuria forskali. Biological Bulletin. 198 (1), pp. 34–49.

Vincken, J.-P., Heng, L., de Groot, A. & Gruppen, H. (2007) Saponins, classification and occurrence in the plant kingdom. Phytochemistry. 68 (3), pp. 275–297.

Vo, N.N.Q., Fukushima, E.O. & Muranaka, T. (2016) Structure and hemolytic activity relationships of triterpenoid saponins and sapogenins. Journal of Natural Medicines. 71 (1), pp. 50–58.

Wang, S.-H., Liu, F.-F., Dong, X.-Y. & Sun, Y. (2010) Thermodynamic Analysis of the Molecular Interactions between Amyloid β-Peptide 42 and (–)-Epigallocatechin-3-gallate. The Journal of Physical Chemistry B. 114 (35), pp. 11576–11583.

Wang, X.-H., Zou, Z.-R., Yi, Y.-H., Han, H., Li, L. & Pan, M.-X. (2014) Variegatusides: New Non-Sulphated Triterpene Glycosides from the Sea Cucumber *Stichopus variegates* Semper. Marine Drugs. 12 (4), pp. 2004–2018.

Watson, G.J., Bentley, M.G., Gaudron, S.M. & Hardege, J.D. (2003) The role of chemical signals in the spawning induction of polychaete worms and other marine invertebrates. Journal of Experimental Marine Biology and Ecology. 294 (2), pp. 169–187.

Wilkie, I.C. (2001) Autotomy as a prelude to regeneration in echinoderms. Microscopy Research and Technique. 55 (6), pp. 369–396.

Winter, WP. (1994) Mechanism of saponin induced red cell hemolysis: Evidence for the involvement of aquaporin CHIP28. Blood 84: Suppl. 1 to 10, Abstr. 445.

Wittstock, U. & Gershenzon, J. (2002) Constitutive plant toxins and their role in defense against herbivores and pathogens. Current Opinion in Plant Biology. 5 (4), pp. 300–307.

Xu, Z.-X., Ding, T., Haridas, V., Connolly, F. & Gutterman, J.U. (2009) Avicin D, a Plant Triterpenoid, Induces Cell Apoptosis by Recruitment of Fas and Downstream Signaling Molecules into Lipid Rafts Gordon Langsley (ed.). PLOS ONE. 4 (12), pp. e8532–11.

Yu, K., Chen, F. & Li, C. (2012) Absorption, Disposition, and Pharmacokinetics of Saponins from Chinese Medicinal Herbs: What Do We Know and What Do We Need to Know More? Current Drug Metabolism. 13 (5), pp. 577–598.

Yuan, W.-H., Yi, Y.-H., Xue, M., Zhang, H.-W. & La, M.-P. (2008) Two Antifungal Active Triterpene Glycosides from Sea Cucumber *Holothuria (Microthele) axiloga*. *Chinese Journal of Natural Medicines*. 6 (2), pp. 105–108.

Yudt, M.R. & Cidlowski, J.A. (2002) The Glucocorticoid Receptor: Coding a Diversity of Proteins and Responses through a Single Gene. Molecular Endocrinology. 16 (8), pp. 1719–1726.

Zabelinskii, S.A., Brovtsyna, N.B., Chebotareva, M.A., Gorbunova, O.B. & Krivchenko, A.I. (1995) Comparative investigation of lipid and fatty acid composition of fish gills and mammalian lungs. A model of the membrane lipid component areas. Comp. Biochem Physiol. 111B (1), pp. 127–140.

Zakanda, F.N., Lins, L., Nott, K., Paquot, M., Lelo, G.M. & Deleu, M. (2012) Interaction of Hexadecylbetainate Chloride with Biological Relevant Lipids. Langmuir. 28 (7), pp. 3524–3533.

Zhang, Y.-F., Fan, X.-J., Li, X., Peng, L.-L., Wang, G.-H., Ke, K.-F. & Jiang, Z.-L. (2008) Ginsenoside Rg1 protects neurons from hypoxic–ischemic injury possibly by inhibiting Ca2+ influx through NMDA receptors and L-type voltage-dependent Ca2+ channels. European Journal of Pharmacology. 586 (1-3), pp. 90–99.